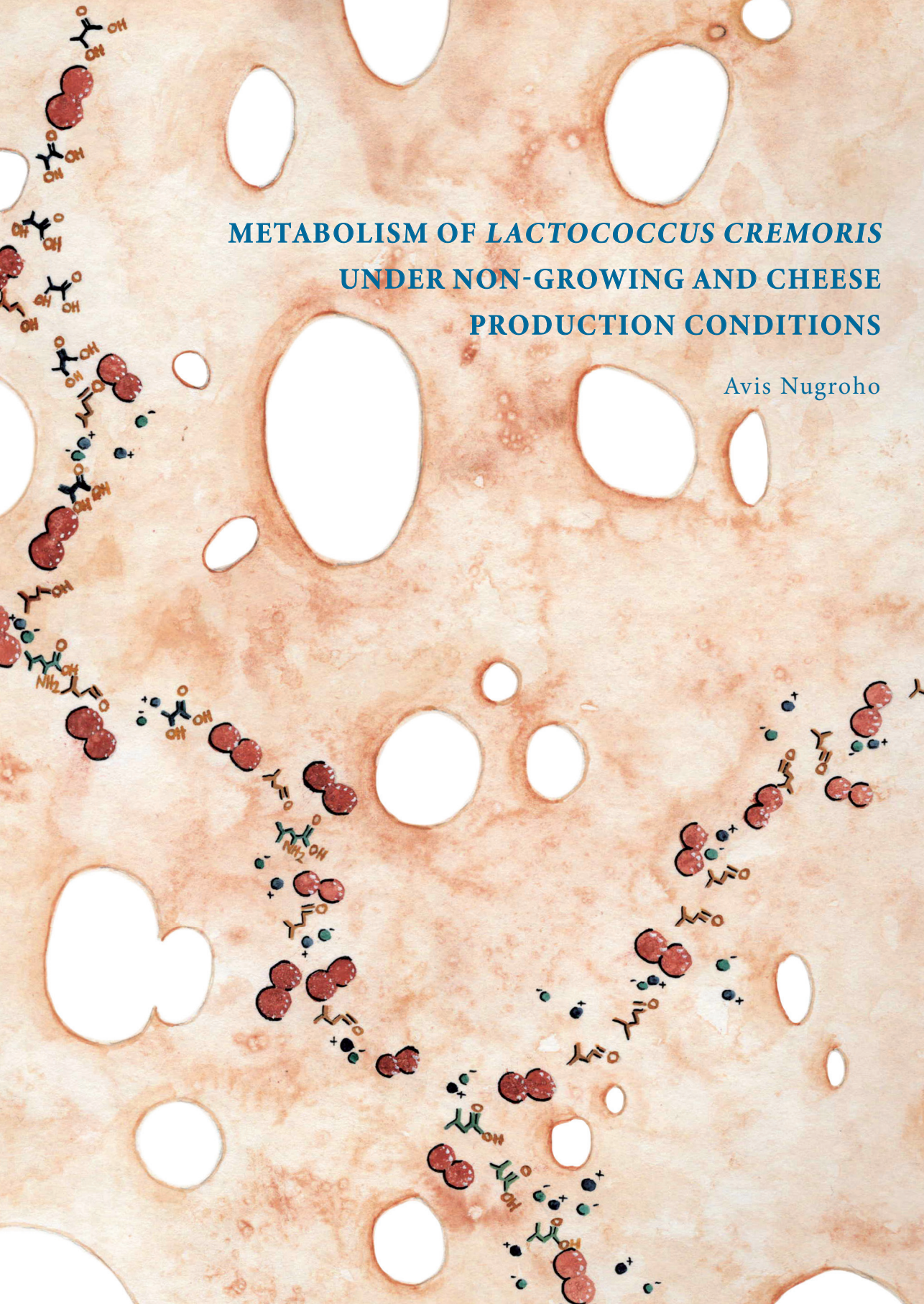

METABOLISM OF *LACTOCOCCUS CREMORIS* UNDER NON-GROWING AND CHEESE PRODUCTION CONDITIONS

Avis Nugroho

Propositions

1. Signature volatiles in cheese are the result of the activity of intact microbial cells rather than the enzymes released by those cells.
   (this thesis)

2. Functionality optimization instead of growth optimization ensures maximum starter performance.
   (this thesis)

3. More research catering to the fact that most microbes spend most of their life in a non-growing state is required.

4. The ambition of applied food science to translate consumer wishes to required technical parameters is strenuous.

5. Progressing from tolerance to acceptance is the challenge of Dutch society.

6. The divide-and-conquer instead of the unite-and-build mentality within minority groups hinders equity and inclusion.

Propositions belonging to the thesis, entitled:

Metabolism of *Lactococcus cremoris* under non-growing and cheese production conditions.

Avis Dwi Wahyu Nugroho

Wageningen, 25 April 2023

Metabolism of *Lactococcus cremoris* under non-growing and cheese production conditions

Avis D. W. Nugroho

Thesis committee

Promotor

Prof. Dr M. Kleerebezem

Personal professor at Host-Microbe Interactomics

Wageningen University & Research

Co-promotor

Dr H. Bachmann

Assistant professor, Systems Bioinformatics,

Vrije Universiteit Amsterdam

Principal scientist, NIZO Food Research, Ede

Other members

Prof. Dr H.M.W. den Besten, Wageningen University & Research

Prof. Dr A.R. Neves, Technical University of Denmark, Lyngby, Denmark

Prof. Dr P.R. Jensen, Technical University of Denmark, Lyngby, Denmark

Dr A. Wegkamp, Royal DSM, Wageningen

This research was conducted under the auspices of VLAG Graduate School (Biobased, Biomolecular, Chemical, Food and Nutrition Sciences).

Metabolism of *Lactococcus cremoris* under non-growing and cheese production conditions

Avis D. W. Nugroho

Thesis

submitted in fulfilment of the requirements for the degree of doctor
at Wageningen University
by the authority of the Rector Magnificus,
Prof. Dr A.P.J. Mol,
in the presence of the
Thesis Committee appointed by the Academic Board
to be defended in public
on Tuesday 25 April 2023
at 1.30 p.m. in the Omnia Auditorium.

Avis D.W. Nugroho

Metabolism of *Lactococcus cremoris* under non-growing and cheese production conditions,
198 pages.

PhD thesis, Wageningen University, Wageningen, The Netherlands (2023)
With references, with summary in English

ISBN 978-94-6447-560-9
DOI https://doi.org/10.18174/585657

·] To those in liminal spaces [·

Table of Contents

Chapter 1

General Introduction

Nugroho, A. D. W.

1.1 The cheese industry: overview and challenges

Cheese is a significant contributor to the Dutch economy. In 2020, 14.2 billion kg of bovine milk was produced in The Netherlands, which contributed 7.8 billion euro to a total of 56.2 billion euro in the Agro & Food sector of the Dutch economy[1]. From this milk production, 7.8 billion kg was processed into cheese and 65% of the resulting cheese was exported globally, bringing a revenue of 3.2 billion euro[1]. Gouda cheese is arguably the most popular cheese in The Netherlands. It is a firm/semi-hard cheese, which is ripened normally at 10-17°C between 1 month and 12 months. Following ripening, additional cooling is required during transport, distribution, and retail to prevent undesired sensory changes and spoilage. Altogether, this makes the overall life cycle of cheese costly and time intensive.

With the global demand for efficient manufacturing, accelerated cheese ripening and post-ripening stability are crucial for cheese industries. During ripening, the majority of key-volatiles in cheese are produced and flavour formation continues during storage, distribution, and until consumption. Unsuitable post-ripening conditions can negatively alter the overall flavour profile due to degradation of key-volatiles, conversion to less odour-active derivatives, or production of undesired volatiles (off-flavours). Ideally, flavour formation during ripening is achieved fast without further changes. To accomplish this, the understanding of metabolic regulation that occurs during starter preparation, cheesemaking, and cheese ripening is vital. Moreover, unconventional cheeses, e.g., with reduced fat or salt content or those made from plant or recombinant proteins, often suffer from flavour discrepancies in comparison to conventional dairy cheeses and will benefit from the knowledge of factors influencing flavour formation.

1.2 Dairy starter Lactic Acid Bacteria (LAB): the trade-offs associated with growth rate

LAB are primarily anaerobic, non-sporulating, Gram-positive bacteria, which produce lactic acid as the prominent metabolite of sugar fermentation. LAB are found in various habitats[2–4] ranging from plant materials, milk environment, fermented foods, to animal hosts, e.g., mouth, guts, and vagina. In the case of dairy starter LAB, it is believed that they derived from plant-origin ancestors[5], and domestication to dairy environment led to reductive genome evolution[6]. This resulted in the loss of functions associated with the utilisation of complex (carbohydrate) polymers and other plant-derived components as well as (oxidative) stress response and exopolysaccharide biosynthesis[7]. Dairy LAB are further characterised by a high number of amino acid auxotrophies and the ability to efficiently utilise milk proteins as the source of amino acids[8]. Such adaptation and evolution lead to LAB that grow and acidify its milk environment much more rapidly than their non-dairy counterparts. These fast-growing dairy LAB are commonly referred as starter LAB, which also include *Lactococcus cremoris* NCDO712 (formerly *L. lactis* subsp. *cremoris* NCDO712) used in this thesis.

Interestingly, empirical observation shows that the use of fast-growing dairy LAB seems to be restricted to the acidification stage of production, which is an early stage of cheese manufacturing and ripening[9]. In contrast, adjunct and non-starter LAB (NSLAB) are associated with limited or slow growth and they contribute to the later stage of cheese ripening when starter LAB viability decreases[10,11] and flavour accumulates. NSLAB originate from raw milk and survive through milk pasteurisation and cheesemaking as well as colonise processing environments, which enable them to be reintroduced in each batch of cheesemaking[12]. While starter LAB have been selected and cultivated in a relatively isolated community and controlled environment, NSLAB experience the contrary. In lactococci, it has been argued that plant isolates are

continuously in an energy-saving mode for growth and maintenance, while dairy isolates only switch to such mode in a non-growing state[13]. While it remains to be investigated, this may influence the available energy for product formation, e.g., flavour formation during cheese ripening. Altogether, it can be argued that starter LAB are selected through human intervention for fast growth, whereas NSLAB are naturally selected for survival, which may subsequently be associated with higher metabolite accumulation. Many of these NSLAB are subsequently screened and cultivated as adjunct starters with the sole aim to improve sensory quality[10,14].

Finally, there seems to be a trade-off between the growing and non-growing state. The latter represents a predominant state of bacterial existence in nature as a result of nutrient starvation and unfavourable environmental conditions such as non-optimal temperature or pH, oxidative stress, and the presence of antibiotics or other growth inhibitors[15]. During cheese ripening or storage of fermented foods, lactococci are primarily in a non-growing state[16,17] and their contribution to flavour formation will be explained in greater depth in **Chapter 2**. In this state, cells remain metabolically active, but their metabolic activity is markedly reduced in comparison to growing cells[15]. The ability to persist in a non-growing state for an extended period, until favourable environmental conditions allow growth to resume, is crucial to the survival of microbial species. In *E. coli*, slower growth led to exponentially slower death of non-growing cells caused by carbon starvation, and it was shown to be caused by the decrease in maintenance rate[18]. It has also been hypothesized that the formation of persister subpopulations is a consequence of a fundamental trade-off between survival and growth where investment in growth-supporting proteins comes at the expense of stress response proteins[19].

1.3 Ribosome allocation and cellular trade-offs in Biology

Ribosomes are required for the synthesis of all proteins. Due to the higher demand on protein production rate with higher growth rates, ribosome concentration in cells scales in parallel with growth rate[20,21]. A linear relation between growth rate and ribosome fraction exists in various microorganisms[22,23] and is referred to as bacterial growth law[24]. Ribosomal proteins make up a large fraction of the total proteome. For example, in rapidly growing yeast cells, ribosomes constitute approximately 50% of the total number of cellular proteins and 30% of the total cellular protein mass[25]. Evidently, allocation of resources to synthesize ribosomes is substantial in a cell. Since cellular growth is constrained by physical and chemical limits, e.g., size and surface-to-volume ratio[26], trade-offs may occur where optimisation of fitness-enhancing traits under a condition comes at the expense of other traits[20]. An example of trade-offs in lactococci can be seen in Figure 1.1. As growth rate increases, cell number, total cell volume (count x volume) and total protein decrease whereas lactic acid production and cell size increase. Recent investigation using a genome-scale metabolic model of *L. cremoris* shows that limited proteome availability at high growth rate favoured lactic acid as opposed to mixed acid fermentation that requires the expression of multiple proteins for ATP production[27].

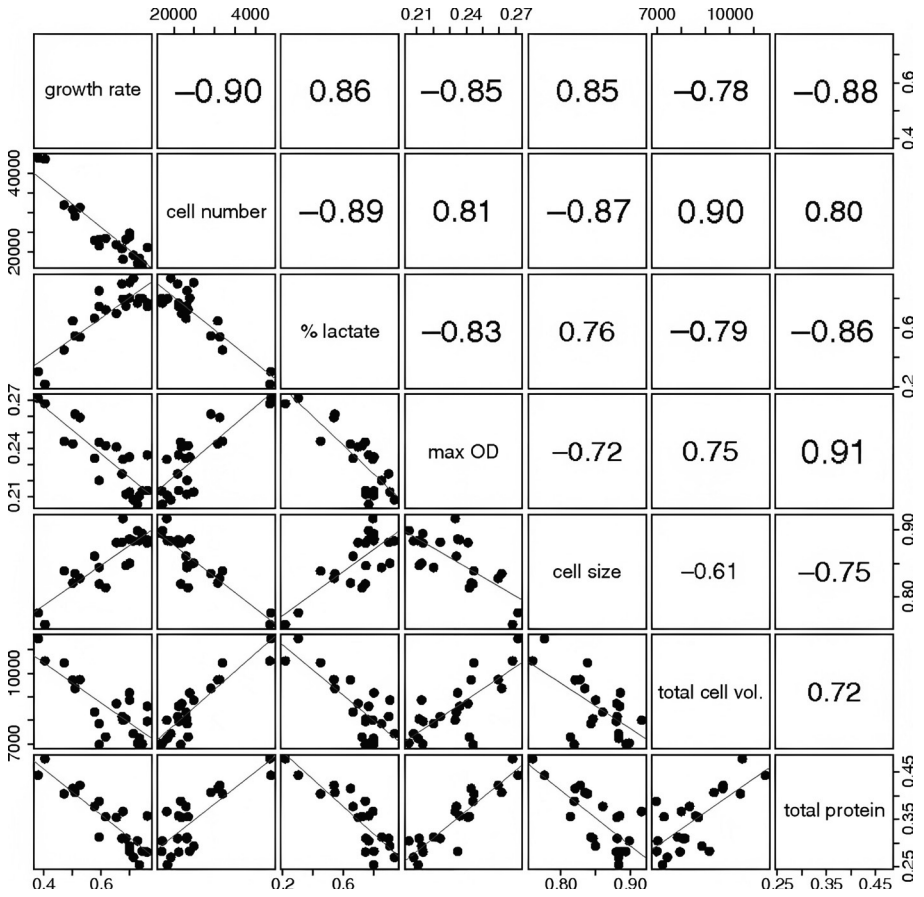

Figure 1.1 *Trade-offs in* Lactococcus cremoris *taken from Bachmann et al. (2013)*[28]*. Correlation matrix of parameters is obtained from the growth of 22 derivatives of* L. cremoris *MG1363 obtained from adaptive evolution. From growth experiments, growth rate (/h) and maximum optical density at 600 nm (max OD) were acquired. Based on Coulter Counter measurements, cell number, cell size, and total cell volume (total cell vol. = cell count x cell volume) were obtained. Fraction of lactic acid as end-metabolites was indicated as % lactate. Total protein content (total protein) was determined with BCA protein assay.*

Since many dairy starter cultures are optimised for growth and acidification rate, high ribosomal allocation and protein synthesis are thought to consume a major fraction of available cellular resources during fast growth, e.g., starter preparation. When a cell encounters unfavourable, stress conditions during cheesemaking, a mechanism is in place to regulate translational

capacity. These mechanisms are those that (1) confer an inactive or hibernating state or (2) inhibit different stages of translation, which eventually ensure reactivation of translation when conditions improve[29,30]. Under such condition, ribosomes do not seem to be actively degraded unless protein damage occurs and triggers proteolysis by Clp proteases, which requires ATP and are thereby executing costly reactions[31]. Furthermore, growth is limited during cheesemaking (3-6 generations)[9], and the subsequent non-growing state occurs under conditions of sugar limitation, as well as low pH and temperature that limit *de novo* synthesis of ribosomes. While proteome changes and cellular adjustments to cheese ripening may occur, this is likely to happen very slowly[32,33]. Recent investigation also shows that *L. cremoris* NCDO712 demonstrates very limited proteome adjustments during 2 weeks of cheese ripening (Berdien van Olst, personal communication). As a consequence of limited growth and a lack of subsequent changes, ribosomal allocation during starter preparation is potentially retained throughout cheesemaking. With a high ribosomal fraction, the remaining fraction for flavour-forming and other relevant proteins, e.g., stress proteins, is limited. Since the effective formation of flavours depend on the level of enzymes, this implies that starter preparation may significantly influence its functionality during cheesemaking and ripening. On the other hand, it suggests that starter preparation is a prospective means of functionality optimisation. Such optimisation can be done by cheesemakers through bulk starter preparation or by starter culture producers through the preparation of direct inoculation cultures (Figure 1.2). However, the question remains how such multi-objective optimisation can be achieved, and System Biology investigations are required to disentangle the influencing factors.

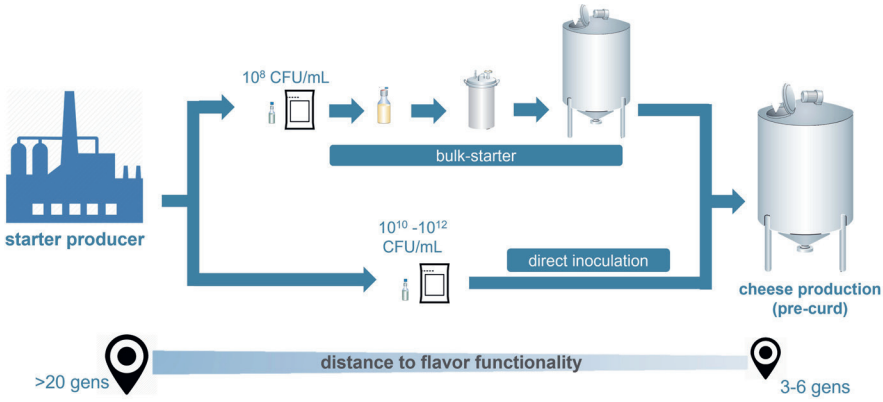

Figure 1.2 *Starter can be prepared as (upper branch) bulk starter or (lower branch) for direct vat inoculation (DVI). Main differences are that DVI cultures are frozen between culturing inoculation while bulk starters are typically produced on-site prior to cheesemaking.*

1.4 Leucine catabolism: the interplay between central carbon metabolism, growth rate, and other metabolic pathways

Leucine is an essential amino acid aside from isoleucine, valine, glutamate, histidine, and methionine in *L. cremoris* NCDO712[34,35]. Leucine is catabolised through transamination, which is initialised through the intermediate formation of α-keto isocaproic acid (KICA)[36]. Subsequent conversions can lead to the production of a diverse array of metabolites that are industrially relevant. Besides flavour compounds, antimicrobial compounds, bioplastic, biofuels, and other commodity chemicals can also be obtained from leucine catabolism by various bacteria[37]. In LAB, leucine catabolism is mostly associated with the formation of flavour compounds such as 3-methylbutanal. In strain NCDO712, formation of 3-methylbutanal from KICA may follow either a single or a multi-step conversion but the corresponding enzymes are yet to be characterised (Figure 1.3). Moreover, leucine catabolism is also associated with survival and stress response. In fact, the correlation between leucine catabolism and survival has been observed in diverse organisms besides LAB[38–40]. For example, the utilisation of branched-

chain amino acids has been shown as an alternative pathway for ATP generation to support survival during long-term carbon starvation[41], and a putative pathway that leads to the production of up to 3 ATP molecules per leucine molecule has been proposed[42]. In *L. cremoris* NCDO712, 1 ATP can be produced from the conversion of leucine to 3-methylbutanoic acid (Figure 1.3). Moreover, overproduction of 3-methylbutanoic acid from leucine (Figure 1.3) during acid stress was proposed to enhance survival by its contribution to redox balance maintenance through the regeneration of NADH[43].

Central carbon metabolism seems to highly interact and influence amino acid metabolism and the formation of 3-methylbutanal. Leucine transamination to produce KICA requires α-ketoglutarate as a co-substrate. In *E. coli*, this co-substrate has been shown to coordinate carbon and nitrogen utilisation through the inhibition of Enzyme I (EI), which facilitates the first step of the sugar–phosphoenolpyruvate phosphotransferase system (PTS)[44] and is highly conserved across bacteria[45]. In the case of leucine transamination, α-ketoglutarate needs to be regenerated. This can be performed by phosphoserine aminotransferase (SerC) that facilitates the conversion of phosphoserine to 3-P-hydroxypyruvate that is subsequently converted by phosphoglycerate dehydrogenase (SerA) to 3-P-glycerate in the glycolytic pathway[46]. Pyruvate is eventually produced, and its dissipation leads to the production of lactic acid, acetic acid, formic acid, and ethanol (Figure 1.3). The composition of metabolites from pyruvate conversion is influenced by growth rate, redox balance, and oxygen availability among others[20,47,48]. Further information of global regulators of central carbon catabolism is explained in **Chapter 2**. Generally speaking, lactic acid is mainly produced at high growth rate, whereas the other metabolites ("mixed-acids") are increasingly produced at low growth rate. For mixed-acid fermentation, pyruvate-formate lyase (Pfl), pyruvate dehydrogenase (Pdh), phosphate acetyltransferase (Pta), acetate kinase (Ack), and alcohol-aldehyde dehydrogenase (Adh) need to be expressed. Among these enzymes, Pdh, Pta, and Ack are also required for the multi-step

conversion of 3-methylbutanal from KICA via 3-methylbutanoic acid. Altogether, this demonstrates how intricately crossed leucine metabolism is with major metabolic pathways that are required for growth and survival. Considering that many cofactors like ADP, ATP and NAD(H) are shared between carbon and nitrogen metabolism, it is not unlikely that metabolic dependencies exist between these pathways.

1.5 Cheese volatiles: bioactive chemicals with roles beyond flavour

The study of flavours and odour-active compounds is relevant beyond food production. Gouda cheesemaking includes various stress conditions for microbes, such as carbon starvation, acid stress, non-optimal temperatures, osmotic stress, and phage infections. Therefore, cheese is an ideal model system for food fermentation and beyond. In fact, cheese has been studied as the representative environment to study the development of multi-species communities[50] in the contexts of genetic studies[51] as well as food safety[52]. Next to flavour perception, odour-active compounds possess biological roles in the environment. Humans evolved roughly 400 olfactory receptors to perceive at least 10,000 chemosensory entities[53]. Although comparably lower than other animal species, the human ability to detect odour active compounds is to this date unmatched with the current analytical tools to measure volatiles, e.g., GC-MS. The coconut-like smelling (3aS,4aS,7aR)-isomer of wine lactone shows an extraordinarily low human odour threshold of 20 fg/L (0.02 pg/L) in air. It is remarkable that our smelling sense retains remarkably high sensitivity to odour compounds. Odour can be indicative of diseases such as isovaleric acidaemia, which is an autosomal recessive inborn error of leucine metabolism[54]. In many species, odour is a form of chemical communication and is a determining factor in mating choice or preference[55–57]. Accumulating evidence has also shown that odorant receptors play versatile roles in health and diseases[58].

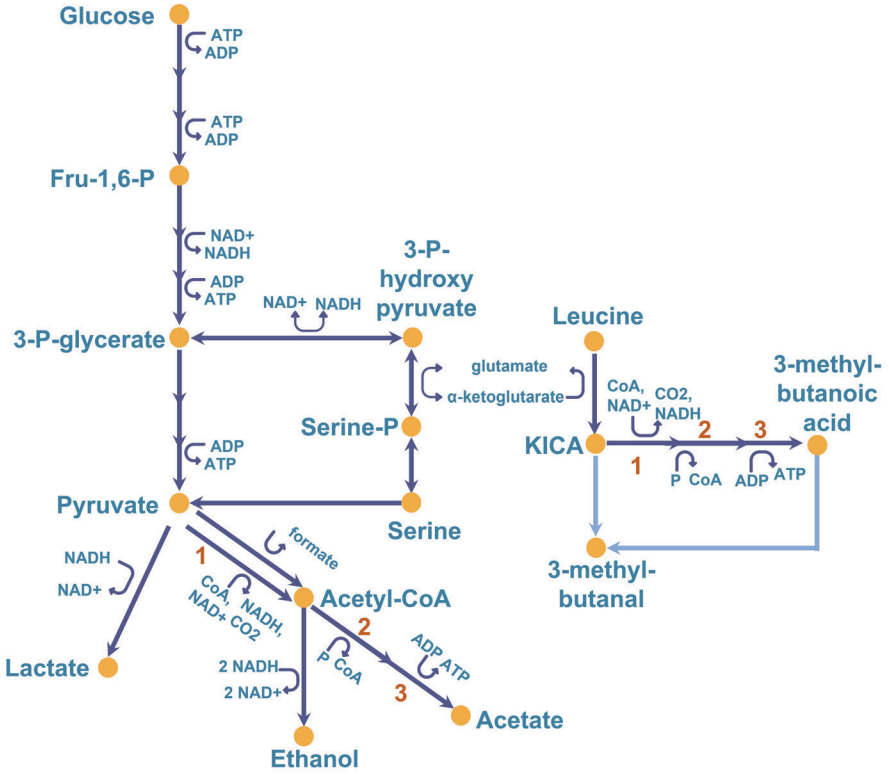

Figure 1.3 *The interplay between sugar and amino acid metabolism. Dark blue arrows represent reactions with known enzymes while light blue arrows represent reported reactions in other species with unknown enzymes in strain NCDO712. The formation of 3-methylbutanal from α-keto isocaproic acid (KICA) has been reported to be either a single-step reaction or a multi-step reaction via 3-methylbutanoic acid. A single step reaction is facilitated by branched-chain ketoacid decarboxylase*[36]*, while a multi-step reaction is facilitated by enzymes*[49] *denoted in dark orange numbers: (1) pyruvate dehydrogenase (Pdh), (2) phosphotransacetylase (Pta), (3) acetate kinase (Ack). Numbered enzymes are more prominently known for their roles in pyruvate dissipation, and these reactions are indicated correspondingly.*

For microorganisms, the functions of flavour formation in cell fitness-determination are not well-established. One argument for yeast cells refers to its role in attracting insects, which subsequently aid in transporting microbes from one environment to another[59–62]. As an example, fermentation of sugar by yeasts produces a diverse array of alcohol and ester by-products that give a fruity aroma and signal the insects the presence of food resources[60–63]. Along

the process, attracted insects transport the yeasts to other locations. Analogously, various flavour compounds synthesized by plants also attract insects that assist with flower pollination. In the case of corpse flower (*Amorphophallus titanium*), dimethyltrisulfide and trimethylamine cause the rotten meat and fish odours, which attracts pollinating flies[64]. Interestingly, 3-methylbutanal, which is a key-volatile in Gouda cheese and other semi-hard cheeses was also found as one of the important flower odours in the same study. Aside from this argument, it is poorly understood why microorganisms produce flavours and whether such production has an evolutionary beneficial purpose that is different than non-odour active compounds.

1.6 Aims and outline of this thesis

This thesis describes the factors influencing microbial formation of flavour volatiles in cheese by *Lactococcus cremoris*. It demonstrates how industrially relevant conditions during starter preparation, cheesemaking and/or ripening contribute to the accumulation of key-volatiles, in relation to other metabolic pathways and in both growing and non-growing states. In particular, volatiles derived from branched-chain amino acids, such as 3-methylbutanal (chocolate, fruity, nutty) are found to be correlated to various environmental perturbations.

Chapter 2 provides further background information on starter culture physiology and cheese flavour formation and emphasizes the implication of optimising starter culture for growth rate. Starter optimisation for cheese production and ripening is far from trivial since multiple environmental adaptations and stresses occur throughout the cheese production process. This chapter presents and discusses various examples and highlights the importance of intact non-growing cells as opposed to cell lysis during cheese ripening.

Chapter 3 describes the development of a method for high throughput long-term analysis of non-growing *L. cremoris.* Such method is important for the combinatorial investigation of the multiple factors that affect starter culture

performance during ripening. We demonstrate that this method can facilitate the continuous monitoring of metabolic activity in non-growing cells for 4 weeks, which corresponds to the minimum ripening time required for Gouda cheese.

Chapter 4 shows the vital role of manganese in the accumulation of potent volatile specimens (aldehydes) rather than their derivatives (alcohols) that have lower odour activities. Manganese is found in limited quantities in the dairy environment and its addition to non-growing cells induces rapid transition towards a non-culturable but metabolically-active state. Such cellular state is shown to be associated with the accumulation of 3-methylbutanal rather than 3-methylbutanol due to limited NADH availability.

Chapter 5 demonstrates that acidification in non-growing cells decays faster with faster production rate, which leads to lower cumulative lactic acid yields. This observation could be replicated independently of the intervention by which the acidification rates were manipulated, demonstrating the robustness of this trade-off between the catalytic rate and product yield of the acid forming pathway in *L. cremoris*. Translating these observations to cheese production leads us to hypothesize that rate manipulation is not only a critical parameter in acceleration of cheese ripening but also in post-ripening stability.

Chapter 6 investigates the influence of growth conditions of starter culture preparations on the global proteome composition of the resulting cells in defined medium and a cheese model. This study demonstrates that growth rate optimisation requires higher ribosomal allocation, which impacts on the eventual flavour formation by non-growing cells. However, the changes in flavour formation were not necessarily correlated with the expression level of the enzymes involved in the corresponding flavour forming pathways. This study establishes the importance of Systems Biology approaches for the optimisation of starters cultures for flavour formation due its complex intertwinement with a variety of metabolic pathways.

Chapter 7 summarises and discusses all findings from previous chapters, including the exemplification case of the key-flavour compound in cheese, 3-methylbutanal. This chapter ends with concluding remarks.

References

1. ZuivelNL. Dutch Dairy in Figures 2020. https://www.zuivelnl.org/uploads/images/Publicaties/Dutch-Dairy-in-Figures-2020-spread.pdf (2021).
2. Cavanagh, D., Fitzgerald, G. F. & McAuliffe, O. From field to fermentation: The origins of *Lactococcus lactis* and its domestication to the dairy environment. *Food Microbiol.* **47**, 45–61 (2015).
3. Shimada, A. *et al.* Oral lactic acid bacteria related to the occurrence and/or progression of dental caries in Japanese preschool children. *Biosci. Microbiota, Food Heal.* **34**, 29-36 (2015).
4. Endo, A. *et al.* Fructophilic lactic acid bacteria, a unique group of fructose-fermenting microbes. *Appl. Environ. Microbiol.* **84**, 1290–1308 (2018).
5. Wels, M., Siezen, R., Van Hijum, S., Kelly, W. J. & Bachmann, H. Comparative genome analysis of *Lactococcus lactis* indicates niche adaptation and resolves genotype/phenotype disparity. *Front. Microbiol.* **10**, 4 (2019).
6. Kelly, W. J., Ward, L. J. H. & Leahy, S. C. Chromosomal diversity in *Lactococcus lactis* and the origin of dairy starter cultures. *Genome Biol. Evol.* **2**, 729–744 (2010).
7. Siezen, R. J. *et al.* Genome-scale genotype-phenotype matching of two *Lactococcus lactis* isolates from plants identifies mechanisms of adaptation to the plant niche. *Appl. Environ. Microbiol.* **74**, 424–436 (2008).
8. Bachmann, H., Starrenburg, M. J. C., Molenaar, D., Kleerebezem, M. & Van Hylckama Vlieg, J. E. T. Microbial domestication signatures of *Lactococcus lactis* can be reproduced by experimental evolution. *Genome Res.* **22**, 115-124 (2012).
9. Bachmann, H., Kruijswijk, Z., Molenaar, D., Kleerebezem, M. & van Hylckama Vlieg, J. E. T. A high-throughput cheese manufacturing model for effective cheese starter culture screening. *J. Dairy Sci.* **92**, 5868–5882 (2009).
10. Briggiler-Marcó, M. *et al.* Nonstarter lactobacillus strains as adjunct cultures for cheese making: *in vitro* characterization and performance in two model cheeses. *J. Dairy Sci.* **90**, 4532–4542 (2007).
11. Peterson, S. D. & Marshall, R. T. Nonstarter lactobacilli in Cheddar cheese: a review. *J. Dairy Sci.* **73**, 1395–1410 (1990).
12. Bokulich, N. A. & Mills, D. A. Facility-specific 'house' microbiome drives microbial landscapes of artisan cheesemaking plants. *Appl. Environ. Microbiol.* **79**, 5214–5223 (2013).
13. Kleerebezem, M. *et al.* Lifestyle, metabolism and environmental adaptation in *Lactococcus lactis*. *FEMS Microbiol. Rev.* **44**, 804-820 (2020).
14. El Soda, M., Madkor, S. A. & Tong, P. S. Adjunct cultures: recent developments and potential significance to the cheese industry. *J. Dairy Sci.* **83**, 609–619

(2000).

15. Lempp, M., Lubrano, P., Bange, G. & Link, H. Metabolism of non-growing bacteria. *Biol. Chem.* **401**, 1479–1485 (2020).
16. Douwenga, S., van Tatenhove-Pel, R. J., Zwering, E. & Bachmann, H. Stationary *Lactococcus cremoris*: energetic state, protein synthesis without nitrogen and their effect on survival. *Front. Microbiol.* **12**, 794316–794316 (2021).
17. van Tatenhove-Pel, R. J., Zwering, E., Solopova, A., Kuipers, O. P. & Bachmann, H. Ampicillin-treated *Lactococcus lactis* MG1363 populations contain persisters as well as viable but non-culturable cells. *Sci. Rep.* **9**, 1–10 (2019).
18. Biselli, E., Schink, S. J. & Gerland, U. Slower growth of *Escherichia coli* leads to longer survival in carbon starvation due to a decrease in the maintenance rate. *Mol. Syst. Biol.* **16**, e9478 (2020).
19. Berkvens, A., Chauhan, P. & Bruggeman, F. J. Integrative biology of persister cell formation: molecular circuitry, phenotypic diversification and fitness effects. *J. R. Soc. Interface* **19**, 20220129 (2022).
20. Molenaar, D., Van Berlo, R., De Ridder, D. & Teusink, B. Shifts in growth strategies reflect tradeoffs in cellular economics. *Mol. Syst. Biol.* **5**, 323 (2009).
21. Bosdriesz, E., Molenaar, D., Teusink, B. & Bruggeman, F. J. How fast-growing bacteria robustly tune their ribosome concentration to approximate growth-rate maximization. *FEBS J.* **282**, 2029–2044 (2015).
22. Xia, J. *et al.* Proteome allocations change linearly with the specific growth rate of *Saccharomyces cerevisiae* under glucose limitation. *Nat. Commun. 2022 131* **13**, 1–12 (2022).
23. Jahn, M. *et al.* Growth of Cyanobacteria is constrained by the abundance of light and carbon assimilation proteins. *Cell Rep.* **25**, 478-486 (2018).
24. Scott, M., Gunderson, C. W., Mateescu, E. M., Zhang, Z. & Hwa, T. Interdependence of cell growth and gene expression: origins and consequences. *Science.* **330**, 1099–1102 (2010).
25. Shore, D. & Albert, B. Ribosome biogenesis and the cellular energy economy. *Curr. Biol.* **32**, R611–R617 (2022).
26. Harris, L. K. & Theriot, J. A. Surface area to volume ratio: a natural variable for bacterial morphogenesis. *Trends Microbiol.* **26**, 815–832 (2018).
27. Chen, Y. *et al.* Proteome constraints reveal targets for improving microbial fitness in nutrient-rich environments. *Mol. Syst. Biol.* **17**, e10093 (2021).
28. Bachmann, H. *et al.* Availability of public goods shapes the evolution of competing metabolic strategies. *Proc. Natl. Acad. Sci. U. S. A.* **110**, 14302–14307 (2013).
29. Prossliner, T., Skovbo Winther, K., Sørensen, M. A. & Gerdes, K. Ribosome hibernation. *Annu. Rev.Genet.* **52**, 321–348 (2015).
30. Puri, P. *et al. Lactococcus lactis* YfiA is necessary and sufficient for ribosome dimerization. *Mol. Microbiol.* **91**, 394–407 (2014).
31. Frees, D., Savijoki, K., Varmanen, P. & Ingmer, H. Clp ATPases and ClpP proteolytic complexes regulate vital biological processes in low GC, Gram-positive bacteria. *Molecular Microbiology* vol. 63 1285–1295 (2007).
32. Ercan, O., Wels, M., Smid, E. J. & Kleerebezem, M. Molecular and metabolic

adaptations of *Lactococcus lactis* at near-zero growth rates. *Appl. Environ. Microbiol.* **81**, 320–331 (2015).

33. van Mastrigt, O., Abee, T., Lillevang, S. K. & Smid, E. J. Quantitative physiology and aroma formation of a dairy *Lactococcus lactis* at near-zero growth rates. *Food Microbiol.* **73**, 216–226 (2018).
34. Flahaut, N. A. L. *et al.* Genome-scale metabolic model for *Lactococcus lactis* MG1363 and its application to the analysis of flavor formation. *Appl. Microbiol. Biotechnol.* **97**, 8729–8739 (2013).
35. Jensen, P. R. & Hammer, K. Minimal requirements for exponential growth of *Lactococcus lactis*. *Appl. Environ. Microbiol.* **59**, 4363-4366 (1993).
36. Smit, B. A. *et al.* Chemical conversion of α-keto acids in relation to flavor formation in fermented foods. *J. Agric. Food Chem.* **52**, 1263–1268 (2004).
37. Díaz-Pérez, A. L., Díaz-Pérez, C. & Campos-García, J. Bacterial l-leucine catabolism as a source of secondary metabolites. *Rev. Environ. Sci. Bio/Technology 2015 151* **15**, 1–29 (2015).
38. Alonso-Sáez, L., Galand, P. E., Casamayor, E. O., Pedrós-Alió, C. & Bertilsson, S. High bicarbonate assimilation in the dark by Arctic bacteria. *ISME J.* **4**, 1581–1590 (2010).
39. Beck, H. C., Hansen, A. M. & Lauritsen, F. R. Catabolism of leucine to branched-chain fatty acids in *Staphylococcus xylosus*. *J. Appl. Microbiol.* **96**, 1185–1193 (2004).
40. Dherbécourt, J., Maillard, M. B., Catheline, D. & Thierry, A. Production of branched-chain aroma compounds by *Propionibacterium freudenreichii*: links with the biosynthesis of membrane fatty acids. *J. Appl. Microbiol.* **105**, 977–985 (2008).
41. Ganesan, B., Stuart, M. R. & Weimer, B. C. Carbohydrate starvation causes a metabolically active but nonculturable state in *Lactococcus lactis*. *Appl. Environ. Microbiol.* **73**, 2498–2512 (2007).
42. Ganesan, B., Dobrowolski, P. & Weimer, B. C. Identification of the leucine-to-2-methylbutyric acid catabolic pathway of *Lactococcus lactis*. *Appl. Environ. Microbiol.* **72**, 4264-4273 (2006).
43. Serrazanetti, D. I. *et al.* Acid stress-mediated metabolic shift in *Lactobacillus sanfranciscensis* LSCE1. *Appl. Environ. Microbiol.* **77**, 2656-2666 (2011).
44. Doucette, C. D., Schwab, D. J., Wingreen, N. S. & Rabinowitz, J. D. A-ketoglutarate coordinates carbon and nitrogen utilization via enzyme I inhibition. *Nat. Chem. Biol.* **7**, 894–901 (2011).
45. Houot, L., Chang, S., Pickering, B. S., Absalon, C. & Watnick, P. I. The phosphoenolpyruvate phosphotransferase system regulates *Vibrio cholerae* biofilm formation through multiple independent pathways. *J. Bacteriol.* **192**, 3055–3067 (2010).
46. Lahtvee, P. J. *et al.* Multi-omics approach to study the growth efficiency and amino acid metabolism in *Lactococcus lactis* at various specific growth rates. *Microb. Cell Fact.* **10**, 1–12 (2011).
47. Garrigues, C., Mercade, M., Cocaign-Bousquet, M., Lindley, N. D. & Loubiere, P. Regulation of pyruvate metabolism in *Lactococcus lactis* depends on the imbalance between catabolism and anabolism. *Biotechnol. Bioeng.* **74**, 108–115

(2001).

48. Abbe, K., Takahashi, S. & Yamada, T. Involvement of oxygen-sensitive pyruvate formate-lyase in mixed-acid fermentation by *Streptococcus mutans* under strictly anaerobic conditions. *J. Bacteriol.* **152**, 175–182 (1982).

49. Liu, M., Nauta, A., Francke, C. & Siezen, R. J. Comparative genomics of enzymes in flavor-forming pathways from amino acids in lactic acid bacteria. *Appl. Environ. Microbiol.* **74**, 4590-4600 (2008).

50. Wolfe, B. E., Button, J. E., Santarelli, M. & Dutton, R. J. Cheese rind communities provide tractable systems for *in situ* and *in vitro* studies of microbial diversity. *Cell* **158**, 422–433 (2014).

51. Bonham, K. S., Wolfe, B. E. & Dutton, R. J. Extensive horizontal gene transfer in cheese-associated bacteria. *Elife* **6**, (2017).

52. Melo, J., Andrew, P. W. & Faleiro, M. L. *Listeria monocytogenes* in cheese and the dairy environment remains a food safety challenge: the role of stress responses. *Food Res. Int.* **67**, 75–90 (2015).

53. Dunkel, A. *et al.* Nature's chemical signatures in human olfaction: a foodborne perspective for future biotechnology. *Angew. Chemie Int. Ed.* **53**, 7124–7143 (2014).

54. Zaki, O. K. *et al.* Genotype–phenotype correlation in patients with isovaleric acidaemia: comparative structural modelling and computational analysis of novel variants. *Hum. Mol. Genet.* **26**, 3105–3115 (2017).

55. Roberts, T. & Roiser, J. P. In the nose of the beholder: Are olfactory influences on human mate choice driven by variation in immune system genes or sex hormone levels? *Exp. Biol. Med. (Maywood).* **235**, 1277–1281 (2010).

56. Havlíček, J., Winternitz, J. & Craig Roberts, S. Major histocompatibility complex-associated odour preferences and human mate choice: near and far horizons. *Philos. Trans. R. Soc. Lond. B. Biol. Sci.* **375**, 20190260 (2020).

57. Richard, F. J. Symbiotic bacteria influence the odor and mating preference of their hosts. *Front. Ecol. Evol.* **5**, 143 (2017).

58. Tong, T., Wang, Y., Kang, S. G. & Huang, K. Ectopic odorant receptor responding to flavor compounds: versatile roles in health and disease. *Pharm.* **13**, 1314 (2021).

59. Ljunggren, J. *et al.* Yeast volatomes differentially affect larval feeding in an insect herbivore. *Appl. Environ. Microbiol.* **85**, e01761-19 (2019).

60. Madden, A. A. *et al.* The ecology of insect–yeast relationships and its relevance to human industry. *Proc. R. Soc. B Biol. Sci.* **285**, 20172733 (2018).

61. Becher, P. G. *et al.* Chemical signaling and insect attraction is a conserved trait in yeasts. *Ecol. Evol.* **8**, 2962–2974 (2018).

62. Christiaens, J. F. *et al.* The fungal aroma gene *ATF1* promotes dispersal of yeast cells through insect vectors. *Cell Rep.* **9**, 425–432 (2014).

63. Knols, B. G. J. & De Jong, R. Limburger cheese as an attractant for the malaria mosquito *Anopheles gambiae s.s*. *Parasitol. Today* **12**, 159–161 (1996).

64. Shirasu, M. *et al.* Chemical identity of a rotting animal-like odor emitted from the inflorescence of the titan arum (*Amorphophallus titanum*). *Biosci. Biotechnol. Biochem.* **74**, 2550–2554 (2010).


2

Chapter 2

Growth, Dormancy, and Lysis: The Complex Relation of Starter Culture Physiology and Cheese Flavour Formation

Nugroho, A. D. W., Kleerebezem, M. & Bachmann, H.

This chapter has been published:
Curr. Opin. Food Sci. **39**, 22-30 (2021)

Abstract

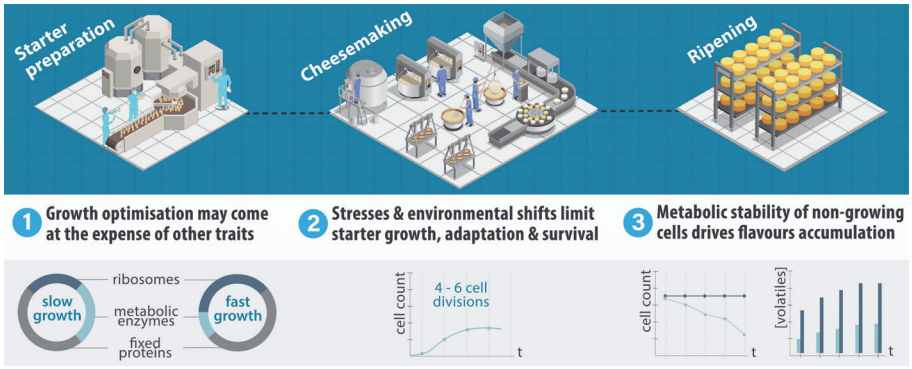

Fast acidification and growth are desired from lactic acid bacteria starter cultures during food fermentation to minimise the risk of spoilage and process failure. In addition, starter cultures play a predominant role in the formation of flavour volatiles. Recent studies in different microbial species have shown that high growth rates come at the expense of the expression level of metabolic enzymes and/or stress proteins. In starter cultures, such a trade-off would affect flavour formation, which depends on the level of flavour-forming enzymes and the prolonged survival of cells. Moreover, starter culture performance during cheese ripening could also be influenced by its cultivation history due to the low number of divisions during cheese manufacturing and limited proteome adjustment during ripening. These findings indicate that changes in (pre)culture conditions can modulate proteome allocation and metabolic stability in starter cultures and thereby provide novel approaches to steer flavour formation.

2.1 Introduction

Dairy fermentation is a dynamic process that encompasses adverse and fluctuating conditions for the fermenting organisms. During cheese manufacturing, environmental parameters such as temperature, pH, osmolarity and lactose concentration change significantly, and they can be stressful to starter bacteria (Figure 2.1). Rapid environmental shifts impose limitations to cell growth and adaptation. In a typical Gouda or Cheddar type cheese, starter cultures only divide up to 6 times[1,2] before entering a non-growing state that is accompanied by environmental changes such as carbon starvation, pH decrease, cold, and salt stress. It is during this ripening period that enzymatic conversion to flavour volatiles through the metabolism of starter cells is most prominent[2,3]. The low number of divisions during the initial cheesemaking combined with limited *de novo* protein synthesis of non-growing cells during ripening suggests that starter culture preparation might influence their functional properties in cheese. This suggestion is based on the notion that upon cell division proteins are divided over daughter cells and these proteins can contribute to cellular behaviour. For example, in *E. coli*, proteins of the *lac*-operon induced by exposure to lactose decreased over 10 generations after cells were transitioned to glucose, but its presence was sufficient to minimise growth delay in the subsequent lactose transition[4]. It is conceivable that similar mechanisms could lead to a cell "memory" that is determined during starter preparation and that would influence starter functionality in a product, but to date these are largely unexplored for food fermentations.

Furthermore, during starter culture selection, specific traits such as biomass yield, acidification rate, stress resistance, or production of specific metabolites are often analysed using standard environmental conditions that do not resemble "in product" conditions. While these selection criteria are potentially relevant for starter performance in the application, disparate performance might be observed during the application due to environmental differences. For example, in the propagation of dairy *L. lactis* strains, haem

supplementation has been shown to significantly alter cellular robustness during freezing and freeze-drying[5] while galactose co-supplementation induces *lacS* expression and shortens lag phase in lactose-grown cultures[6]. During cheesemaking, strains prepared under different preculture conditions might therefore vary in their survival, e.g., after curd scalding, possibly resulting in altered flavour formation during the subsequent ripening process[7,8]. In lactococci, retentostat experiments have also shown that aroma formation during cheese ripening is best resembled by bacteria at near-zero growth rates[9,10]. This suggests that long-term cell integrity is of importance to flavour formation, but this is often overshadowed by the argument that lysis and release of cytoplasmic enzymes into the cheese matrix is an important part of cheese ripening[11].

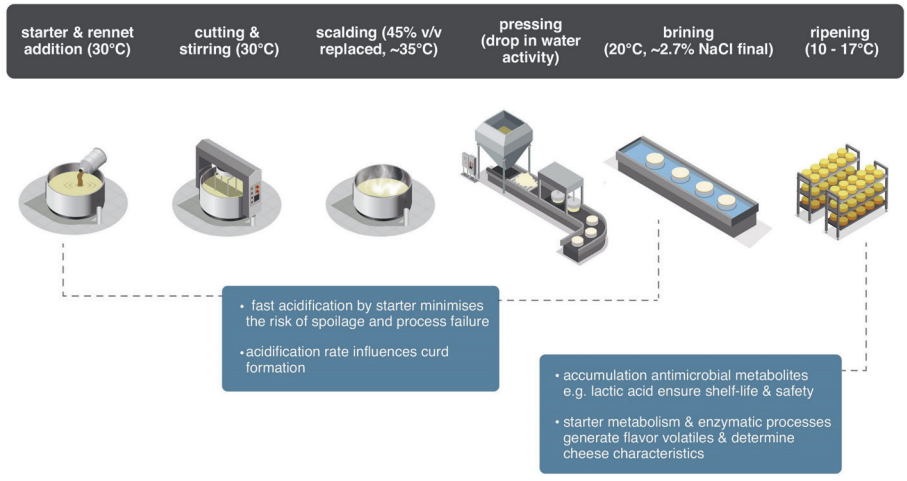

Figure 2.1 *Schematic representation of Gouda-type cheese production including the changes in conditions that starter cultures are exposed to.*

In the ideal situation, one might desire a strain that is optimised for all situations and functions throughout fermentation. However, the optimisation of a trait often comes at the expense of another due to biological and physical constraints, which dictates the allocation of a cell's resources[12]. To some extent, these trade-offs may be explained from a protein economy perspective, where nutrient and energy resource allocation in cells is constrained by their

proteome synthesis and adjustment[13]. However, our fundamental and detailed understanding of mechanisms that govern the interplay of microbial growth and metabolism remains limited, especially in the context of microbes participating in food production processes[14].

This review summarises important conceptual advances in our understanding of the effect of various growth modulations on the stress tolerance and metabolic capacities of bacteria. While growth optimisation of a bacterial population gives more offspring and leads to predomination in natural habitats, it does not guarantee optimised starter functionality. We will highlight how the functionality of lactic acid bacteria (LAB) starter cultures might be affected through culturing & fermentation conditions, especially during the non-growing phase, e.g., throughout the ripening of cheese. A better understanding of the constraints that shape trade-offs in industrially relevant traits will open new avenues to modify process conditions and to steer functionalities of starter cultures. Such adjustments can influence application performance and product properties through modulation of a variety of traits, including lag-time, flavour formation and processing robustness.

2.2 Growth rate optimisation and the evidence of trade-offs

Fast microbial growth is often desired since it enables shorter test and trial time in research and development, as well as the higher production rate and cost-efficiency of manufacture[15]. In the dairy industry (Figure 2.1), high acidification rate as a result of fast growth is considered an important physiological trait of starter LAB, based on the important role of acidification rate in determining texture properties of fermented milk[16,17] and the effective prevention of growth of undesired spoilage bacteria. The rapid accumulation and high concentrations of metabolic end-products like lactic acid and acetic acid ensures a long shelf-life and safety of the products[18]. Consequently, research has aimed to select and investigate specific strains that display naturally high growth rates in standard production conditions. For example, studies in *Streptococcus thermophilus* have focused on understanding the

genomic requirements for fast acidification[19] and investigating the role of specific enzymes such as protease[20] and urease[21]. Nonetheless, we are not aware of comprehensive reports on the consequences of culture optimisation towards rapid growth and acidification affecting other relevant metabolic traits such as flavour formation.

In contrast, Systems Biology approaches in model microorganisms have defined quantitative links and interactions between growth rate and physiological subsystems using coarse-grain analysis[22] of global proteome data. Studies in *E. coli* have underpinned the robust relation between growth rate and the relative abundance of the protein synthesis machinery (i.e., ribosomal fraction)[23]. By varying carbon and energy source, increasing growth rates were found to coincide with increasing relative abundance of the ribosomal proteins within the overall cytoplasmic proteome. Importantly, increased proteome allocation toward ribosomes also coincided with decreased proteome allocation towards metabolic proteins[24]. This trade-off could be constrained by the total cytoplasmic proteome 'size' and global regulatory processes that govern proteome adjustment to support maximal growth rate under a specific condition (Figure 2.2). Although not explicitly addressed in these studies, growth-rate mediated modulation of the abundances of enzymes relevant for biotechnological processes is plausible, since these enzymes are part of the metabolic-protein fraction.

Similar results were also obtained in yeasts under steady-state growth conditions limited by carbon, nitrogen, phosphorus, and sulphur. A linear correlation was found between growth rate and the expression level of more than one quarter of all yeast genes (1470 out of 5537 imputed genes) independent of the limiting nutrient[25]**.** In a similar study[26], 493 protein coding genes were upregulated, and 398 protein-coding genes were downregulated with increasing growth rate. Positively correlated genes mainly corresponded to the production of growth-related functions, e.g., protein translation, macromolecules synthesis and organelle production, whereas negatively

correlated genes were enriched in stress-related functions[25,26]. Taken together, contemporary 'omics studies in *E. coli* and yeasts suggest that optimisation towards fast growth may reduce desired metabolic capacity as well as stress robustness. Arguably, the constant environmental parameters of chemostats, where most of the evidence was obtained, may select for proliferation rather than protection and robustness. Nonetheless, the relation between growth rate and metabolic functions was also observed in bacterial cells grown in batch cultures, albeit at slightly lesser extent[27]. Therefore, these trade-offs associated with growth rate were suggested to apply universally and they are suggested to describe a bacterial growth law[23].

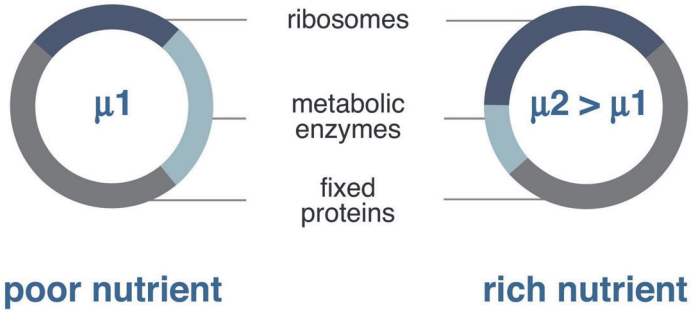

Figure 2.2 *Schematic simplification of bacterial proteome allocation. The cellular proteome can be partitioned into a fixed, metabolic, and ribosome-related fraction. Growth rate (μ) is finely tuned to the fraction of ribosomal and metabolic proteins. Faster growth due to, e.g., a better carbon source in the medium requires more ribosomes to ensure fast synthesis of proteins needed for cell division. Due to a cytoplasmic proteome constraint this is suggested to come at the expense of metabolic enzymes and proteins. Figure adapted from Scott et al[23].*

2.3 Growth rate optimisation and LAB starter functionality

The observed trade-offs in *E. coli* and yeast raise the question whether growth rate influences the performance of dairy starter cultures. Although we are not aware of dedicated investigations in LAB, empirical observations in *L.*

lactis reported that strains with ssp. *lactis* phenotype* generally grow fast but generate less flavours during cheese ripening in comparison to the slower-growing strains that have a ssp. *cremoris* phenotype[28]. Intriguingly, the lower flavour generating properties of the ssp. *lactis* phenotype strains seem to correlate with their ability to utilise alternative ATP sources, like arginine and maltose, but also with their higher temperature and salt tolerance[29]. Hence, a relation between growth rate and starter functionality seems to be apparent when comparing the two *L. lactis* subspecies. While the fast growth of ssp. *lactis* seems to be a consequence the evolutionary history of the strains and the adaptation towards dairy environments[14,29], there is evidence that growth rate modulation within a strain correlates with changes in its metabolic capacity and/or stress resistance. For instance, upon valine or isoleucine starvation, *L. lactis* cultures displayed 3 hours extended lag-phase and an approximate 30% reduced maximum cell density when reaching the stationary phase of growth, while at the same time increasing their formation of flavour compounds by 1.5- to 2.0-fold[30]. However, it cannot be concluded to which extent altered flavour formation can be attributed to differences in growth rate or amino acid availability in this experiment. In a better controlled study, cells cultivated at low dilution rate (D=0.1 /h) showed only 3% of damaged cells after freezing, which is quite different compared to cells cultivated at high dilution rate (D = 0.8 /h) that showed approximately 15% of damaged cells after freezing[5]. Taken together, these observations appear to support that, analogous to the observations in *E. coli* and yeast, the growth rate of lactococci also affects cellular metabolism, physiology and robustness.

On the other hand, the adaptation of lactococci and other LAB to nutrient-rich environments such as milk has led to them being remarkably

* Prior to the phylogenetic reclassification:
Li, T. T., Tian, W. L. & Gu, C. T. Elevation of *Lactococcus lactis* subsp. *cremoris* to the species level as *Lactococcus cremoris* sp. nov. and transfer of *Lactococcus lactis* subsp. *tructae* to *Lactococcus cremoris* as *Lactococcus cremoris* subsp. *tructae* comb. nov. *Int. J. Syst. Evol. Microbiol.* **71**, 004727 (2021).

fastidious and metabolically squandering in comparison to *E. coli*. For example, during growth, glycolysis in *L. cremoris* cells runs close to its maximal capacity and is barely controlled by ATP demand[31], which is in clear contrast to *E. coli*[32]. Moreover, while the interplay of growth rate, glycolytic flux and redox-balance in lactococci has been proposed to control the metabolic shift from homo-lactic (ATP-inefficient) to mixed-acid (ATP-efficient) metabolism[2], the proteome associated with these two metabolic 'states' hardly differs[33], which appears to disagree with the cytoplasmic proteome constraints that are predicted by the proposed bacterial growth law. Alternatively, a scenario where growth rate is primarily restricted by membrane proteome capacity rather than a cytoplasmic proteome capacity may control growth-rate associated metabolic adaptations in lactococci[34,35].

Taken together, evaluating the empirical observations in lactococci and some other LAB in the light of the robust scientific evidence available for *E. coli*, it is tempting to speculate that similar proteome-constraint dependent trade-offs are applicable in these species. However, some of the observations in lactococci appears to contradict such similarity, and it is important to realise that there are major differences between *E. coli* (Gram-negative proteobacteria) and lactococci (Gram positive low G+C-content Firmicutes). It remains to be seen whether similar trade-offs are applicable in these bacteria. Notably, unravelling of the constraints that are applicable under various environmental conditions in lactococci and other LAB is a requirement to further understand the relations between growth rate and physiological or metabolic adaptations, and to subsequently employ such knowledge for the optimisation of starter culture preparations.

2.4 Cellular adaptation to (stationary) non-growing state

In various fermentation processes, starter cultures enter a non-growing state during ripening or product maturation where viability and metabolic activity are maintained for a prolonged period. The environmental causes for growth cessation include nutrient starvation, environmental

stresses, and the presence of inhibitory compounds such as organic acids[36]. In applications such as cheese ripening by LAB[37], wine fermentation by yeasts[38], or sausage ripening by staphylococci[39,40], the metabolism of non-growing cells is desired for metabolite production[3] as well as safety, e.g., through the conversion of biogenic amines[40] or the depletion of nutrients. The metabolic activity of non-growing cells is also important in biotechnology applications since metabolic resources allocated to growth can be diverted to the production of desired metabolites[41] and allows its continuous production, e.g., by cell immobilisation[42], retentostat[43] or partial cell recycling chemostat cultivation[44]. While there is little quantitative data available for the length of time that enzymatic conversions can proceed during ripening of fermented products, it was shown that lactococci stored in a sugar-depleted buffered medium for over 3.5 years was still able to catabolise amino acids[45]. Recently, a novel method was described that allows to follow metabolic activity continuously in translationally-blocked/non-growing cells for weeks to months, offering new approaches to study metabolism, enzyme decay and functional properties in non-growing cells to mimic the roles of starter culture cells during ripening[46]

As cells enter a non-growing state, various metabolic changes occur to aid in cell survival under non-optimal conditions. In the case of carbon exhaustion, lactococci gradually lose its ability to grow on solid media within weeks, but remarkably maintained intact cell membrane and metabolic ability for over 3.5 years[45]. Under such starvation, cell response might vary between species, but stringent responses are generally observed. Overall, transcription and translational machineries, DNA replication, and cell division are strongly repressed[47]. At the same time, general stress resistance including heat, acid, and oxidative stress are significantly induced[47,48], while autolytic genes are significantly repressed[45]. Cells consequently redirect their catabolic activity from the exhausted carbohydrate by upregulating the activity of alternative pathways that can provide ATP[49], which may include other carbon or nitrogen sources. These are indicated by the alleviation of repression by central transcriptional regulators such as the catabolite repression protein CcpA and

the global nitrogen metabolism regulating protein CodY, which together affect roughly 200 genes in lactococci[47,50,51]. Interestingly, amino acids such as arginine[51,52], branched-chain amino acids[45], and citrate[53] are commonly found to be the alternative source of ATP generation under carbohydrate starvation[50]. Their catabolic pathways are directly responsible for the production of potent flavour volatiles in (dairy) fermentation[3]. Hence, the flavour forming capacity of LAB seem to be highly dependent on the adaptation toward nutrient starvation and its corresponding non-growing state.

2.5 Metabolic stability of non-growing LAB during cheese ripening

A number of studies assessed the transcriptional response of lactococci during cheese ripening[54–56]. Lactococci typically reach stationary phase of growth within 24 hours after milk inoculation, which is accompanied by the downregulation of ribosomal protein levels[55]. While the total residual lactose concentrations vary in different cheese types[57], the limited diffusion and exhaustion of lactose in a cell's proximity is described to induce a carbon starvation response[55]. General stress responses, including increased expression of acidic and oxidative stress proteins, are induced at the early stage of cheese ripening and support long term cell survival[55]. Although starter culture colony forming unit recovery declines quite drastically during cheese ripening, e.g., 20-fold in 28 days[1], cell membranes of these non-growing starter cultures are reported to remain mostly intact for extended periods[37,58], despite a higher level of observed permeability[59,60]. These apparently intact but non-growing/ dormant cells[2,37] are probably of key-importance for the flavour volatiles that keep accumulating throughout a year of ripening, particularly those derived from amino acids[61].

It is remarkable that the production of volatiles as a result of cell metabolism can be observed for prolonged periods in non-growing cells because proteins are considered to be notoriously instable and at constant risk of misfolding, damage, and aggregation[62]. However, intracellular macromolecular crowding is suggested to prolong enzyme functionality and

stability by interactions between proteins[63] that can even contribute to renaturation of partially misfolded proteins. In contrast to the observed stability of amino acid conversion in intact cells for up to years[45], *in vitro* activity of enzymes typically declines dramatically within a few hours of conversion at maximum rate. In intact cells, protein integrity is ensured by chaperons[64] as well as the recycling of denatured and damaged proteins after active degradation through, e.g., Clp proteins[65]. These mechanisms that minimise enzyme decay is not only crucial for general survival and adaptability[66] but also potentially for prolonged metabolic conversion.

Taken together, we hypothesize the proteome changes, turnover, and repair and renaturation processes in starter cultures are important for their functionality throughout cheese manufacturing and ripening. However, little is known about the protein dynamics under these conditions. This lack of investigation is likely due to technical challenges of working in food matrices. Due to the instability of mRNA, transcriptome data does not reflect the actual level of enzymes well[67] especially after prolonged incubation where translation is hampered by energy and resource deprivation. The combination of the very few generations made in cheese with the limited protein turnover during non-growing cheese ripening raises the question whether at least part of the cellular functionality established during starter preparation is retained throughout ripening. In the absence of active protein degradation, growth of 4-6 cellular divisions during cheese production implies that the initial starter culture proteome may still constitute 1.5-12.5% of the cellular proteome during ripening[1]. This suggests that proteins that are expressed at a low level during starter preparation might disappear or get reduced to a level that has no impact on a functional property. On the other hand, highly expressed proteins may still be present in a small but adequate amount to influence metabolite formation over the extended period of ripening time. Understanding whether such a lasting impact of biological response exists and if it has functional consequences is relevant for the optimisation of starter cultures through altering preculture conditions.

2.6 Flavour formation and the role of cell lysis during cheese ripening

In cheese and other fermented foods, volatile formation is most prominent during the ripening or maturation stage. The use of processes or strains that result in cell lysis during cheese ripening has been widely investigated in the last few decades and considered as an important factor[8,68,69]. The underlying reasoning is that cell lysis leads to the release of intracellular enzymes into the food matrix and consequently enhance macromolecule degradation, e.g., proteins[8,70] and fats[69]. Their degradation products subsequently become the precursors for the following cascade of reactions that lead to flavour volatiles. For example, the formation of key-volatiles in cheese such as 3-methylbutanal, phenylacetaldehyde, and methanethiol is derived from amino acid conversions[3,71]. Therefore, it is believed that enhanced lysis leads to increased flavour formation. However, we consider that the evidence available for a direct and quantitative relation between cell lysis and specific production of flavour compounds remains unconvincing. The main reason for our doubts arises from the fact that many of the conversions required to achieve volatile formation depend on complete pathways involving multiple cofactor-dependent enzymes (Figure 2.3). Without the efficient cofactor regeneration that can occur within an intact cell, these reactions are not likely to be sustained and thus would rapidly decline in extracts of lysed cell that are released in the cheese matrix. Moreover, compared to freely dispersed enzymes, intracellular enzyme activity could persist much longer due to renaturation and chaperone-mediated enzyme maintenance and repair[72].

Nevertheless, enhanced lysis was shown to consistently correlate with increased abundance of peptides and amino acids[8,68,70,73] and fatty acids in the cheese matrix[69] and has also been reported to enhance removal of bitter-peptides[68,70,73]. However, the relation to product-flavour was mostly demonstrated by descriptive sensory studies[73], without actual measurement of volatile compounds using GC-MS analysis or similar approaches. In addition, these *in situ* lysis studies compared different bacterial strains with highly different flavour forming phenotypes[69,70] or mixtures of different starter

strains[68,73] with highly variable genomic content and physiological characteristics[29]. These variations, disallow generic conclusions about flavour formation resulting from increased cell-lysis rather than from confounding factors such as metabolic diversity of genotypically distinct strains[69,70], microbial interactions in mixed starters[68,73] and/or distinct physico-chemical characteristics, e.g., pH or protein degradation, resulting from differences in acidification rates or proteolytic activity[70,73]. Despite our doubts concerning the importance of cell-lysis in flavour volatile formation during ripening, there may be a prominent role of subpopulation lysis especially in mixed-culture starters. In such mixed starter cultures, the lysis of one of the community members may contribute to milk-protein degradation and increased peptide and amino acid availability for other members of the starter culture that remained intact and effectively convert these compounds to their flavour volatile derivatives. However, to the best of our knowledge such cross-feeding interactions or syntrophic chains that lead to flavour compound production have not been reported to date[68,73].

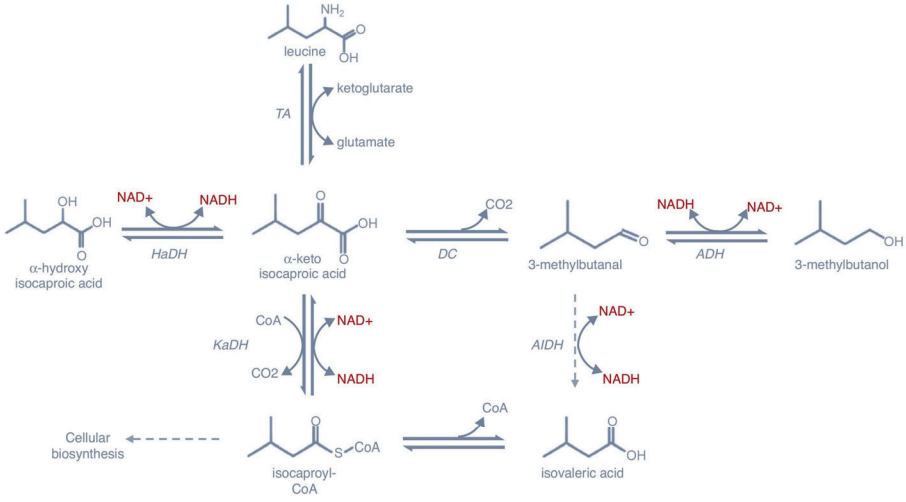

Figure 2.3 *Metabolic pathway of leucine degradation to important volatile compounds, e.g., 3-methybutanal, 3-methylbutanol, and isovaleric acid. Reactions that rely on NAD+ and NADH are highlighted in red. TA = transaminase, HaDH = hydroxy acid dehydrogenase, DC = keto acid decarboxylase, ADH = alcohol dehydrogenase, AlDH = aldehyde dehydrogenase and KaDH = keto acid dehydrogenase. Adapted from Smit et al[71].*

In conclusion, at present, the evidence favouring a prominent role of cell lysis in flavour volatile formation during cheese ripening appears circumstantial, and more importantly, the majority of key-volatiles that determine cheese flavour can only be formed through an intact multi-enzyme pathway that in our opinion depends on cellular integrity. It is likely that volatile formation relies on the interplay and the balance between lysed, intact non-growing, as well as (slow-) growing cells throughout cheese ripening.

2.7 Modulation of prolonged biocatalysis processes

For semi-hard cheeses, the ripening step can take place from 4 weeks to >1 year at controlled temperature <20°C. This process is relatively slow and expensive, and thus ways to modulate (i.e., accelerate) ripening is of economic interest. Current technologies to accelerate volatile formation include elevated temperature, high pressure, as well as the addition of exogenous enzymes[74]. Such technological development mostly focuses on the quality[75–77] and safety aspect of cheese rather than on the biological understanding of starter culture's behaviour, which remains largely unexplored even in the standard conditions. Recent publications have trended to study the expression of genes important for flavour development and adaptation towards ripening conditions by employing techniques such as RT-qPCR[78,79], RNA-seq[55] and metatranscriptomics[80,81]. However, the eventual accumulation of flavour volatiles produced by non-growing starter cells heavily relies on the actual catalytic activity rate of the enzymes present in a cell, which is typically not the subject of such studies. A remaining key-question is related to the mechanisms that underlie such long-term activity and its maintenance, and whether it is possible to modulate and steer these mechanisms to control the kinetics and persistence of *in situ* flavour formation. The aforementioned method that allows the determination of long-term measurement of metabolic activities in non-growing bacterial cells[46] can provide information about the stability of

product formation, which has been reported to vary between (pre)culture conditions and strains[7,45,46,82].

2.8 Summary

Resource allocation theory suggests that growth modulation, e.g., during starter preparation might result in starter cells with altered level of metabolic enzymes. Due to limited divisions in cheesemaking, the impact of cultivation history during starter preparation might eventually influence cheese manufacturing since small differences in proteome composition can have significant functional consequences in a non-growing state. We think that the cell's ability to maintain membrane integrity and retain metabolic activity is important for the accumulation of flavour volatiles, and that this is predominantly dictated by (the lack of) time-dependent decay of enzymatic conversions. The postulated importance of culture history for *in situ* starter functionality raises the question whether biomass-, growth-rate-, and acidification-rate- optimised starter culture production regiments could have trade-offs for the downstream starter functionality. Alternatively, adjusting starter production regiments to optimise for cellular robustness and flavour pathway expression could lead to starter cultures with improved functional properties during application in cheese production (and ripening).

References

1. Bachmann, H., Kruijswijk, Z., Molenaar, D., Kleerebezem, M. & van Hylckama Vlieg, J. E. T. A high-throughput cheese manufacturing model for effective cheese starter culture screening. *J. Dairy Sci.* **92**, 5868–5882 (2009).
2. Kleerebezem, M. *et al.* Lifestyle, metabolism and environmental adaptation in *Lactococcus lactis*. *FEMS Microbiol. Rev.* **44**, 804-820 (2020).
3. Smid, E. J. & Kleerebezem, M. Production of aroma compounds in lactic fermentations. *Annu. Rev. Food Sci. Technol.* **5**, 313–326 (2014).
4. Lambert, G. & Kussel, E. Memory and fitness optimization of bacteria under fluctuating environments. *PLoS Genet.* **10**, e1004556 (2014).
5. Johanson, A., Goel, A., Olsson, L., Franzén, C. J. & Dudley, E. G. Respiratory physiology of *Lactococcus lactis* in chemostat cultures and its effect on cellular robustness in frozen and freeze-dried starter cultures. *Appl. Environ. Microbiol.*

74, 6178-6186 (2020).

6. Lorántfy, B. *et al.* Presence of galactose in precultures induces *lacS* and leads to short lag phase in lactose-grown *Lactococcus lactis* cultures. *J. Ind. Microbiol. Biotechnol.* **46**, 33–43 (2019).
7. Settachaimongkon, S. *et al.* Influence of *Lactobacillus plantarum* WCFS1 on post-acidification, metabolite formation and survival of starter bacteria in set-yoghurt. *Food Microbiol.* **59**, 14–22 (2016).
8. Meijer, W., Dobbelaar, C. & Hugenholtz, J. Thermoinducible lysis in *Lactococcus lactis* subsp. *cremoris* SK110: implications for cheese ripening. *Int. Dairy J.* **8**, 275–280 (1998).
9. van Mastrigt, O., Gallegos Tejeda, D., Kristensen, M. N., Abee, T. & Smid, E. J. Aroma formation during cheese ripening is best resembled by *Lactococcus lactis* retentostat cultures. *Microb. Cell Fact.* **17**, 1–8 (2018).
10. van de Bunt, B., Bron, P. A., Sijtsma, L., de Vos, W. M. & Hugenholtz, J. Use of non-growing *Lactococcus lactis* cell suspensions for production of volatile metabolites with direct relevance for flavour formation during dairy fermentations. *Microb. Cell Fact.* **13**, 1-9 (2014).
11. Crow, V. L. *et al.* The role of autolysis of lactic acid bacteria in the ripening of cheese. *Int. Dairy J.* **5**, 855–875 (1995).
12. Bachmann, H., Bruggeman, F. J., Molenaar, D., Branco dos Santos, F. & Teusink, B. Public goods and metabolic strategies. *Curr. Opin. Microbiol.* **31**, 109–115 (2016).
13. Hui, S. *et al.* Quantitative proteomic analysis reveals a simple strategy of global resource allocation in bacteria. *Mol. Syst. Biol.* **11**, 784 (2015).
14. Teusink, B. & Molenaar, D. Systems biology of lactic acid bacteria: for food and thought. *Curr. Opin. Syst. Biol.* **6**, 7–13 (2017).
15. Pei, L. & Schmidt, M. Fast-growing engineered microbes: new concerns for gain-of-function research? *Front. Genet.* **9**, 207 (2018).
16. Aichinger, P. A. *et al.* Fermentation of a skim milk concentrate with *Streptococcus thermophilus* and chymosin: structure, viscoelasticity and syneresis of gels. in *Colloids and Surfaces B: Biointerfaces* vol. 31 243–255 (Elsevier, 2003).
17. Lucey, J. A. Acid coagulation of milk. in *Advanced Dairy Chemistry: Volume 1B: Proteins: Applied Aspects: Fourth Edition* 309–328 (Springer New York, 2016).
18. Adams, M. R. & Hall, C. J. Growth inhibition of food-borne pathogens by lactic and acetic acids and their mixtures. *Int. J. Food Sci. Technol.* **23**, 287–292 (1988).
19. Proust, L. *et al.* Complete genome sequence of the industrial fast-acidifying strain *Streptococcus thermophilus* N4L. *Microbiol. Resour. Announc.* **7**, e01029-18 (2018).
20. Galia, W., Jameh, N., Perrin, C., Genay, M. & Dary-Mourot, A. Acquisition of PrtS in *Streptococcus thermophilus* is not enough in certain strains to achieve rapid milk acidification. *Dairy Sci. Technol.* **96**, 623–636 (2016).
21. Yamauchi, R., Maguin, E., Horiuchi, H., Hosokawa, M. & Sasaki, Y. The critical role of urease in yogurt fermentation with various combinations of *Streptococcus thermophilus* and *Lactobacillus delbrueckii* ssp. *bulgaricus*. *J. Dairy Sci.* **102**,

1033–1043 (2019).

22. Molenaar, D., Van Berlo, R., De Ridder, D. & Teusink, B. Shifts in growth strategies reflect tradeoffs in cellular economics. *Mol. Syst. Biol.* **5**, 323 (2009).
23. Scott, M., Klumpp, S., Mateescu, E. M. & Hwa, T. Emergence of robust growth laws from optimal regulation of ribosome synthesis. *Mol. Syst. Biol.* **10**, 747 (2014).
24. Scott, M., Gunderson, C. W., Mateescu, E. M., Zhang, Z. & Hwa, T. Interdependence of cell growth and gene expression: origins and consequences. *Science.* **330**, 1099–1102 (2010).
25. Brauer, M. J. *et al.* Coordination of growth rate, cell cycle, stress response, and metabolic activity in yeast. *Mol. Biol. Cell* **19**, 352–367 (2008).
26. Castrillo, J. I. *et al.* Growth control of the eukaryote cell: a systems biology study in yeast. *J. Biol.* **6**, 1–25 (2007).
27. Korem Kohanim, Y. *et al.* A bacterial growth law out of steady state. *Cell Rep.* **23**, 2891–2900 (2018).
28. Kim, W. S., Ren, J. & Dunn, N. W. Differentiation of *Lactococcus lactis* subspecies *lactis* and subspecies *cremoris* strains by their adaptive response to stresses. *FEMS Microbiol. Lett.* **171**, 57–65 (1999).
29. Wels, M., Siezen, R., Van Hijum, S., Kelly, W. J. & Bachmann, H. Comparative genome analysis of *Lactococcus lactis* indicates niche adaptation and resolves genotype/phenotype disparity. *Front. Microbiol.* **10**, 4 (2019).
30. Gómez de Cadiñanos, L. P., García-Cayuela, T., Martínez-Cuesta, M. C., Peláez, C. & Requena, T. Expression of amino acid converting enzymes and production of volatile compounds by *Lactococcus lactis* IFPL953. *Int. Dairy J.* **96**, 29–35 (2019).
31. Koebmann, B. J. *et al.* The extent to which ATP demand controls the glycolytic flux depends strongly on the organism and conditions for growth. *Mol. Biol. Rep.* **29**, 41–45 (2002).
32. Koebmann, B. J., Westerhoff, H. V., Snoep, J. L., Nilsson, D. & Jensen, P. R. The glycolytic flux in *Escherichia coli* is controlled by the demand for ATP. *J. Bacteriol.* **184**, 3909–3916 (2002).
33. Goel, A. *et al.* Protein costs do not explain evolution of metabolic strategies and regulation of ribosomal content: Does protein investment explain an anaerobic bacterial Crabtree effect? *Mol. Microbiol.* **97**, 77–92 (2015).
34. Price, C. E. *et al.* Adaption to glucose limitation is modulated by the pleotropic regulator CcpA, independent of selection pressure strength. *BMC Evol. Biol.* **19**, 1-15 (2019).
35. Szenk, M., Dill, K. A. & de Graff, A. M. R. Why do fast-growing bacteria enter overflow metabolism? testing the membrane real estate hypothesis. *Cell Systems* **5**, 95–104 (2017).
36. van Tatenhove-Pel, R. J., Zwering, E., Solopova, A., Kuipers, O. P. & Bachmann, H. Ampicillin-treated *Lactococcus lactis* MG1363 populations contain persisters as well as viable but non-culturable cells. *Sci. Rep.* **9**, 1–10 (2019).
37. Erkus, O. *et al.* Use of propidium monoazide for selective profiling of viable microbial cells during Gouda cheese ripening. *Int. J. Food Microbiol.* **228**, 1-9 (2016).

38. Millet, V. & Lonvaud-Funel, A. The viable but non-culturable state of wine micro-organisms during storage. *Lett. Appl. Microbiol.* **30**, 136–141 (2000).

39. Tjener, K., Stahnke, L. H., Andersen, L. & Martinussen, J. Growth and production of volatiles by *Staphylococcus carnosus* in dry sausages: influence of inoculation level and ripening time. *Meat Sci.* **67**, 447–452 (2004).

40. Bover-Cid, S., Izquierdo-Pulido, M. & Vidal-Carou, M. C. Effect of the interaction between a low tyramine-producing *Lactobacillus* and proteolytic staphylococci on biogenic amine production during ripening and storage of dry sausages. *Int. J. Food Microbiol.* **65**, 113–123 (2001).

41. Sonderegger, M., Schümperli, M. & Sauer, U. Selection of quiescent *Escherichia coli* with high metabolic activity. *Metab. Eng.* **7**, 4–9 (2005).

42. Fidaleo, M. *et al.* A model system for increasing the intensity of whole-cell biocatalysis: Investigation of the rate of oxidation of D-sorbitol to L-sorbose by thin bi-layer latex coatings of non-growing *Gluconobacter oxydans*. *Biotechnol. Bioeng.* **95**, 446–458 (2006).

43. Ercan, O. *et al.* Physiological and transcriptional responses of different industrial microbes at near-zero specific growth rates. *Appl. Environ. Microbiol.* **81**, 5662–5670 (2015).

44. van Mastrigt, O., Egas, R. A., Lillevang, S. K., Abee, T. & Smid, E. J. Application of a partial cell recycling chemostat for continuous production of aroma compounds at near-zero growth rates. *BMC Res. Notes* **12**, 1-6 (2019).

45. Ganesan, B., Stuart, M. R. & Weimer, B. C. Carbohydrate starvation causes a metabolically active but nonculturable state in *Lactococcus lactis*. *Appl. Environ. Microbiol.* **73**, 2498–2512 (2007).

46. Nugroho, A. D. W., Kleerebezem, M. & Bachmann, H. A novel method for long-term analysis of lactic acid and ammonium production in non-growing *Lactococcus lactis* reveals pre-culture and strain dependence. *Front. Bioeng. Biotechnol.* **8**, 580090 (2020).

47. Ercan, O., Wels, M., Smid, E. J. & Kleerebezem, M. Genome-wide transcriptional responses to carbon starvation in non-growing *Lactococcus lactis*. *Appl. Environ. Microbiol.* **81**, 2554–2561 (2015).

48. Ercan, O. *Physiological and Molecular Adaptations of Lactococcus lactis to Near-Zero Growth Conditions*. (Wageningen University and Research, 2014).

49. Redon, E., Loubiere, P. & Cocaign-Bousquet, M. Transcriptome analysis of the progressive adaptation of *Lactococcus lactis* to carbon starvation. *J. Bacteriol.* **187**, 3589–3592 (2005).

50. Guédon, E., Sperandio, B., Pons, N., Ehrlich, S. D. & Renault, P. Overall control of nitrogen metabolism in *Lactococcus lactis* by CodY, and possible models for CodY regulation in Firmicutes. *Microbiology* **151**, 3895–3909 (2005).

51. Zomer, A. L., Buist, G., Larsen, R., Kok, J. & Kuipers, O. P. Time-resolved determination of the CcpA regulon of *Lactococcus lactis* subsp. *cremoris* MG1363. *J. Bacteriol.* **189**, 1366–1381 (2007).

52. Gaudu, P., Lamberet, G., Poncet, S. & Gruss, A. CcpA regulation of aerobic and respiration growth in *Lactococcus lactis*. *Mol. Microbiol.* **50**, 183–192 (2003).

53. van Mastrigt, O., Mager, E. E., Jamin, C., Abee, T. & Smid, E. J. Citrate, low pH and amino acid limitation induce citrate utilization in *Lactococcus lactis* biovar

diacetylactis. *Microb. Biotechnol.* **11**, 369–380 (2018).

54. Bachmann, H., De Wilt, L., Kleerebezem, M. & Van Hylckama Vlieg, J. E. T. Time-resolved genetic responses of *Lactococcus lactis* to a dairy environment. *Environ. Microbiol.* **12**, 1260–1270 (2010).

55. Cretenet, M. *et al.* Dynamic analysis of the *Lactococcus lactis* transcriptome in cheeses made from milk concentrated by ultrafiltration reveals multiple strategies of adaptation to stresses. *Appl. Environ. Microbiol.* **77**, 247–257 (2011).

56. Ulve, V. M. *et al.* RNA extraction from cheese for analysis of *in situ* gene expression of *Lactococcus lactis*. *J. Appl. Microbiol.* **105**, 1327–1333 (2008).

57. Bylund, G. *Dairy Processing Handbook*. (Tetra Pak Processing Systems, 1995).

58. Chapot-Chartier, M. P., Deniel, C., Rousseau, M., Vassal, L. & Gripon, J. C. Autolysis of two strains of *Lactococcus lactis* during cheese ripening. *Int. Dairy J.* **4**, 251–269 (1994).

59. Aburjaile, F. F. *et al.* The long-term survival of *Propionibacterium freudenreichii* in a context of nutrient shortage. *J. Appl. Microbiol.* **120**, 432–440 (2016).

60. Bunthof, C. J., Van Schalkwijk, S., Meijer, W., Abee, T. & Hugenholtz, J. Fluorescent method for monitoring cheese starter permeabilization and lysis. *Appl. Environ. Microbiol.* **67**, 4264–4271 (2001).

61. Bergamaschi, M. & Bittante, G. From milk to cheese: Evolution of flavor fingerprint of milk, cream, curd, whey, ricotta, scotta, and ripened cheese obtained during summer Alpine pasture. *J. Dairy Sci.* **101**, 3918–3934 (2018).

62. Mateus, A. *et al.* Thermal proteome profiling in bacteria: probing protein state *in vivo*. *Mol Syst Biol* **14**, e8242 (2018).

63. Sarkar, M., Lu, J. & Pielak, G. J. Protein crowder charge and protein stability. *Biochemistry* **53**, 1601–1606 (2014).

64. Schramm, F. D., Schroeder, K. & Jonas, K. Protein aggregation in bacteria. *FEMS Microbiol. Rev.* **44**, 54–72 (2019).

65. Frees, D., Savijoki, K., Varmanen, P. & Ingmer, H. Clp ATPases and ClpP proteolytic complexes regulate vital biological processes in low GC, Gram-positive bacteria. *Mol, Microbiol*. **63**, 1285–1295 (2007).

66. Lahtvee, P. J., Seiman, A., Arike, L., Adamberg, K. & Vilu, R. Protein turnover forms one of the highest maintenance costs in *Lactococcus lactis*. *Microbiol. (United Kingdom)* **160**, 1501–1512 (2014).

67. Jin, L. *et al.* Integrative analysis of transcriptomic and proteomic profiling in inflammatory bowel disease colon biopsies. *Inflamm. Bowel Dis.* **25**, 1906–1918 (2019).

68. Hannon, J. A. *et al.* Use of autolytic starter systems to accelerate the ripening of Cheddar cheese. *Int. Dairy J.* **13**, 313–323 (2003).

69. Collins, Y. F., McSweeney, P. L. H. & Wilkinson, M. G. Evidence of a relationship between autolysis of starter bacteria and lipolysis in Cheddar cheese during ripening. *J. Dairy Res.* **70**, 105–113 (2003).

70. El Soda, M. *et al.* Autolysis of lactic acid bacteria: impact on flavour development in cheese. *Dev. Food Sci.* **37**, 2205–2223 (1995).

71. Smit, B. A. *et al.* Chemical conversion of α-keto acids in relation to flavor

formation in fermented foods. *J. Agric. Food Chem.* **52**, 1263–1268 (2004).

72. Wolff, S., Weissman, J. S. & Dillin, A. Differential scales of protein quality control. *Cell* **157**, 52–64 (2014).

73. Morgan, S., Ross, R. P. & Hill, C. Increasing starter cell lysis in Cheddar cheese using a bacteriocin-producing adjunct. *J. Dairy Sci.* **80**, 1–10 (1997).

74. Khattab, A. R., Guirguis, H. A., Tawfik, S. M. & Farag, M. A. Cheese ripening: a review on modern technologies towards flavor enhancement, process acceleration and improved quality assessment. *Trends Food Sci. Technol.* **88**, 343–360 (2019).

75. Walsh, E. A., Diako, C., Smith, D. M. & Ross, C. F. Influence of storage time and elevated ripening temperature on the chemical and sensory properties of white Cheddar cheese. *J. Food Sci.* **85**, 268–278 (2020).

76. Giannoglou, M. *et al.* Effect of high pressure treatment applied on starter culture or on semi-ripened cheese in the quality and ripening of cheese in brine. *Innov. Food Sci. Emerg. Technol.* **38**, 312–320 (2016).

77. Ávila, M., Gómez-Torres, N., Delgado, D., Gaya, P. & Garde, S. Application of high pressure processing for controlling *Clostridium tyrobutyricum* and late blowing defect on semi-hard cheese. *Food Microbiol.* **60**, 165–173 (2016).

78. Ruggirello, M. *et al.* Study of *Lactococcus lactis* during advanced ripening stages of model cheeses characterized by GC-MS. *Food Microbiol.* **74**, 132–142 (2018).

79. Ruggirello, M., Cocolin, L. & Dolci, P. Fate of *Lactococcus lactis* starter cultures during late ripening in cheese models. *Food Microbiol.* **59**, 112–118 (2016).

80. Duru, I. C. *et al.* Metagenomic and metatranscriptomic analysis of the microbial community in Swiss-type Maasdam cheese during ripening. *Int. J. Food Microbiol.* **281**, 10–22 (2018).

81. Mataragas, M. Investigation of genomic characteristics and carbohydrates' metabolic activity of *Lactococcus lactis* subsp. *lactis* during ripening of a Swiss-type cheese. *Food Microbiol.* **87**, 103392 (2020).

82. Settachaimongkon, S. *et al.* Effect of sublethal preculturing on the survival of probiotics and metabolite formation in set-yoghurt. *Food Microbiol.* **49**, 104–115 (2015).

Chapter 3

A Novel Method for Long-Term Analysis of Lactic Acid and Ammonium Production in Non-Growing *Lactococcus cremoris* Reveals Preculture and Strain Dependence

Nugroho, A. D. W., Kleerebezem, M. & Bachmann, H.

This chapter has been published:
Front. Bioeng. Biotechnol. **8**, 580090 (2020)

Abstract

In various (industrial) conditions, cells are in a non-growing but metabolically active state in which *de novo* protein synthesis capacity is limited. The production of a metabolite by such non-growing cells is dependent on the cellular condition and enzyme activities such as the amount, stability, and degradation of the enzyme(s). For industrial fermentations in which the metabolites of interest are mainly formed after cells enter the stationary phase, the investigation of prolonged metabolite production is of great importance. However, current batch model systems do not allow prolonged measurements due to metabolite accumulation driving product-inhibition. Here we developed a protocol that allows high-throughput metabolic measurements to be followed in real-time over extended periods (weeks). As a validation model, sugar utilisation and arginine consumption by a low density of translationally-blocked *Lactococcus cremoris* was designed in a defined medium. In this system *L. cremoris* MG1363 was compared with its derivative HB60, a strain described to achieve higher metabolic yield through a shift towards heterofermentative metabolism. The results showed that in a non-growing state HB60 is able to utilise more arginine than MG1363, and for both strains the decay of the measured activities were dependent on preculture conditions. During the first 5 days of monitoring a ~25-fold decrease in acidification rate was found for strain HB60 as compared to a ~20-fold decrease for strain MG1363. Such measurements are relevant for the understanding of microbial metabolism and for optimising applications in which cells are frequently exposed to long-term suboptimal conditions such as microbial cell factories, fermentation ripening, and storage survival.

3.1 Introduction

The widespread use of bacteria in many biotechnological applications is not only attributed to their growth ability but also to their metabolic persistence under non-growing/dormant condition. The arrest of cell division coincides with limited *de novo* protein synthesis, whereas metabolic activity and survival can be maintained over a long period of time[1,2]. This non-growing state can be induced by adverse circumstances, e.g., starvation, lethal stress or inhibitory compounds[3–5], as commonly found in industrial processes such as bioreactor metabolite production[6], wastewater treatment[7], and food processes[8]. In some applications, for example microbial cell factories, such physiological state might be desired since metabolic fluxes are diverted away from cell growth, resulting in the increase of metabolic yield[9]. In food fermentation applications, the long-term metabolic activity is an important function of starter cultures that contributes to product quality, stability and safety[10,11]. Therefore, the study of persisting metabolic activity in non-growing cells is of relevance for food fermentation processes, and the ability to steer the activity of such cells can strongly contribute to process control.

Lactic acid bacteria (LAB) and lactococci, in particular, are important industrial microorganisms and the ability to steer their metabolic activities in non-growing cultures is of great interest. As an example, the majority of flavour volatiles is produced by the starter culture during cheese ripening, where the most relevant ones are derived from nitrogen catabolism such as 3-methylbutanal, 2-methylbutanal and 2-methylpropanal[12]. The combination of cheese production-related environments such as the dynamic processing conditions, low temperatures, high salt concentrations, and carbon starvation results in non-growing but metabolically active starter culture cells. Despite the loss of culturability during cheese ripening, it has been shown that a high level of cellular intactness was retained and only a small fraction of the starter population appeared to exhibit membrane injury[2]. Furthermore, studies on the

metabolite production of lactococci have shown that the cheese-related volatile profile can be mimicked best with near-zero growth conditions achieved by retentostat cultivation[13] or by incubation in nutrient-free buffer[14]. Conversely, the prolonged metabolic activity of non-growing starter cultures can also pose challenges in ensuring product quality during storage. Post-production acidification is an important example of such phenomenon in which slow but persistent lactic acid production in stored yoghurts eventually leads to shorter shelf life due to perceivable changes in flavour and acidity leading to lower consumer appreciation and acceptance[15,16].

Since the renewal of proteins is limited, the role of repair, maintenance and active degradation becomes particularly important. During prolonged incubation of non-growing cells, enzyme decay is inevitable but can be minimised by intracellular mechanisms that ensure protein quality control such as the Clp-related protease machinery[17,18]. Upon carbon starvation, lactococci were shown to lose the ability to be cultured but at the same time they could maintain intact membranes and showed metabolic activity for up to 3.5 years[19]. The overall cell fitness and performance can be greatly affected by the cellular proteome composition that is dependent on the conditions applied during the growing phase[20,21]. Consequently, the initial enzyme amount and the rate of enzyme-activity decay will influence the overall production of metabolites over prolonged periods of incubation. In addition, environmental conditions, such as pH, and temperature, as well as the level of oxidative conditions and inhibitor exposure also affect protein and cellular stability. Collectively, these environmental parameters determine the actual rate and stability of metabolite formation, but they are often determined as separate entities and/or in a simplified *in vitro* system.

In this study, we developed a method that allows us to measure catalytic activity of a complete pathway based on continuous pH monitoring through a fluorescent readout in a 384-well plate format. pH-monitoring is employed as a model since it applies to primary metabolism but also amino

acid catabolism, that both involve a substantial metabolic flux. The system is designed to prevent product inhibition, which is achieved by employing cultures at low cell densities combined with the translation-inhibiting antibiotic erythromycin. Blockage of *de novo* protein synthesis enabled us to compare the impact on acidification and arginine consumption rate of distinct strains and cellular proteome compositions, that were generated through different (pre)culture conditions. The method allowed continuous pH measurements in real-time over periods of several weeks, without the emergence of detectable product inhibition as commonly found in batch systems.

3.2 Materials and methods

3.2.1 Strain and cultivation conditions

Lactococcus cremoris NCDO712[22], HB60[23] and MG1363[24] were grown on chemically defined medium for prolonged cultivation (CDMPC) as described previously[25]. Medium was supplemented with either lactose 30 mM, galactose 55 mM or glucose 55 mM depending on experimental design. All precultures were standardised and started with a single use aliquot of glycerol stock, which was 1,000-fold diluted in medium and cultured overnight (as described in Price et al). Overnight cultures were subcultured (40-fold dilution) in fresh medium and harvested during the early exponential phase (OD_{600} 0.1-0.2). *Lactococcus cremoris* was routinely cultured at 30°C without aeration. The growth rate of *L. cremoris* NCDO712 in CDMPC+0.5% glucose is approximately 0.7 /h, which is a bit slower compared to 0.8 /h reached in the rich medium M17 supplemented with 0.5% glucose.

3.2.2 Prolonged measurements of culture pH

Exponentially growing cells were centrifuged at 5,000 g for 10 minutes and washed twice with an equal volume of PBS, followed by resuspending the cells at a standard density between 1E+07 and 2.5E+07 cells/mL in fresh CDMPC (Mn-omitted) supplemented with erythromycin (5 µg/mL) and 10 µM

5(6)-carboxyfluorescein (Sigma-Aldrich 21877). Individual sugar was supplemented as the sole carbon source in the media depending on experimental design at concentration of 30 mM (lactose) or 55 mM (glucose or galactose). In experiments measuring arginine utilisation, the CDMPC pH was set to 5.5 (rather than 6.5 in standard CDMPC) and instead of one of the sugars, L-arginine was supplemented at a final concentration of 30 mM. All measurements were performed with at least 4 replicates in black clear bottom 384-well plate (Greiner Bio-One 781076). Fluorescence (λex/em: 485/535 nm) was measured at constant gain, at 30-minute intervals during a period of up to 3 weeks at 30°C in a microplate reader (Tecan Safire 2). The gain was determined to ensure standard pH solutions (4.0 – 7.0) were in the detectable range.

3.2.3 Viable count and membrane integrity determination

Measurements of culturable bacteria were performed through plating on CDMPC supplemented with 1% glucose and 0.5% UltraPure agarose (Invitrogen 16500500). Serial dilutions were prepared in PBS and 100 µL of the diluted cultures were plated on agar plates. Plates were incubated at 30°C for 24-48 hours and colonies were enumerated.

Membrane integrity of cells during prolonged incubation was analysed using Live/Dead® BacLight™ Bacterial viability and counting kit (Invitrogen L34856) and a BD LSR Fortessa Flow Cytometry instrument (BD Biosciences), according to manufacturer instructions with some modifications. A staining mixture was prepared with 1.5 µL of PI, 1.5 µL of SYTO 9 stock-solutions, 5 µL microsphere standard (1E+08 beads/mL), 892 µL of running buffer (FACS Flow), and 100 µL of sample resulting in a total of 1 mL assay reaction. Fluorescence signals were measured with FITC and PE-Texas Red detectors. Gating was set on the basis of fresh overnight culture (live) and cells incubated in 60% ethanol (dead).

3.2.4 Fermentation end product analysis

The concentrations of organic acids in media (lactic acid, formic acid, acetic acid, and ethanol) were determined by high performance anion exchange chromatography (HPAEC) with UV and refractive index (RI) detection as previously described[26]. Culture supernatant samples were collected and filtered using 0.20 µm polyethersulfone (PES) membranes and stored at -20°C before analysis.

3.2.5 Calculation of lactic acid or ammonia production rate

Raw data files from the microplate reader were analysed and plotted with R (v 3.6.1). Fluorescent signals were converted to pH values based on a standard curve obtained with fluorophore-containing medium set at a range of pH values. To correct for buffering capacity, the proton equivalent of the pH values was calculated. Subsequently, the acid production was determined based on the logarithmic equation, which relates the accumulation of acid and the change in proton equivalent. This relation was obtained from a titration curve, which was prepared by stepwise addition of lactic acid (2 M) to CDMPC in the presence of 2.5E+07 cells/mL for the extended operational range of the measurement (pH 6.5 to 4.0). In case of arginine consumption, the ammonia production was analogously determined using a titration curve of ammonia from pH 5.5 to 7.0. The production rate (M/h) was calculated periodically in equal intervals of lactate or ammonium production, e.g., every 0.001 M.

3.3 Results

3.3.1 Optimisation of cell density and medium composition allows acidification measurements for weeks without product inhibition in non-growing cells

The glycolytic flux of *Lactococcus cremoris* has been reported to run at maximal rate during balanced growth in batch culture[27]. The high flux through glycolysis and lactic acid production leads to a fast decline in pH and high accumulation of lactate, which eventually stops acidification. In non-growing cells of *L. cremoris*, the glycolytic flux was found to be 37% of exponentially growing cells[28], which is still relatively high. To enable a prolonged measurement of the product formation rate, a number of challenges such as product inhibition, continuous monitoring, sufficient throughput and the maintenance of non-growing state need to be overcome. To achieve this, we established a microplate-based assay in which the pH of non-growing cells can be continuously followed in a microplate reader through the use of commercially-available fluorescent pH indicator (5/6-carboxyfluorescein). The assay consists of a defined medium in which cells are fully translationally-blocked with erythromycin (5 μg/mL) and provided with excess supply of a catabolisable substrate. Under circumstances with, e.g., sugar (1% w/v) as a substrate and high cell densities, e.g., 1E+08 cells/mL, this setup leads to full acidification of the solution within 24-48 hours, when further acidification is blocked by product inhibition. In contrast, in the absence of translation inhibition, the exponential growth of cells and the concomitant increase of glycolytic flux will typically lead to complete acidification within less than 8-12 hours. Therefore, to enable long term acidification online monitoring, we ensured the cell density is kept constant by complete inhibition of protein translation.

Cell concentration in the range of 1-2.5E+07 /mL in 20 mM phosphate buffer resulted in slow but detectable acidification activity that remains in a

high-buffering range. This allowed us to follow measurements for 3 weeks. The results consistently showed that acidification ranged in pH from 6.5 to 5.75 and produced less than 20 mM lactate over the complete period. Considering the pKa of lactate at 3.8, the majority of lactate (~99%) will be in a deprotonated state, which will not readily diffuse across the cell membrane. During the long period of measurement, the fluorescent signal was stable and showed negligible change in signal intensity (Figure 3.1A). The detection accuracy and frequent reading interval (30 minutes) allows real-time and precise monitoring. We opted to use a defined medium as it allows well defined alterations of individual constituents, however it is possible to use undefined medium such as M17, but medium-composition manipulations will be less defined and higher fluorescence background might reduce measurement resolution. Furthermore, the use of assay medium that closely resembles growing medium of the bacteria aims to optimise conditions for all cellular processes. In combination with the use of a microplate (384-wells), the setup allows high-throughput comparisons of prolonged acidification profiles.

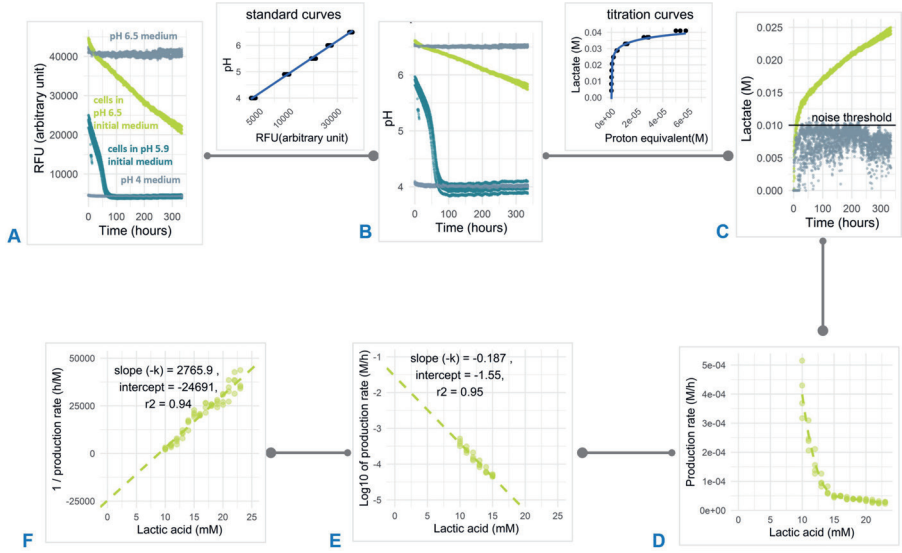

Figure 3.1 *Analysis pipeline of prolonged acidification in non-growing cells.* L. cremoris *NCDO712 cells were precultured in lactose 1%, harvested at mid-exponential growth and transferred to the assay medium with lactose 1%. (A) Fluorescent signal was measured for assay medium without cells at pH 4 and 6.5 (light grey), cells (2.5E+07 /ml) in assay medium at an initial pH of 6.5 (light green) and an initial pH of 5.9 (dark green). (B) Based on a standard curve, the RFU were converted to pH. In samples with a low starting pH (dark green) acidification stopped due to product inhibition at pH 4 while for a high starting pH acidification was still ongoing after more than 300 hours. (C) Based on a titration curve, the pH profile was converted to the amount of lactic acid produced. The noise threshold was determined from the non-biological fluctuation of signal based on a negative control at pH 6.5. (D) The lactate production rate is plotted as a function of the total amount of lactic acid produced. Decline in production could be calculated following first order (E) or second order (F) reaction kinetics. The experiment was carried out 3 times with 4 replicates with reproducible results. Four replicate curves are shown in this plot.*

3.3.2 Conversion of the fluorescent signal to acid production rate

The fluorescent signal in our assay was not directly reflecting organic acid production because of the buffer capacity being higher at the initial (near neutral) pH compared to the buffering capacity towards the end of the fermentation (> pH 5). To get a better representation of lactic acid production, we established an analysis pipeline where the fluorescent signal (Figure 3.1A) is first converted to pH (Figure 3.1B) based on a calibration curve of medium prepared at different pH values (pH was set by hydrochloric acid addition). Subsequently, the pH value is converted to the proton equivalent, which is then used to obtain the equivalent of acid produced (Figure 3.1C). The latter conversion was based on the titration of pure lactic acid to the assay medium in the presence of cells to accommodate the contribution of cells to buffering capacity. Once the acid formation over time was calculated, the rate of formation and its decline could be derived as a function of time. However, large differences in rate could result in unfair comparison due to the difference in total reaction number per enzyme. Therefore, the production rate was calculated within periods of equal production of acid, e.g., 1 mM starting from the period above the noise threshold determined from a negative control (Figure 3.1C). In multiple experiments, the signal considered as noise was consistently found to be the first 7.5-10 mM of lactate produced. This can be seen in the negative control that showed signal noise at 5-10 mM of lactate produced (Figure 3.1C). This sensitivity to noise is possibly due to the high buffering capacity in this pH region, which leads to small signal variation resulting in relatively large noise in lactate production (with a relatively constant signal of approximately 40,000 RFU in the control sample (Figure 3.1A) noise of 1,000-1,500 RFU is responsible for the observed 5-10 mM variation in lactate). The measurements from this initial region were therefore not considered in the data analysis. The decline in lactic acid production rate over time was plotted against lactate accumulation (Figure 3.1D) and typically resulted in a straight-line when transformed to its log-values (Figure 3.1E) or

its inverse (Figure 3.1F), following the first order or second order of rate kinetic, respectively. From this plot, the kinetic of rate decline could be determined from the slope and the maximum/initial production rate was predicted from Y-intercept. Based on these kinetic parameters, the behaviour in longer period of time could be estimated, e.g., lactate yield in 2 months. As an exemplary case, *L. cremoris* NCDO712 (2.5E+07 cells/mL) precultured in lactose was transferred into the assay medium containing the same sugar and followed for 2 weeks. A 15-fold reduction of the lactic acid production rate from 3.98E-04 to 2.51E-05 M/h was observed (Figure 3.1D).

3.3.3 Translational blocking leads to non-culturable cells and has no influence on organic acid profiles

The addition of erythromycin results in the physical blocking of the nascent-peptide exit tunnel in the ribosome, which halts translation[29]. We tested different erythromycin concentrations and found that 5 µg/mL was sufficient to prevent an increase in culture density over 2 weeks, indicating that cell growth was blocked due to continuous translational blocking. Such treatment may cause cell dormancy or induce cell death, which is influenced by not only the kinetics of drug-ribosome interactions, but also species or strains, growth conditions, cell density and the antibiotic concentration[30]. When prolonged translation inhibition is applied, cell death is inevitable and can be responsible to the decline in product formation to some extent. Antibiotic exposure to *Lactococcus cremoris* has also been reported to induce heterogenous population response regarding dormancy states and the corresponding death rates and metabolic activity[31]. To characterise the effects of erythromycin in our experiments, a combination of CFU counting and live-dead staining measurements was employed to determine how cellular viability and integrity relate to the observed decline in acidification. For *L. cremoris* NCDO712 precultured and transitioned to lactose, the amount of colony forming units was decreasing from 7.25 to 5.65 log10 CFU/mL in 11 days

(Figure 3.2A), which is equivalent to roughly a 40-fold overall decline. On the other hand, the number of intact cells according to live-dead stained flow cytometry counts was more or less constant at approximately 7 log cells/mL. Moreover, the fraction of cells classified as intact (live+injured-cells) remained constantly above 75% (Figure 3.2B), displaying a slow progression towards cell populations with compromised membrane-integrity ('injured cells' in the analysis). In the 2-week incubation period, approximately 40% of the cells initially qualified as 'live' cells progressed to the 'injured' population, representing only a 2.5-fold reduction of the 'live' population, which is much less than the observed 40-fold reduction in CFU enumerations. This observation is in agreement with the detection of so-called 'viable but non-culturable' (VBNC) lactococcal cells during 2 weeks of retentostat cultivation[32] and cheese ripening[2]. Overall, the 40-fold decrease in CFU does not match the 15-fold decrease in acidification rate and the results of the live-dead staining. This suggests that VBNC cells appear in the population, but the current methodology does not allow to discern the contribution of different cell populations to the acidification profiles.

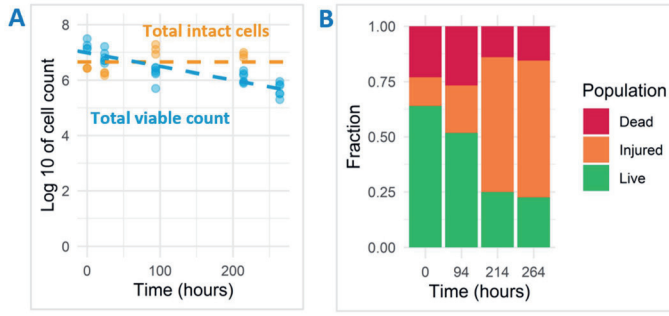

D

Time (h)	Lactate (mM)	Formate (mM)	Acetate (mM)
24	4.21±0.05	0.21±0.09	0.20±0.09
94	9.81±0.06	0.10±0.00	0.26±0.08
214.5	15.79±0.12	0.39±0.11	0.26±0.13
264	17.32±0.08	0.57±0.02	0.29±0.05

Figure 3.2 *Prolonged observation of* L. cremoris *NCDO712 precultured in CDMPC-lactose 1%, harvested at mid-exponential growth and transferred to the assay medium with lactose 1%.* ***(A)*** *Colony forming units and intact cell count as measured by flow-cytometry.* ***(B)*** *The different cell fractions of the life-dead staining as measured by flow-cytometry.* ***(C)*** *Lactate accumulation derived from fluorescent measurements and HPLC determination show good agreement (R-squared value of 0.94) (dashed lines indicate semi-logarithmic fit).* ***(D)*** *The organic acid production profiles as determined by HPLC were dominated by lactic acid throughout the experiment.*

Besides cell viability, we also determined the concentration of organic acids during the prolonged acidification measurements to confirm the fluorescence-based result. While it is known that the strain used produces predominantly lactic acid (>90%) during growth on lactose, low levels of acetic acid production might lead to slight misestimation of the lactic acid production level. The switch to heterofermentative metabolism (acetic and lactic acid formation) is known to occur in conditions with reduced glycolytic flux[33,34] or increased exposure to molecular oxygen and intracellular redox balance[35–37], which could both be apparent during the prolonged assay developed here. Therefore, we investigated whether the induced non-growing state led to

changes in fermentation pathways. Under the experimental conditions used, the cells remained a homofermentative (>90% of carbon flux towards lactic acid) metabolite profile during the 2-week incubation (Figure 3.2D). The final concentrations of lactic acid determined reached almost 20 mM, whereas concentrations of formic and acetic acid did not exceed 1 mM (Figure 3.2D). Moreover, the lactic acid concentrations determined matched accurately (R-squared value of 0.94) with the concentrations estimated based on fluorescence measurements using the lactic acid titration curve (Figure 3.2C).

3.3.4 Sugar and arginine utilisation are strain and preculture dependent

The presented standardised protocol allows for the testing of numerous modulations of environmental parameters as well as the comparison of different strains. To demonstrate this, the developed protocol was used to test the influence of preculture conditions on the long-term acidification activity using different preculture and assay substrates. In addition, the wild-type strain *L. cremoris* MG1363 (plasmid-free derived of NCDO712) and its experimentally evolved derivative HB60[23] were employed to further characterise the phenotype difference of these strains. Expression for carbon source utilisation pathways is governed by carbon catabolite repression to ensure hierarchical utilisation of preferred carbon source. As a consequence of catabolite repression, it was not unexpected to find that mid-exponential *L. cremoris* MG1363 and HB60 precultured in glucose showed no detectable utilisation of galactose when it was provided to translationally-blocked cells in the assay medium (data not shown). Growth on glucose is known to effectively repress the expression of the enzymes of the Leloir pathway that is required to import and utilise galactose as a carbon and energy source. In contrast, galactose-precultured *L. cremoris* could effectively utilise either glucose or galactose during the translationally-blocked assay conditions (Figure 3.3A middle and left). However, the glucose utilisation rate (as measured by lactic

acid formation rate) rapidly declined and halted within 75 hours (Figure 3.3B middle). Interestingly, we observed higher acidification rates in MG1363 than HB60, which is in agreement with previous findings where due to a point-mutation (F65L) in *ptnD*, HB60 displays reduced glucose import activity and consequently a lower glycolytic flux compared to its parental strain[23]. Higher acidification rates were also observed for galactose-precultured MG1363 in the prolonged assay in comparison to galactose-precultured HB60, irrespective of the carbon source provided during the assay (glucose or galactose). Notably, the acidification rates seem to decline faster in HB60 as compared to MG1363 (Figure 3.3B) under all assay conditions. Within 5 days of measurement, up to 25-fold decrease in acidification rates was found for strain HB60 as opposed to roughly 20-fold for strain MG1363. Since *L. cremoris* MG1363 grown on galactose and HB60 displays a mixed-acid fermentation profile, it may be that the calculated acid production is somewhat misestimated, but the kinetics of production decline remains reliable due to normalisation to the produced amount of acid. Moreover, the pH values during the prolonged acidification assay are between 5.75 and 6.5, where both acetic (pKa = 4.75) and formic (pKa = 3.75) acid are predominantly present in their deprotonated form (>90% & >99%, respectively). The calculated proton equivalent is barely affected by undissociated H^+ ions from formic acid, but rather slightly affected by undissociated H^+ ions from acetic acid. In our setup, a higher flux towards acetate would potentially result in more protons released due to the stoichiometry of the end products and the high buffer pH, which ensures that lactate and acetate are deprotonated. This means our system might underestimate the differences in acidification rate between MG1363 and HB60 and the discussed effect might actually be larger than what is shown.

Next to lowering the pH by carbon fermentation and organic acid production, the presented method also allows for similar measurements of pathways that lead to metabolite production that increase the environmental pH. To exemplify this possibility, we characterised the arginine utilisation

pathway activity over extended periods of time in *L. cremoris* strains MG1363 and HB60 that were incubated in assay media that lack a carbon source and with an initial pH set to 5.5. This enables the detection of a pH increase due to the formation of one of the arginine pathway products, ammonium (Figure 3.3C). Besides ammonium, arginine catabolism by the arginine deiminase (ADI) pathway also generates ornithine, CO_2 and ATP[38], which contribute to the enhanced acid stress tolerance observed in cells that actively express this pathway[39]. The detected pH-increase curves established that there is significant ammonium production in *L. cremoris* HB60, but that this activity could not readily be detected in MG1363 (Figure 3.3C). Especially glucose-precultured cells of MG1363 appeared to lack ammonium production entirely, whereas the very modest pH increase observed in galactose-precultured MG1363 cells suggests that these cells did convert arginine to ammonium, albeit at a marginal and barely detectable level. Strikingly, when analysing the ammonium production rates decline over time in *L. cremoris* HB60 (Figure 3.3D), we observed a faster decline in galactose-precultured cells compared to glucose-precultured cells. Overall, this demonstrates the suitability and sensitivity of the method to capture the metabolic pathway activity levels over prolonged periods of time, and it enables the study of strain- and preculture-dependent differences.

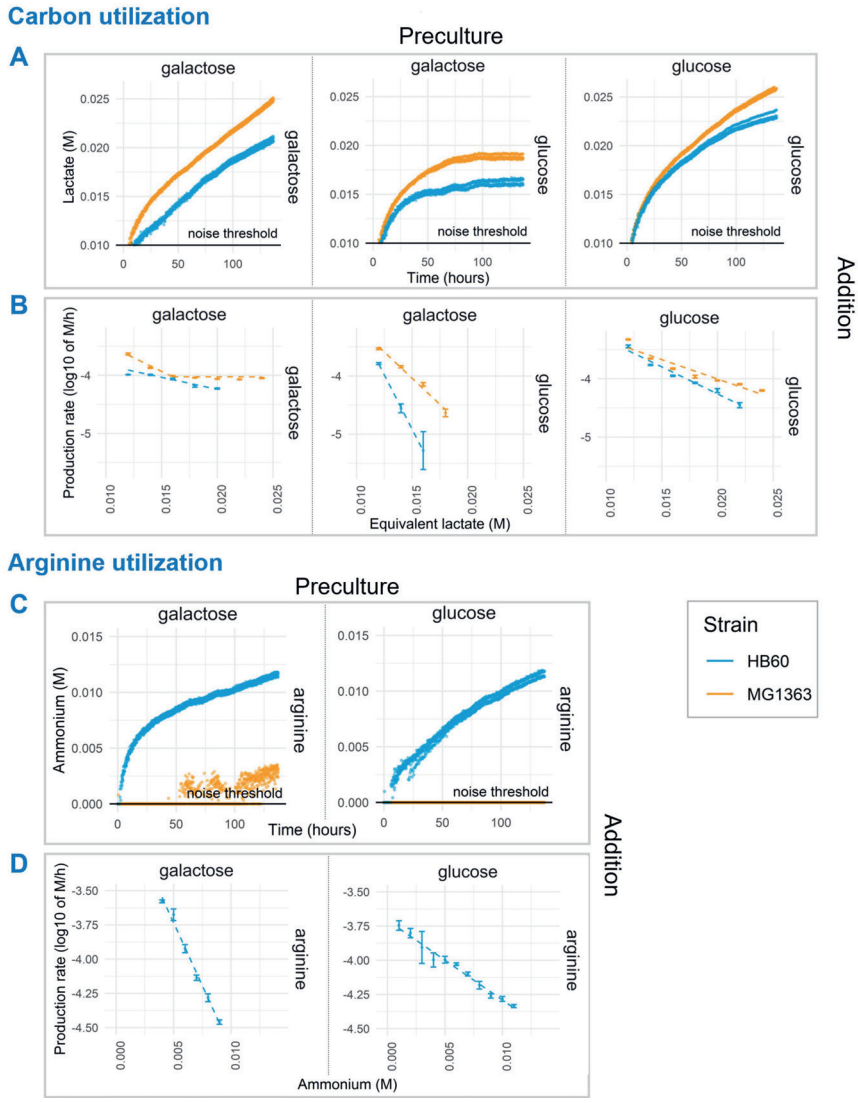

Figure 3.3 *Prolonged assay of carbon and arginine utilisation.* L. cremoris *MG1363 (orange) and HB60 (blue) were harvested at mid-exponential growth following preculture (top label) in 1% w/v of glucose or galactose and subsequently transferred to translationally-blocked assay mediums with different carbon source (right side label) at 2.0E+07 /mL cell density.* ***(A)*** *Lactate production.* ***(B)*** *The decline in lactate production rates.* ***(C)*** *Ammonium production.* ***(D)*** *The decline in ammonium production rates. Dashed lines indicate the linear fits of the data. Noise threshold was determined from the non-biological fluctuation of signal based on a negative control at pH 6.5 (lactate production) and pH 5.5 (ammonium production). Error bars indicate standard deviation of the experiment (n=4).*

3.4 Discussion

Here we describe a high-throughput approach and analysis pipeline for prolonged measurements of metabolic activity using translationally-blocked *L. cremoris* cells. As model pathways, we employed carbohydrate and amino acid utilisation of which the products can be readily detected by measurement of the pH of the medium. The novelty in the presented approach lies in the fact that real-time monitoring of lactic acid formation or ammonium accumulation due to arginine deamination can be performed for up to several weeks by a relatively straightforward and simple microplate-based assay. Prolonged product-formation measurements can be readily tracked in low-density, translation-blocked cells, which is critical to prevent cell growth and adaptation and product inhibition. To some extent, these translationally-blocked cells may also mimic aspects of cellular physiology and pathway persistence in the non-growing state that many cells experience during environmental and industrial conditions. This possible parallel opens several avenues to test industrially and environmentally interesting phenotypic properties in changing environments. In the case that strains of interest carry erythromycin resistance cassettes, there are multiple antibiotic alternatives that could likely be employed for the same purpose, such as chloramphenicol and azithromycin[30,40]. Alternatively, a non-growing state can be achieved by nitrogen starvation or omission of essential nutrients, although in such a system the complete inhibition of translation cannot be guaranteed as internal turnover of the limiting molecules might occur.

The presented method was used to compare the metabolic capacity of two closely related strains. *L. cremoris* MG1363 and HB60, which is a derivative of MG1363 that contains a point-mutation (F65L) in its *ptnD* gene. HB60 is reported to have a higher ATP yield when growing on glucose at the expense of its growth rate[23]. However, the expression of other ATP-generating pathways such as arginine deiminase pathway was not investigated in this strain, to date. While the mutated phosphotransferase system (PTS^{Man}) serves mainly as a

high-affinity glucose transport system in *L. cremoris*, it has also been suggested to be involved in galactose transport in *L. cremoris* MG1363[41]. Investigating carbon and arginine utilisation, we demonstrated that acidification rates of MG1363 were higher than those of HB60 not only for glucose utilisation, but also for galactose utilisation. Interestingly, we also observed significantly higher ammonium production through arginine deimination in translationally-blocked cells of strain HB60 than MG1363. While the amount of arginine in the initial study with this strain was relatively low, the catabolisation of arginine in HB60 could potentially contribute to the observed increased biomass yield. It has been reported that arginine utilisation during active growth could increase biomass yield up to 25% in an *L. lactis* strain[42]. The expression of the arginine deiminase pathway has been linked to carbon catabolite repression[43,44]. The lower growth rate of HB60 might possibly play a role in relieving repression of this pathway either directly through interaction of CcpA with the *cre* elements in the *arc* operon or indirectly through, e.g., FBP levels, which are expected to be lower in the slow-growing HB60[23]. In chemostat cultures, it was observed that arginine consumption increases up to a dilution rate of 0.5 /h above which it rapidly drops again[45]. Based on this data it seems plausible that a reduction of the maximum growth rate can result in a higher arginine utilisation, indicating that exploration of this activity in strains that are known to display reduced growth rates, e.g., *ldh* or *ccpA* mutants[46–48] would be of interest.

Next to the ability of the assay to measure pathway activities, we also observed differences in production rate decline in relation to preculture conditions or strains. A prominent example was the glucose-utilisation assay of galactose-precultured cells, which showed rapid acidification decline and complete halt within 100 hours of measurement. The underlying mechanism that caused acidification to stop after the transition to the preferred carbon source glucose remains to be deciphered, but it has been suggested that large overshoots in intracellular metabolites can be toxic due to osmotic and hydration effects[49]. Such activity decline could potentially be associated with

changes in the physiological state of the population over time, including rate of cellular viability and membrane integrity loss. Detailed analysis of such underlying effects, may reveal heterogeneity in the bacterial population, including the potential presence of persister subpopulations in cultures produced under different preculture conditions that may explain the (bi-phasic) decline in metabolic activities during the subsequent assay conditions. The current approach is a valuable addition toward answering fundamental questions on catalytic stability and cellular fitness, particularly in non-growing environmental conditions.

The presented method provides additional insight on the complete pathway activity of intact cells. While 'omics analysis produces substantial information on composition and level of transcripts and proteins in response to variation in a specific growth condition, they have a reduced throughput and are not necessarily able to distinguish between active and non-active proteins/pathways. The combination of 'omics technologies with extensive physiological measurement contributes to our understanding of cellular performance during long-term incubations under non-growing conditions. In addition, determination of the specific activity level of relevant enzymes or pathways in cells harvested from the assay conditions could be used to determine enzyme decay. The simplicity of the method developed is very attractive, while it does not compromise on the level of assay condition definition. Consequently, omission, addition and dose titration of single components, e.g., metals, vitamins, amino acids, etc can be performed in a high throughput manner to decipher the effect of environmental conditions on the flux through certain pathways. Moreover, the influence of biochemical parameters on pathway activities such as allosteric regulation, cofactor availability, pH, and temperature, can also be explored and related to its longevity. Although the present assay was on pathways that modulate the environmental pH (i.e., carbon flux and lactic acid production as well as arginine utilisation and ammonium formation) that is monitored by a pH-

dependent fluorescent reporter, one can envision the expansion to other metabolic pathways provided that product formation can be measured by fluorescence or other means of detection, e.g., luminescence and absorbance that are compatible with high-throughput methodologies. Ultimately, this approach will allow to investigate the effect of environmental and genetic modulation on phenotypic properties and the optimisation during prolonged catalysis in biotechnological applications, which is largely unexplored despite of its commercial interest.

3.5 Acknowledgments

The authors would like to thank Stephanie Agnes Bachtiar for technical assistance in viability and membrane integrity measurement and Roelie Holleman for the HPLC measurement of organic acids.

References

1. Ercan, O., Wels, M., Smid, E. J. & Kleerebezem, M. Molecular and metabolic adaptations of *Lactococcus lactis* at near-zero growth rates. *Appl. Environ. Microbiol.* **81**, 320–31 (2015).
2. Erkus, O. *et al.* Use of propidium monoazide for selective profiling of viable microbial cells during Gouda cheese ripening. *Int. J. Food Microbiol.* **228**, 1-9 (2016).
3. Keren, I., Kaldalu, N., Spoering, A., Wang, Y. & Lewis, K. Persister cells and tolerance to antimicrobials. *FEMS Microbiol. Lett.* **230**, 13–18 (2004).
4. Oliver, J. D., Hite, F., McDougald, D., Andon, N. L. & Simpson, L. M. Entry into, and resuscitation from, the viable but nonculturable state by *Vibrio vulnificus* in an estuarine environment. *Appl. Environ. Microbiol.* **61**, 2624–30 (1995).
5. Magajna, B. A. & Schraft, H. *Campylobacter jejuni* biofilm cells become viable but non-culturable (VBNC) in low nutrient conditions at 4 °C more quickly than their planktonic counterparts. *Food Control* **50**, 45–50 (2015).
6. Förberg, C., Enfors, S. O. & Häggström, L. Control of immobilized, non-growing cells for continuous production of metabolites. *Eur. J. Appl. Microbiol. Biotechnol.* **17**, 143–147 (1983).
7. Witzig, R. *et al.* Microbiological aspects of a bioreactor with submerged membranes for aerobic treatment of municipal wastewater. *Water Res.* **36**, 394–402 (2002).
8. Millet, V. & Lonvaud-Funel, A. The viable but non-culturable state of wine micro-organisms during storage. *Lett. Appl. Microbiol.* **30**, 136–141 (2000).

9. Sonderegger, M., Schümperli, M. & Sauer, U. Selection of quiescent *Escherichia coli* with high metabolic activity. *Metab. Eng.* **7**, 4–9 (2005).

10. Liu, J. *et al.* Discovery and control of culturable and viable but non-culturable cells of a distinctive *Lactobacillus harbinensis* strain from spoiled beer. *Sci. Rep.* **8**, 1-10 (2018).

11. Marcobal, Á., Martín-Álvarez, P. J., Polo, M. C., Muñoz, R. & Moreno-Arribas, M. V. Formation of biogenic amines throughout the industrial manufacture of red wine. *J. Food Prot.* **69**, 397–404 (2006).

12. Smid, E. J. & Kleerebezem, M. Production of aroma compounds in lactic fermentations. *Annu. Rev. Food Sci. Technol.* **5**, 313–326 (2014).

13. van Mastrigt, O., Gallegos Tejeda, D., Kristensen, M. N., Abee, T. & Smid, E. J. Aroma formation during cheese ripening is best resembled by *Lactococcus lactis* retentostat cultures. *Microb. Cell Fact.* **17**, 1–8 (2018).

14. van de Bunt, B., Bron, P. A., Sijtsma, L., de Vos, W. M. & Hugenholtz, J. Use of non-growing *Lactococcus lactis* cell suspensions for production of volatile metabolites with direct relevance for flavour formation during dairy fermentations. *Microb. Cell Fact.* **13**, 1-9 (2014).

15. Settachaimongkon, S. *et al.* Influence of *Lactobacillus plantarum* WCFS1 on post-acidification, metabolite formation and survival of starter bacteria in set-yoghurt. *Food Microbiol.* **59**, 14–22 (2016).

16. Shah, N. P., Lankaputhra, W. E. V., Britz, M. L. & Kyle, W. S. A. Survival of *Lactobacillus acidophilus* and *Bifidobacterium bifidum* in commercial yoghurt during refrigerated storage. *Int. Dairy J.* **5**, 515–521 (1995).

17. Frees, D., Varmanen, P. & Ingmer, H. Inactivation of a gene that is highly conserved in Gram-positive bacteria stimulates degradation of non-native proteins and concomitantly increases stress tolerance in *Lactococcus lactis*. *Mol. Microbiol.* **41**, 93–103 (2001).

18. Kock, H., Gerth, U. & Hecker, M. The ClpP peptidase is the major determinant of bulk protein turnover in *Bacillus subtilis*. *J. Bacteriol.* **186**, 5856–5864 (2004).

19. Ganesan, B., Stuart, M. R. & Weimer, B. C. Carbohydrate starvation causes a metabolically active but nonculturable state in *Lactococcus lactis*. *Appl. Environ. Microbiol.* **73**, 2498–2512 (2007).

20. Dijkstra, A. R. *et al.* Fermentation-induced variation in heat and oxidative stress phenotypes of *Lactococcus lactis* MG1363 reveals transcriptome signatures for robustness. *Microb. Cell Fact.* **13**, 1-11 (2014).

21. Settachaimongkon, S. *et al.* Effect of sublethal preculturing on the survival of probiotics and metabolite formation in set-yoghurt. *Food Microbiol.* **49**, 104–115 (2015).

22. Gasson, M. J. Plasmid complements of *Streptococcus lactis* NCDO712 and other lactic streptococci after protoplast-induced curing. *J. Bacteriol.* **154**, 1–9 (1983).

23. Bachmann, H. *et al.* Availability of public goods shapes the evolution of competing metabolic strategies. *Proc. Natl. Acad. Sci. U. S. A.* **110**, 14302–14307 (2013).

24. Wegmann, U. *et al.* Complete genome sequence of the prototype lactic acid bacterium *Lactococcus lactis* subsp. *cremoris* MG1363. *J. Bacteriol.* **189**, 3256–

3270 (2007).

25. Price, C. E. *et al.* Adaption to glucose limitation is modulated by the pleotropic regulator CcpA, independent of selection pressure strength. *BMC Evol. Biol.* **19**, 1-15 (2019).

26. Hugenholtz, J. & Starrenburg, M. J. C. Diacetyl production by different strains of *Lactococcus lactis* subsp. *lactis* var. *diacetylactis* and *Leuconostoc* spp. *Appl. Microbiol. Biotechnol.* **38**, 17–22 (1992).

27. Koebmann, B. J. *et al.* The extent to which ATP demand controls the glycolytic flux depends strongly on the organism and conditions for growth. *Mol. Biol. Rep.* **29**, 41–45 (2002).

28. Koebmann, B. J., Andersen, H. W., Solem, C. & Jensen, P. R. Experimental determination of control of glycolysis in *Lactococcus lactis*. In *Lactic Acid Bacteria: Genetics, Metabolism and Applications* 237–248 (Springer Netherlands, 2002).

29. Tenson, T., Lovmar, M. & Ehrenberg, M. The mechanism of action of macrolides, lincosamides and streptogramin B reveals the nascent peptide exit path in the ribosome. *J. Mol. Biol.* **330**, 1005–1014 (2003).

30. Svetlov, M. S., Vázquez-Laslop, N. & Mankin, A. S. Kinetics of drug-ribosome interactions defines the cidality of macrolide antibiotics. *Proc. Natl. Acad. Sci. U. S. A.* **114**, 13673–13678 (2017).

31. van Tatenhove-Pel, R. J., Zwering, E., Solopova, A., Kuipers, O. P. & Bachmann, H. Ampicillin-treated *Lactococcus lactis* MG1363 populations contain persisters as well as viable but non-culturable cells. *Sci. Rep.* **9**, 1–10 (2019).

32. van Mastrigt, O., Abee, T., Lillevang, S. K. & Smid, E. J. Quantitative physiology and aroma formation of a dairy *Lactococcus lactis* at near-zero growth rates. *Food Microbiol.* **73**, 216–226 (2018).

33. Thomas, T. D., Ellwood, D. C. & Longyear, V. M. C. Change from homo- to heterolactic fermentation by *Streptococcus lactis* resulting from glucose limitation in anaerobic chemostat cultures. *J. Bacteriol.* **138**, 109–117 (1979).

34. Thomas, T. D., Turner, K. W. & Crow, V. L. Galactose fermentation by *Streptococcus lactis* and *Streptococcus cremoris*: pathways, products, and regulation. *J. Bacteriol.* **144**, 672–82 (1980).

35. Garrigues, C., Loubiere, P., Lindley, N. D. & Cocaign-Bousquet, M. Control of the shift from homolactic acid to mixed-acid fermentation in *Lactococcus lactis*: predominant role of the NADH/NAD+ ratio. *J. Bacteriol.* **179**, 5282–5287 (1997).

36. Lopez de Felipe, F., Kleerebezem, M., de Vos, W. M. & Hugenholtz, J. Cofactor engineering: a novel approach to metabolic engineering in *Lactococcus lactis* by controlled expression of NADH oxidase. *J. Bacteriol.* **180**, 3804–8 (1998).

37. Melchiorsen, C. R. *et al.* Synthesis and posttranslational regulation of pyruvate formate-lyase in *Lactococcus lactis*. *J. Bacteriol.* **182**, 4783–4788 (2000).

38. Poolman, B., Driessen, A. J. M. & Konings, W. N. Regulation of arginine-ornithine exchange and the arginine deiminase pathway in *Streptococcus lactis*. *J. Bacteriol*. **169**, 5597-5604 (1987).

39. Budin-Verneuil, A., Maguin, E., Auffray, Y., Dusko Ehrlich, S. & Pichereau, V. An essential role for arginine catabolism in the acid tolerance of *Lactococcus lactis*

MG1363. *Lait* **84**, 61–68 (2004).

40. Yerlikaya, O. Probiotic potential and biochemical and technological properties of *Lactococcus lactis* ssp. *lactis* strains isolated from raw milk and kefir grains. *J. Dairy Sci.* **102**, 124–134 (2019).

41. Neves, A. R. *et al.* Towards enhanced galactose utilization by *Lactococcus lactis*. *Appl. Environ. Microbiol.* **76**, 7048–7060 (2010).

42. Palmfeldt, J., Paese, M., Hahn-Hägerdal, B. & Van Niel, E. W. J. The pool of ADP and ATP regulates anaerobic product formation in resting cells of *Lactococcus lactis. Appl. Environ. Microbiol.* **70**, 5477–5484 (2004).

43. Gaudu, P., Lamberet, G., Poncet, S. & Gruss, A. CcpA regulation of aerobic and respiration growth in *Lactococcus lactis*. *Mol. Microbiol.* **50**, 183–192 (2003).

44. Zomer, A. L., Buist, G., Larsen, R., Kok, J. & Kuipers, O. P. Time-resolved determination of the CcpA regulon of *Lactococcus lactis* subsp. *cremoris* MG1363. *J. Bacteriol.* **189**, 1366–1381 (2007).

45. Goel, A. *et al.* Protein costs do not explain evolution of metabolic strategies and regulation of ribosomal content: Does protein investment explain an anaerobic bacterial Crabtree effect? *Mol. Microbiol.* **97**, 77–92 (2015).

46. Platteeuw, C., Hugenholtz, J., Starrenburg, M., Van Alen-Boerrigter, I. & De Vos, W. M. Metabolic engineering of *Lactococcus lactis*: influence of the overproduction of α-acetolactate synthase in strains deficient in lactate dehydrogenase as a function of culture conditions. *Appl. Environ. Microbiol.* **61**, 3967–3971 (1995).

47. Luesink, E. J., van Herpen, R. E. M. A., Grossiord, B. P., Kuipers, O. P. & de Vos, W. M. Transcriptional activation of the glycolytic *las* operon and catabolite repression of the *gal* operon in *Lactococcus lactis* are mediated by the catabolite control protein CcpA. *Mol. Microbiol.* **30**, 789–798 (1998).

48. Bongers, R. S. *et al.* IS981-mediated adaptive evolution recovers lactate production by *ldhB* transcription activation in a lactate dehydrogenase-deficient strain of *Lactococcus lactis*. *J. Bacteriol.* **185**, 4499–4507 (2003).

49. Korem Kohanim, Y. *et al.* A bacterial growth law out of steady state. *Cell Rep.* **23**, 2891–2900 (2018).


4

Chapter 4

Manganese Modulates Metabolic Activity and Redox Homeostasis in Translationally-Blocked Lactococcus cremoris, Impacting Metabolic Persistence, Cell-Culturability, and Flavour Formation

Nugroho, A. D. W., van Olst, B., Bachtiar, S. A., Boeren, S.,
Kleerebezem, M. & Bachmann, H.

This chapter has been published:
Microbiol. Spectr. **10**, e02708-21 (2022)

Abstract

Manganese (Mn) is an essential trace element that is supplemented in microbial media with varying benefits across species and growth conditions. We found that growth of *Lactococcus cremoris* was unaffected by manganese omission from the growth medium. The main proteome adaptation to manganese omission involved increased manganese transporter production (up to 2,000-fold), while the remaining 10 significant proteome changes were between 1.4- and 4.0-fold. Further investigation in translationally-blocked (TB), non-growing cells showed that Mn supplementation (20 μM) led to approximately 1.5-fold faster acidification compared to Mn-free conditions. However, this faster acidification stagnated within 24 hours, likely due to draining of intracellular NADH that coincides with substantial loss of culturability. Conversely, without manganese, non-growing cells persisted to acidify for weeks, albeit at a reduced rate, but maintaining redox balance and culturability. Strikingly, despite being unculturable, α-keto acid-derived aldehydes continued to accumulate in cells incubated in the presence of manganese, whereas without manganese cells predominantly formed the corresponding alcohols. This is most likely reflecting NADH availability for the alcohol dehydrogenase-catalysed conversion. Overall, manganese influences the lactococcal acidification rate and flavour formation capacity in a redox-dependent manner. These are important industrial traits especially during cheese ripening, where cells are in a non-growing, often unculturable state.

4.1 Introduction

Growth and survival of microorganisms heavily relies on the environmental availability of metal cofactors, particularly for essential alkaline earth and transition metals such as magnesium, calcium, manganese, iron, cobalt, copper, and zinc. In this group, manganese is especially important because of its relatively high solubility, abundance, and distinctive redox abilities[1]. In comparison to other biologically important redox-active metals, i.e., Fe^{2+}, Mn^{2+} is a weaker electron donor or reducing agent[1]. Consequently, cells can accumulate and tolerate high cytoplasmic concentration of free Mn^{2+} without negative redox outcomes under conditions that will normally promote formation of toxic free radicals through Fenton-type reactions[2,3]. Based on structural similarity among other transition metals, only manganese is able to replace magnesium in its cofactor binding site and activate the corresponding enzymes, which are ubiquitous in carbon, nucleic acid, and protein metabolism[1,4,5].

Therefore, intracellular manganese homeostasis is essential for optimal cellular activities. In bacteria, the intracellular Mn^{2+} concentration is typically maintained relative to other metals as an inverse of the Irving-Williams series (Mg^{2+} and Ca^{2+} (weakest cofactor binding) < Mn^{2+} < Fe^{2+} < Co^{2+} < Ni^{2+} < Cu^{2+} > Zn^{2+})[6,7]. This universal order predicts the stabilities of (transitional) metal complexes independent of the ligands[7] and highly influences the metal competition to cofactor binding sites that depends on both its abundance and affinity. To ensure specific metal cofactors are inserted to metalloenzymes, a cell finely tunes its intracellular metal pools by employing cytosolic metal sensors and transporters. In the case of manganese, two main transporters are reported in lactic acid bacteria (LAB), which are an ABC transport system (*mtsCBA*) and Nramp transporters (*mntH*)[8]. Typically, intracellular manganese is maintained at micromolar levels, which is 1,000- 10,000-fold lower than intracellular Mg^{2+} but 10,000-100,000-fold higher than other metals in the

Irving-Williams series, with an exception for iron that is commonly present in comparable amount to manganese[6]. The maintenance of intracellular manganese levels is especially relevant for cellular bioenergetics where various enzymes related to carbon metabolism, e.g., lactate dehydrogenase, phosphoglycerate mutase, and fructose-1,6-bisphosphate phosphatase are either strictly Mn-dependent or highly stimulated by manganese[1,9]. Many bacterial superoxide dismutases, which act as scavenger of reactive oxygen species also incorporates manganese in their active site[10]. Therefore, manganese is generally considered to be crucial not only in survival under oxidative stress conditions but also in ATP generation[10,11].

In Lactic Acid Bacteria, manganese supplementation has frequently been shown to contribute to cell growth and functionality during fermentation applications. The bioavailability of manganese has been found to enhance *in vitro* formation of flavours such as benzaldehyde[12] and the aldehydes derived from α-keto acids, e.g., 3-methylbutanal[13]. In the latter case, the conversion of branched-chain α-keto acids (BCAAs) was reported to serve as a redox sink and the utilisation of BCAAs can result in a marked increase of biomass, possibly due to additional ATP formation[14]. On the other hand, lactococci grown without manganese supplementation have shown higher survival following a heat shock[15]. Although the underlying mechanism to this observation is not known, it is plausible that manganese deprivation leads to stress responses that provide cross-protective resistance[16]. Nonetheless, manganese supplementation is generally favoured for microbial cultivation media despite these variations in physiological consequences in various species and growth conditions[17]. While various studies have investigated the effect of manganese on growth and stress resistance, no studies investigated its effect on the metabolism of non-growing cells, which have distinct metabolic strategies and requirements. A non-growing state is commonly encountered in various biotechnological applications such as in the production of pharmaceuticals[18,19], fermented foods[20], or biofuels[21]. It is especially relevant in various long-term

fermentation processes such as cheese ripening where a significant portion of volatile flavour metabolites are generated for up to years after cell growth has ceased.

In the present study, we investigated the physiological and molecular (proteome) adaptation of *Lactococcus cremoris* to the presence and absence of manganese supplementation to a chemically defined medium. Furthermore, we investigated the role of manganese in cellular survival and metabolic activity in growing and translationally-blocked (TB) cells. The results indicate that cells in the absence of manganese can maintain their growth rate with relatively modest adjustment in cytoplasmic proteins compared to membrane transporters. However, in non-growing, TB-cells manganese omission led to a striking prolongation of acidification capacity, cell-survival as well as maintenance of redox homeostasis. These observations demonstrate that manganese omission strongly influences the *L. cremoris* metabolism under TB conditions while it does not appear to have apparent consequences for growth or physiology of *L. cremoris* during cultivation.

4.2 Materials and methods

4.2.1 Strain and Mn-omission cultivation

Lactococcus cremoris NCDO712[22], MG1363[23], MG1363 (pAK80)[24], MG1363(pCPC75::atpAGD)[24], and MG1363 (pNZ5519) (this study, Supplementary Methods SM4.1) were grown on chemically defined medium for prolonged cultivation (CDMPC[25], Supplementary Methods SM4.2) at 30°C without aeration. Strains were precultured in the presence or absence of Mn for 25 generations (4 direct transfers with a 100-fold dilution) to minimise carry-over effects. Details on strain-specific ingredients and growth rate measurement and can be found in Supplementary Methods SM4.3 and SM4.4.

4.2.2 Proteome analysis

Proteome samples were harvested in quadruplicates from exponentially growing cultures of strain NCDO712 that was precultured for 20 generations in the presence or absence of manganese. Protein extraction and analysis were performed as described previously[26]. Details and modifications to the proteomics methods can be found in Supplementary Methods SM4.5. The mass spectrometry proteomics data have been deposited to the ProteomeXchange Consortium via the PRIDE[27] partner repository with the dataset identifier PXD030123.

4.2.3 Acidification and luminescence measurements of translationally-blocked (TB-) cells

Long term analysis of metabolite production was performed as described earlier[28]. Exponentially growing cells precultured in the presence or absence of Mn were harvested and resuspended at a density between 1.0E+07 and 2.5E+07 cells/mL in their corresponding growth medium supplemented with erythromycin (5 μg/mL) and 10 μM 5(6)-carboxyfluorescein (Sigma-Aldrich 21877), with or without Mn (20 μM). For volatile production measurement, aliquots of TB-cultures were transferred to sterile GC-MS vials. Time-course samples were analysed for organic acids, volatiles, viability, and membrane integrity (Supplementary Methods SM4.6 and SM4.7)

Luminescence measurement was performed as described earlier[29]. Aliquot of TB-*L. cremoris* MG1363 harbouring pNZ5519 (1E+07 cells/mL, precultured without manganese) was concentrated at selected time points of incubation by centrifugation and resuspension in less volume of supernatant to a concentration of 1E+08 cells/mL. Nonanal 1% in silicon oil was supplied as reaction substrate and added either into empty wells or the empty space between the wells of the microplate. A regular lid was used to cover the microplate, which allows sufficient oxygen exposure required for the luciferase

reaction. Luminescence was determined at 20-min intervals over a period of 6 hours after nonanal addition in a Genios microplate reader (Tecan, Zurich, Switzerland). The gain was set at 200 and integration time was set at 1,000 ms.

4.3 Results

4.3.1 Manganese omission did not lead to changes in growth characteristics or metabolic end products

Growth rate changes in many organisms are accompanied by metabolic shifts and they are suggested to reflect re-allocations in cellular protein investment and constraints on microbial growth[30,31]. In lactococci, such metabolic shift has been described, where homofermentative acidification predominated by lactic acid occurs at high growth rate but switches to heterofermentative acidification at low growth rate[32]. To investigate the requirement of manganese on growth, we removed manganese from the preparation of our standard chemically-defined medium for lactococci. Remarkably, changes in the growth of strain NCDO712 were not detected in the absence of manganese. Since a carry-over effect from the previous growth medium might be sufficient to compensate for the lack of manganese, we further cultivated NCDO712 for 4 subcultures and a total of 25 generations to ensure complete removal of manganese. At the end of this subculturing, no apparent effect on the growth rates of NCDO712 was seen in relation to manganese availability (Figure 4.1A). The growth rate remained high in the absence of manganese throughout the transfers and under excess or limited supply of lactose (Supplementary Data Figure SD4.1), which implies that cells can grow with minute amounts of manganese available in their environment. In line with the high growth rate, the composition of produced organic acids remained unchanged and was predominated by lactic acid when manganese was omitted (Figure 4.1B). These results suggest that Mn omission led to no changes in flux[33] through the central energy generation pathway, i.e., glycolysis

coupled to pyruvate conversion to lactic acid by lactate dehydrogenase (LDH), nor in the energy and redox state of the cells i.e., ADP/ATP ratio, or NAD^+/NADH ratio[34].

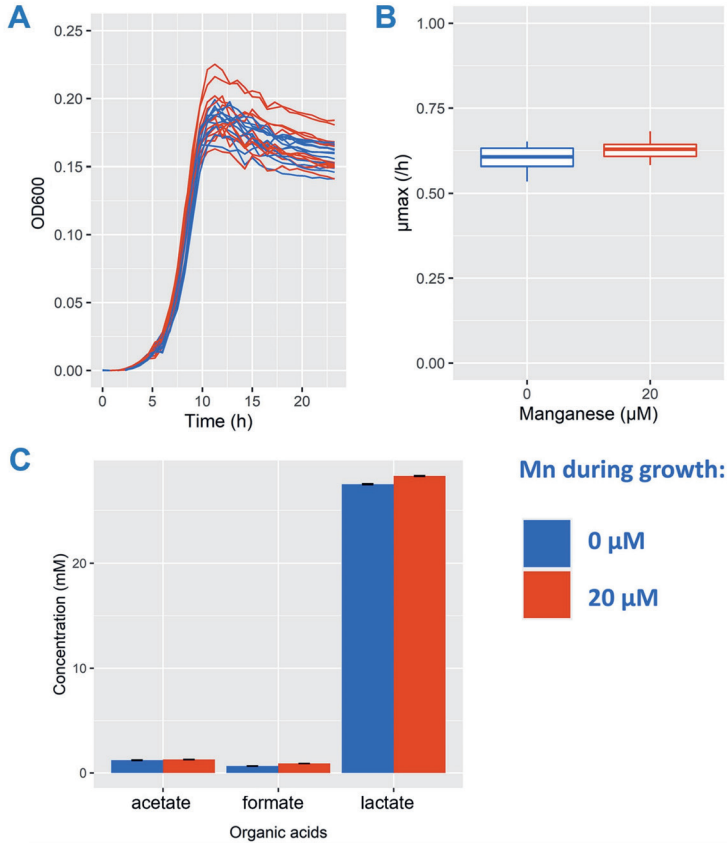

Figure 4.1 Lactococcus cremoris *NCDO712 was serially propagated 4 times (25 generations) in defined medium supplemented with lactose at excess (12.5 mM – growth stops due to acid accumulation) concentration in the presence (red) and absence (blue) of manganese (20 μM). The growth curve (panel A, n=8), maximum specific growth rate (panel B, n=3), and concentrations of organic acids (panel C, n=2) are shown. Error bars indicate the standard deviation from the stated n biological replicates.*

4.3.2 Proteome adjustments to manganese omission mainly upregulated Mn transporters

Growth data suggests that cells are apparently unaffected by manganese deprivation. To characterise the cellular responses to manganese omission from the growth medium, we performed a global proteome analysis. Manganese omission led to only 17 significantly differentially expressed proteins, encompassing 11 upregulated and 6 downregulated expression levels (Table 4.1). By far the most prominent proteome adaptation occurred in the expression of membrane transporters such as MntH, MtsA, and MtsB. There an up to 2,000-fold increase of expression was observed for the ABC transporter MtsA upon the omission of manganese. The expression of proton-dependent NRAMP-related manganese transporter $MntH_P$ (plasmid encoded) increased under manganese omission by 4-fold. Next to these transporters, the putative manganese transporter llmg_1024 and llmg_1025 increased by 4-fold. This is comparable to the fold-change observed for MntH and it may potentially be involved in the regulation of intracellular Mn concentration. Additionally, the genome-encoded MntH (*llmg*_1490) was not captured by differential analysis (Table 4.1) due to its level being below the detection limit with Mn supplementation. When taking into account the estimated minimum detection level in our proteomics data (4.8 LFQ intensity), this genome-encoded MntH increased by at least 20-fold upon Mn omission to an average LFQ intensity of 6.1, which is comparable with the upregulation of plasmid-encoded $MntH_P$. The upregulation of these Mn transporters indicates that cells detected Mn shortage despite no apparent changes in growth rate or acidification profile. However, it cannot be excluded that trace amounts of Mn that might be present as contaminants of medium constituents are compensating or masking any effects of Mn omission on growth. Moreover, it is unknown whether the upregulated transport functions would allow the cells to accumulate these trace amount to a sufficient intracellular level for growth.

Aside from these transporters, manganese omission also led to 12 more modest, but significant changes in cytoplasmic protein levels (ranging from 1.4- to 4-fold changes). Notably, the majority of these proteins are associated with redox metabolism and many catalyse NAD-dependent reactions. Manganese omission from the growth medium increased the expression of 2-dehydropantoate 2-reductase (3-fold) and a putative pyridoxamine 5'-phosphate oxidase (2.5-fold), while the expression of NADH oxidase (0.27-fold), aldehyde-alcohol dehydrogenase (0.41-fold), and a putative ferredoxin protein (0.48-fold) decreased. Moreover, manganese availability seems to correspond to changes in a few proteins related to stress response. For example, expression of the peptide methionine sulfoxide reductase (PMSR), which catalyses the reduction of methionine sulfoxide in proteins back to methionine. This enzyme may protect cells against oxidative stress[35]. It was found to be approximately 2-fold decreased in the absence of manganese. Conversely, manganese omission led to more than 3-fold increased expression of universal stress protein UspA, which is associated with resistance against various stresses. Intriguingly, aside from PMSR, differential expression of superoxide dismutase (MnSOD) and/or other oxidative stress related functions were not observed in the absence of manganese, illustrating a lack of prominent changes in the oxidative stress levels experienced by these cells. Overall, the changes in proteome data are dominated by major changes in Mn-transport proteins and more modest changes in a number of cytosolic proteins that suggest that cells might experience a shift in the redox balance.

Table 4.1 *Significant differentially expressed proteins in manganese omitted compared to manganese supplemented cultures. Proteins were selected based on cut-off parameters of s0 = 0.01 and a False Discovery Rate (FDR) of 0.05. LFQ (Label Free Quantitation) values represent the average from 4 biological replicates.*

Protein Names	Gene Names	LFQ (+Mn)	LFQ (-Mn)	Fold Change	-Log10 p-value
Manganese ABC transporter substrate binding protein	*mtsA* llmg_1138	4.9±0.04	8.26±0.11	2269.43	8.29
Manganese ABC transporter ATP binding protein	*mtsB* llmg_1136	5.72±0.22	7.77±0.1	110.67	5.17
Mn^{2+}/Fe^{2+} transporter, NRAMP family	*mntH* pNZ712_01	6.43±0.13	7.05±0.04	4.19	3.69
Uncharacterised protein	llmg_1025	6.5±0.1	7.12±0.04	4.15	4.14
Putative membrane protein	llmg_1024	6.4±0.09	6.97±0.03	3.78	4.33
Universal stress protein UspA	*uspA*	7±0.05	7.5±0.06	3.20	4.54
2-dehydropantoate 2-reductase (EC 1.1.1.169) (Ketopantoate reductase)	*panE* llmg_1131	5.52±0.15	5.99±0.08	2.99	2.49
Uncharacterised protein	llmg_2395	5.7±0.1	6.11±0.07	2.55	2.92
Ribonuclease J (RNase J) (EC 3.1.-.-)	*rnj* llmg_0876	7.2±0.01	7.51±0.07	2.02	3.63
Lipoprotein	*plpB* llmg_0336	6.82±0.03	7.06±0.05	1.75	3.30
Ribonuclease J (RNase J) (EC 3.1.-.-)	*rnj* llmg_0302	7.32±0.02	7.47±0.03	1.40	3.20
NADH oxidase (EC 1.6.-.-)	*noxC* llmg_1770	6.76±0.14	6.19±0.11	0.27	2.77
Aldehyde-alcohol dehydrogenase	*adhE* llmg_2432	8.1±0.05	7.72±0.13	0.41	2.53
Putative electron transport protein	llmg_1916	6.9±0.1	6.58±0.04	0.48	2.64
Peptide methionine sulfoxide reductase *MsrA* (Protein-methionine-S-oxide reductase) (EC 1.8.4.11)	*pmsR msrA* llmg_2281	6.25±0.06	5.97±0.07	0.52	2.71
Glycine betaine/proline ABC transporter (EC 3.6.3.32)	*busAA* llmg_1048	8.17±0.04	7.92±0.02	0.56	4.22
Glycine betaine-binding protein	*busAB* llmg_1049	7.7±0.03	7.46±0.02	0.59	4.62

4.3.3 Acidification is maintained for a prolonged period in TB-cells only in the absence of manganese

The proteome data implied that cells cultured without Mn addition might be in an altered physiological state, which may depend on the intracellular Mn levels and/or NAD^+/NADH availability to maintain metabolic fluxes. We investigated if cellular adaptation to manganese omission affects central metabolism, which we performed in a previously described model system of non-growing cells with inhibited protein synthesis[28]. In this system we can follow acid production of non-growing cells with continuous measurements for up to three weeks, compared to growing cells, which fully acidifies in a few hours. Inhibition of protein synthesis with the antibiotic erythromycin enables the preservation of protein levels, e.g., manganese transporters. It allows comparing of cells grown in the presence or absence of manganese, while manganese concentration in the assay medium can be precisely adjusted. In line with the growth data, lactic acid was still the predominant fermentation end-product, making up more than 90% (Cmol-based) of the produced organic acids (Supplementary Data Figure SD4.2A) during prolonged incubation irrespective of the treatments. The calculated lactic acid production from the continuous pH measurement (Figure 4.2B) is in good agreement with the HPAEC measurements (Figure 4.2A).

In the presence of manganese, acidification by TB-cells was initially approximately 1.5-fold faster (Supplementary Data Figure SD4.2B) but stagnated within 24 hours (Figure 4.2A & 4.2B, left panel) reaching a relatively low final lactate concentration (~ 4 mM) and a final pH of 6.16. In contrast, when cells were transferred to assay medium containing no manganese, acidification continued at a lower rate for more than a week, reaching drastically higher final lactic acid concentrations (~ 25 mM) and a lower final pH of ~ 4.0. The latter conditions (25 mM lactic acid and pH 4.0) are likely the environmental conditions that prevented further acidification (Figure 4.2A,

4.2B). Moreover, in the absence of Mn in TB-cell assay (Figure 4.2B), Mn-precultured cells produced 20 mM lactic acid in 100 h compared to 150 h when cells were precultured without Mn, potentially as a result of trace amount of Mn carry over. Importantly, these results demonstrate that the absence of manganese in these acidification assays prominently changes the persistence of flux through the central energy-generating pathway. This seems to be irrespective of the accompanying cellular proteome changes as demonstrated by preculture both in the presence or absence of Mn showing prolonged activity following transition to Mn-omitted non-growing assay medium (Figure 4.2A, 4.2B middle and right panel). Despite of the prominent role of manganese in oxidative stress tolerance in many organisms, there were no indications that this stagnated acidification was explained by substantial difference in oxidative stress levels in the absence or presence of Mn in this TB assay (Supplementary Information Figure SD4.3). Overall, this data shows that the omission of manganese during sugar conversion of translationally-blocked cells allows for a much longer persistence of acidification and, therefore, a higher total product formation.

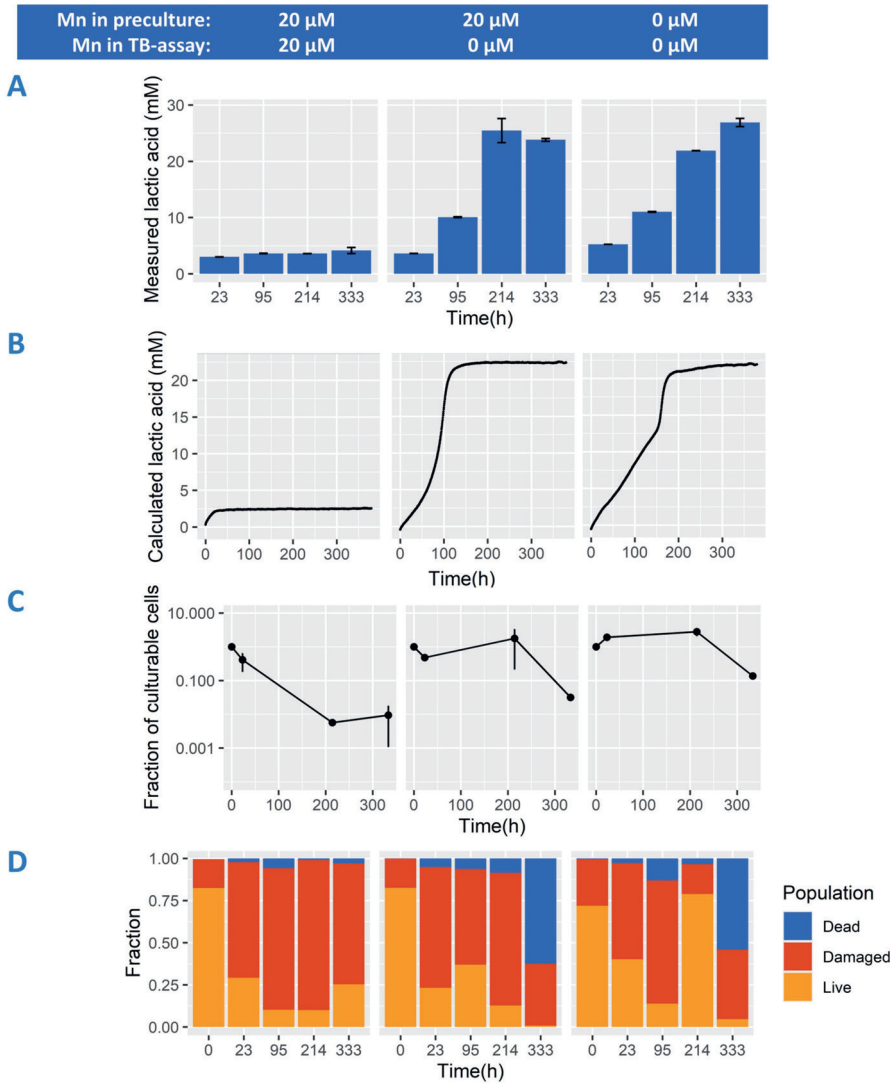

Figure 4.2 Lactococcus cremoris *NCDO712 (n= 3 biological replicates) was precultured in the presence (left and middle panel) and absence (right panel) of manganese (20 µM). Cells (2.5E+07 cells/mL) were transferred into fresh medium containing erythromycin (5 µg/mL) and 20 µM manganese (left panel) or 0 µM manganese (middle and right panel). Concentration of lactic acid (panel A) was measured with HPAEC at selected time points. Continuous measurement of medium pH to calculate lactic acid production overtime can be seen in panel B (replicates behaved nearly identically). Average population fractions based on membrane integrity (panel C) was measured for dead (blue), damaged (red), and live (orange) cells throughout incubation. Fractions of culturable cells based on plate counts can be seen in panel D. Error bars indicate the standard deviation.*

4.3.4 Manganese induces the appearance of viable but non-culturable (VBNC) populations in TB-cells after acidification stagnates

The observed stagnation of acidification within 24 hours for Mn supplemented conditions implies that the generation of ATP through glycolysis would also stagnate, which could also affect the viability and integrity of the cells. In this context it is relevant to note that lactococci is known to remain metabolically-active for prolonged periods of carbon starvation, e.g., more than 3.5 years, in a viable but non-culturable (VBNC) state[36]. To investigate the influence of manganese on cellular integrity and culturability during acidification in TB-cells, we determined the colony forming unit and membrane integrity over time. Within 9 days of prolonged incubation, non-growing cells incubated with manganese showed an approximate 100-fold reduction in culturable cells (Figure 4.2C). This is sharply contrasted by results obtained for cells incubated without manganese, where culturability was maintained close to 100% in the same timeframe. Under the conditions used, rapidly declining culturability of the cells incubated in absence of manganese was only observed after 2 weeks of incubation, which is likely the consequence of the combined stress of low pH and increased lactic acid concentrations. These results are in good agreement with our previous observations that an approximate 40-fold decline of viability was observed under similar conditions after approximately 2 weeks[28]. Analogous to the acidification observations presented above, the presence or absence of manganese during the preculturing and the corresponding proteome adaptations did not significantly influence the culturability results we obtained.

Membrane integrity analysis (Figure 4.2D) of the same time series revealed a prominent decline of the subpopulation with an apparent intact membrane (“live”) that increasingly progressed towards the subpopulation characterised by slightly damaged (“damaged”) or severely damaged (“dead”) membrane integrity over the course of incubation. Under all conditions, the

damaged subpopulation became more predominant over time and on average ranged from 60% to 80% of the total population in cells incubated between 23 h and 214 h. Notably, in the absence of manganese the subpopulation classified as 'dead' increased to approximately 60% of the total population after 333 h of incubation, whereas less than 5% of the total population was classified as 'dead' when incubated for the same time in media containing manganese. Analogous to the culturability results, this drastic decline of viability is likely due to prolonged exposure to low pH and high lactic acid concentrations inducing increasing cell damage that coincides with loss of culturability (and viability). Conversely, the observed decline in culturability of cells incubated in the presence of Mn was very poorly reflected by an increasing subpopulation of cells characterised as 'dead' according to these membrane-staining procedures. Apparently, the loss of culturability of these cells is not related to loss of cellular integrity but could be related to an unbalanced metabolism because of their high rate of acidification. Potential metabolic consequences of rapid acidification could induce stagnation of acidification and loss of culturability. This could be related to an excessive increase of the ATP/ADP balance, where the depletion of the intracellular ADP pool halts glycolytic flux. Alternatively, the disruption of the intracellular redox balance ($NADH/NAD^+$ ratio) could lead to depletion of either form of this cofactor that would also effectively halt glycolytic flux and/or lactate formation. Loss of either ATP/ADP or $NADH/NAD^+$ homeostasis may also negatively affect culturability by creating an inability to re-initiate energy generation or biosynthesis pathways required for regrowth.

4.3.5 Manganese leads to NADH depletion in acidifying TB-cells

To investigate whether manganese induces the proposed ADP depletion and, thereby, stagnates acidification in TB-cells, we used strain MG1363 (a prophage-cured and plasmid-free derivative of strain NCDO712) harbouring pCPC75::atpAGD[24]. This strain constitutively overexpresses the F1 domain of the membrane-bound F1F0-ATPase, which modulates intracellular energy levels by accelerating the ATP to ADP conversion[24]. However, in the presence of manganese TB-cells of this F1-ATPase overexpressing strain displayed the same stagnation of acidification within 24 hours as the control strain (MG1363 harbouring the empty vector pAK80), whereas manganese omission allowed continued acidification at a reduced rate for weeks (Figure 4.3A). These results demonstrated that preventing the postulated ATP accumulation by its conversion to ADP through the F1-ATPase failed to sustain prolonged acidification. This indicates that the disruption of the ATP/ADP homeostasis is not the mechanism underlying the observed phenomenon.

To investigate whether a redox balance disruption is able to explain the manganese-induced stagnation of acidification, we used strain MG1363 harbouring pNZ5519[37], which constitutively expresses *luxAB*, a bacterial luciferase of *Vibrio harveyi*. This luciferase catalyses the reaction of a long chain aldehyde, e.g., nonanal, oxygen, and reduced flavin mononucleotide ($FMNH_2$) to form a carboxylic acid, FMN, and light (490 nm). Regeneration of intracellular $FMNH_2$ is dependent on the availability of NADH, which is thereby required to maintain the luciferase reaction and the corresponding detection of the luminescence signal. In an initial experiment, the LuxAB substrate nonanal was provided immediately after transferring cells to the TB acidification conditions. In this experiment, the initial luminescence signal was approximately equal in absence and presence of manganese and subsequently declined over time, to become undetectable after approximately 6 hours (Figure 4.3B). This result indicates that the high NADH demand of the luminescence reaction effectively

drains the cellular NADH pool, which leads to the rapid decline of the luminescence signal over time. Notably, the decline rate of the luminescence signal was higher when manganese was supplemented and reached undetectable luminescence levels 2 hours earlier compared to the condition when manganese was omitted, suggesting that NADH is depleted more rapidly when manganese is present. In a follow up experiment, TB-cell suspensions were left to acidify for 20 hours prior to the addition of nonanal to initiate the luminescence reaction (Figure 4.3B). Under these conditions, the impact of manganese presence in the incubation medium was very pronounced, where the condition lacking manganese generated an initial luminescence level and a subsequent signal-decline curve that were very similar to those observed when nonanal was added from the start, whereas in the presence of Mn there was hardly any detectable luminescence signal (Figure 4.3B). These results suggest that NADH is depleting during acidification in the presence of Mn, whereas intracellular levels of NADH and redox homeostasis are maintained in the absence of manganese. Taken together these experiments show that manganese-mediated acceleration of acidification correlates with a disruption of redox homeostasis rather than energy homeostasis (ATP/ADP), leading to depletion of NADH and thereby stagnating acidification and possibly inducing a VBNC state. This loss of redox homeostasis is not seen in absence of manganese where NADH pools are apparently kept constant, and acidification can be sustained for weeks[28] in these TB-cell suspensions.

4.3.6 NADH-dependent conversion of aldehydes to alcohols increases in TB-cells upon manganese omission.

Next to acidification, NADH depletion might influence or re-route other (industrially-relevant) metabolic pathways that are dependent on the redox state of the cell, such as branched-chain amino acid catabolism. This catabolic pathway is initiated by the transamination of the amino acid leading to the formation of the corresponding α-keto-iso-caproic acid (KICA), which serves as

the major metabolic precursor that can be converted to 3 different intermediate products. Only the keto acid conversion to the corresponding aldehyde intermediate, e.g., 3- or 2-methylbutanal, is independent of NAD^+ or NADH as a cofactor and is also enhanced by Mn[13]. The other keto acid conversions include the NADH-dependent conversion to α-hydroxyisocaproic acid via hydroxyacid dehydrogenase and the NAD^+ and CoA-dependent conversion to isocaproyl-CoA via ketoacid dehydrogenase.

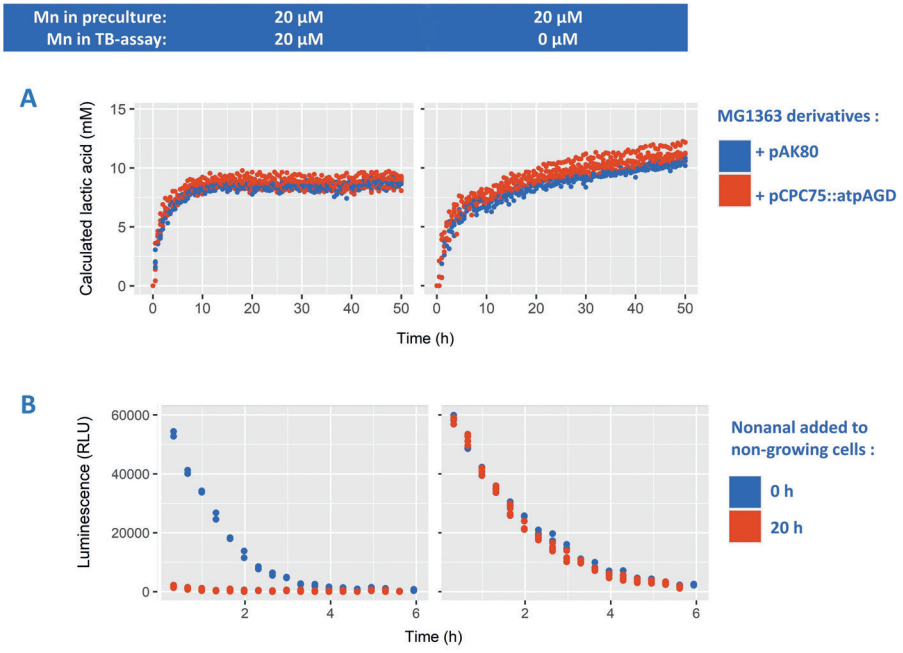

Figure 4.3 *Cells precultured with 20 µM Mn were transferred into TB assay with 20 µM Mn (left column) or 0 µM Mn (right column). (Panel A)* Lactococcus cremoris *MG1363 that harbours empty vector pAK80 (upper) or F1-ATPase encoding pCPC75::*atpAGD *(lower) at 2.0E+07 cells/mL were analysed for continuous measurement of medium pH to calculate lactic acid production overtime. (Panel B)* Lactococcus cremoris *MG1363 (pNZ5519) encoding bacterial* luxAB *luciferase was analysed for luminescence signal maintenance when starting the reaction after 0 h (blue) and 20 h (red) of incubation with TB. Cells were incubated at 1.0E+07 cells/mL and concentrated to 1E+08 cells/mL prior to luminescence detection. Experiment was carried out at least with 3 biological replicates.*

Volatile analysis from TB-cultures shows that the production of 3- and 2-methylbutanal within the first 23 to 95 hours was comparable throughout all conditions (Figure 4.4). However, in the presence of Mn, 3- and 2-methylbutanal continued to accumulate during 2 weeks of incubation to reach an average peak area of 7.5E+06 (arbitrary unit), which is approximately 3-fold higher than the maximum level reached in the absence of Mn. In contrast, BCAA-derived aldehydes were not further accumulating after the first 23 hours in absence of Mn and actually declined after 95 hours, suggesting their utilisation in aldehyde-consuming reactions. A known reaction for aldehyde conversion leads to formation of the corresponding alcohol (3- and 2-methylbutanol) catalysed by aldehyde-alcohol dehydrogenase, which is NADH dependent. We found that in the absence of manganese, the maximum peak area of 3-methylbutanol and 2-methylbutanol were increased approximately 10-fold and 5-fold, respectively, in the conditions without manganese compared to those where manganese was supplemented. In the presence of Mn, it is apparent that the reaction cascade stalls at the aldehyde formation and fails to convert to the alcohol, which agrees with the proposed NADH depletion.

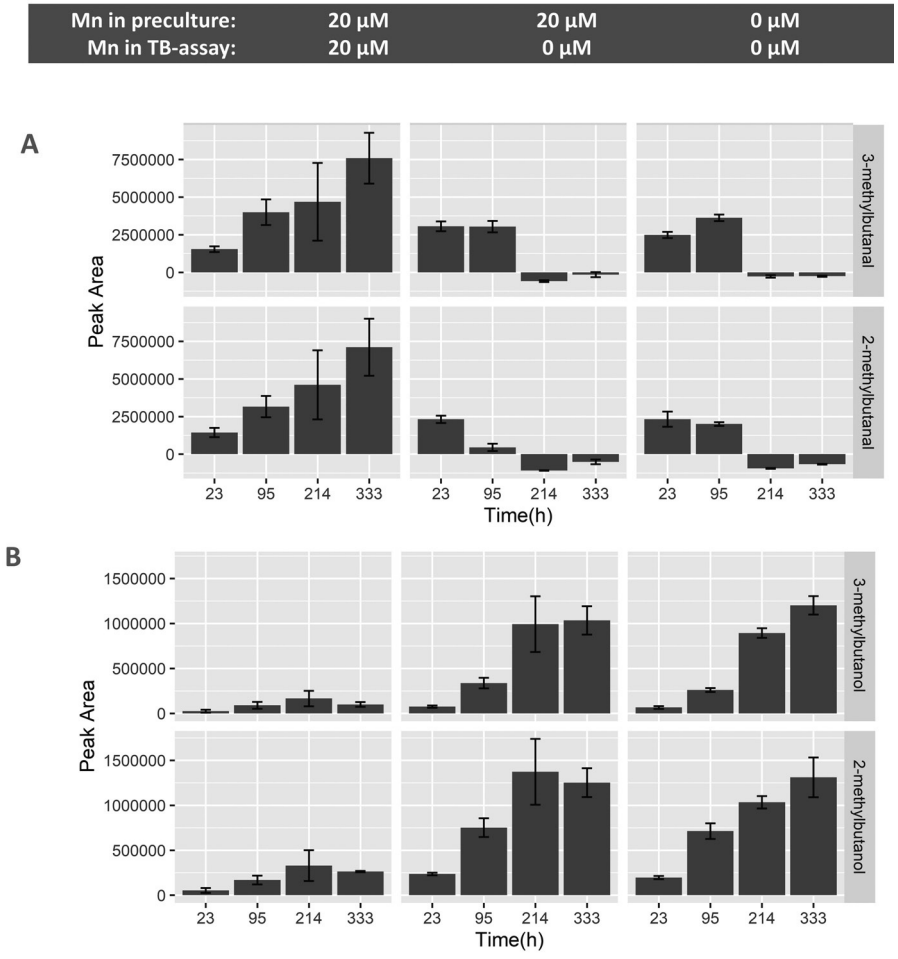

Figure 4.4 Lactococcus cremoris *NCDO712 was precultured in the presence (left and middle panel) and absence (right panel) of manganese (20 µM). Cells (2.5E+07 cells/mL) were transferred into fresh medium containing erythromycin (5 µg/mL) and 20 µM manganese (left panel) or 0 µM manganese (middle and right panel). GC-MS peak areas of 3-methylbutanal and 2-methylbutanal (panel A) as well as 3-methylbutanol and 2-methylbutanol (panel B) were measured throughout incubation. Error bars indicate the standard deviation from 3 biological replicates.*

4.4 Discussion

In this study, we evaluated how manganese influenced the physiology of *L. cremoris* and show that manganese omission from the growth medium did not impose a measurable growth rate reduction, while bringing a substantial survival advantage upon translational blocking. We observed that the adaptation of the cellular proteome to growth conditions that lack manganese mainly involves the upregulation of Mn importers. This may allow for the accumulation of minute levels of Mn contaminations from medium constituents inside the cell to achieve Mn levels that support a high growth rate. Although we did not determine intracellular Mn concentrations, it has previously been reported that *Lactococcus cremoris* MG1363, accumulated up to 0.7 mM Mn intracellularly during growth in the medium that was also employed in this study[38]. The study implied that manganese is required for lactococcal enzyme activities, making our finding that we can omit this metal from the medium without consequences in terms of growth or central energy metabolism even more striking. In addition, the results we report here are also contrasting the apparent dependency for Mn in other lactic acid bacteria species, to sustain rapid growth and oxygen tolerance[39,40].

Cytoplasmic manganese is important in lactococci, which is supported by the extensive transport systems dedicated for Mn homeostasis. Four Mn transport systems were suggested from the MG1363 genome, which includes the chromosomal NRAMP-family transporter (encoded by *mntH)*, an ABC transporter (encoded by *mtsAB* - see below*)*, and the putative Mn-Fe importer (encoded by *llmg1024-1025* - see below). Additionally, *L. cremoris* strain NCDO712 used in this study also harbours 6 plasmids, one of which encodes an extra copy of NRAMP-family transporter MntHp (encoded by $mntH_p$). Next to the characterised transport systems, the proteins encoded by *llmg*_1024-1025 (domain PF01988; detected with E-value 3.1E-41 and 3.1E-40, respectively) show the presence of a VIT1 domain that is also found in various Fe^{2+}/Mn^{2+}

import systems. The upregulation we found for these genes support the role of this protein in Mn import. From an evolutionary perspective, dairy lactococci need to acquire manganese of which the availability is limited in their natural environment. In bovine milk, Mn concentrations are reported to vary between 4 and 6.5 μM[41], which is in the same order of the concentration supplied in the present study. The total concentration of Mn in cheese was found at a similar level, which was between 5 and 20 μmol per kg cheese[42], but its bioavailability might be influenced by the pH, salt concentration, association with other (metal) ions or casein micelles, water activity, and various other factors[43]. The availability of redundant transporter systems is likely to ensure sufficient uptake under dynamic environmental conditions.

It was unexpected that in non-growing cells, we found that manganese supplementation at a physiological concentration for growth led to rapidly stagnating acidification and a culturability decline. This effect on acidification may result from the manganese-mediated modulation of the activity of enzymes in the central energy generating pathway. Within this metabolic pathway, various enzymes were reported to be dependent or activated by manganese such as FBPase, PGM, and LDH[1,9,44]. As a result, manganese addition might affect the homeostasis of this pathway. The balance of ADP/ATP and NAD^+/NADH are especially important as both have been implicated in controlling metabolic flux as well as fermentation end-product profiles from homolactic to mixed acids[34,45]. We demonstrated that in our setup the effects on central metabolism were associated with NAD^+/NADH rather than ADP/ATP disbalance.

Manganese deficiency might not be fully compensated by overproduction of Mn importers as demonstrated by the changes of NADH-utilising enzymes in the absence of Mn. If NADH is a rate-limiting factor, such changes might be an effort to tune the flux through those reactions and thereby preventing an excessive drain of the intracellular NADH pool. Alternatively,

regulating the level of these enzymes at low intracellular NADH concentrations may be necessary to maintain their flux at the required level. In contrast, translational blocking disallows proteome changes that may serve as cell's coping mechanism against NAD imbalance. Without proteome adjustment, a slight disbalance in NAD(H) regeneration might lead to a substantial depletion of NAD(H) over a prolonged period of time, which potentially explains the stagnating acidification of non-growing cells. Consequently, the lack of NADH also blocks other pathways that rely on its availability such as alcohol production in BCAA catabolism as well as $FMNH_2$ regeneration required for luminescence reaction (Figure 4.5). Nevertheless, it is remarkable that the long-term conversion of keto acids to aldehydes in this study was maintained even when central energy-generating pathway has halted for an extended period, implying that cells are likely to maintain a sufficiently high energetic state to import amino acids and that NADH depletion rather than ATP depletion corresponds to the emergence of VBNC state. In yeasts, it has been reported that NAD(P)H depletion is associated with VBNC state resulting from sulphite exposure[46,47]. In non-growing cells of retentostats, where the carbon source is continuously supplied albeit rapidly utilised[48], the production of various aldehydes from amino acid degradation such as benzaldehyde, benzeneacetyladehyde, 3-(methylthio)-propanal was not only highly correlated with the low growth rate but also with the increased loss of culturability on agar. While intracellular NADH concentration was not measured in these retentostat studies, it could be that NADH disbalance coincides with the emergence of VBNC populations and coinciding accumulation of aldehyde-volatiles under those conditions.

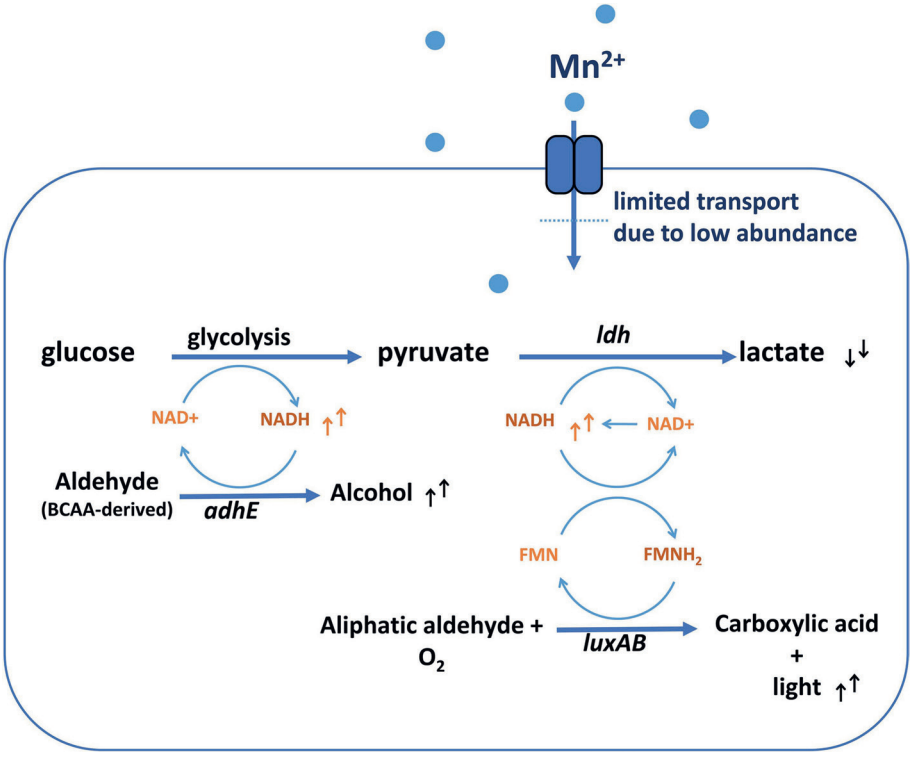

Figure 4.5 *Schematic simplification of the effect of manganese omission on the metabolism of TB-*L. cremoris *NCDO712. Limited manganese import might reduce glycolysis flux or LDH activity, but prevents NADH depletion and allows other NADH-dependent reactions to take place for a prolonged period. Increase or decrease of metabolic compounds measured upon manganese omission are indicated with the corresponding arrows.*

Our study is relevant for biotechnological and fermentation purposes, especially when the metabolism of non-growing cells that rely on cofactor recycling is of interest. As demonstrated, the prolonged stability of acidification and NADH regeneration are potentially crucial for the transition toward non-culturable state. Such transition is potentially relevant for various applications where cells are stored under suboptimal conditions such as commercial starters and probiotic products. In line with other investigations of lactococci at near-zero growth[49], the distinct end-metabolite and its accumulated formation by viable but non-culturable lactococci substantiate their potential important

role in flavour formation during ripening. This was exemplified by BCAA-derived volatiles that are particularly critical for the flavour characteristics of fermented foods. Aldehyde intermediates from BCAA catabolism are more potent flavour volatiles than their alcohol derivatives with an odour threshold that differs by two orders of magnitude[50]. The prolonged aldehyde formation in cells that no longer acidify and presumably no longer generating substantial levels of ATP imply that this metabolite formation is uncoupled from cellular energy status and growth and potentially very suitable for cell factory applications. Next to volatile production, the present study further highlights the relevance of our high-throughput non-growing model system for the investigation of starter cultures in cheese ripening where flavour formation by non-acidifying VBNC cells with limited protein synthesis can be mimicked. Finally, understanding the factors that influence the stability of prolonged metabolism through the presented TB model may provide new approaches in modulating the yield of desired compounds produced by non-growing cells.

4.5 Acknowledgments

The authors would like to thank Roelie Holleman for the HPAEC measurement of organic acids, Wilma Wesselink for the HS-SPME GC-MS measurement of volatiles, Peter Ruhdal Jensen who kindly provided strain MG1363(pAK80) and MG1363(pCPC75::atpAGD), as well as Jacques Vervoort for the constructive discussion.

References

1. Kehres, D. G. & Maguire, M. E. Emerging themes in manganese transport, biochemistry and pathogenesis in bacteria. *FEMS Microbiol. Rev.* **27**, 263–290 (2003).
2. Archibald, F. S. & Duong, M. N. Manganese acquisition by *Lactobacillus plantarum*. *J. Bacteriol.* **158**, 1–8 (1984).
3. Nies, D. H. The biological chemistry of the transition metal transportome of: *Cupriavidus metallidurans*. *Metallomics* **8**, 481–507 (2016).
4. Cowan, J. A. Structural and catalytic chemistry of magnesium-dependent enzymes. *BioMetals* **15**, 225–235 (2002).

5. Vernon, W. B. The role of magnesium in nucleic-acid and protein metabolism. *Magnesium* **7**, 234–248 (1988).

6. Foster, A. W., Osman, D. & Robinson, N. J. Metal preferences and metallation. *J. Biol. Chem.* **289**, 28095–28103 (2014).

7. Irving, H. & Williams, R. J. P. Order of stability of metal complexes. *Nature* **162**, 746–747 (1948).

8. Nierop Groot, M. N. *et al.* Genome-based in silico detection of putative manganese transport systems in *Lactobacillus plantarum* and their genetic analysis. *Microbiology* **151**, 1229–1238 (2005).

9. Holland, R. & Pritchard, G. G. Regulation of the l-lactate dehydrogenase from *Lactobacillus casei* by fructose 1,6 diphosphate and metal ions. *J. Bacteriol.* **121**, 777–784 (1975).

10. Archibald, F. S. & Fridovich, I. Manganese, superoxide dismutase, and oxygen tolerance in some lactic acid bacteria. *J. Bacteriol.* **146**, 928–936 (1981).

11. Barnese, K., Gralla, E. B., Valentine, J. S. & Cabelli, D. E. Biologically relevant mechanism for catalytic superoxide removal by simple manganese compounds. *Proc. Natl. Acad. Sci. U. S. A.* **109**, 6892–6897 (2012).

12. Nierop Groot, M. N. & De Bont, J. A. M. Involvement of manganese in conversion of phenylalanine to benzaldehyde by lactic acid bacteria. *Appl. Environ. Microbiol.* **65**, 5590–5593 (1999).

13. Smit, B. A. *et al.* Chemical Conversion of α-keto acids in relation to flavor formation in fermented foods. *J. Agric. Food Chem.* **52**, 1263–1268 (2004).

14. Ward, D. E. *et al.* Branched-chain α-keto acid catabolism via the gene products of the *bkd* operon in *Enterococcus faecalis*: a new, secreted metabolite serving as a temporary redox sink. *J. Bacteriol.* **182**, 3239–3246 (2000).

15. Dijkstra, A. R. *Spray Drying of Starter Cultures: Diverse Solutions within Lactococcus lactis to Improve Robustness*. (Universiteit van Amsterdam, 2015).

16. Rangel, D. E. N. Stress induced cross-protection against environmental challenges on prokaryotic and eukaryotic microbes. *World J. Microbiol. Biotechnol.* **27**, 1281–1296 (2011).

17. Anjem, A., Varghese, S. & Imlay, J. A. Manganese import is a key element of the OxyR response to hydrogen peroxide in *Escherichia coli*. *Mol. Microbiol.* **72**, 844–858 (2009).

18. Masuda, A., Toya, Y. & Shimizu, H. Metabolic impact of nutrient starvation in mevalonate-producing *Escherichia coli*. *Bioresour. Technol.* **245**, 1634–1640 (2017).

19. Wang, W. *et al.* Harnessing the intracellular triacylglycerols for titer improvement of polyketides in *Streptomyces*. *Nat. Biotechnol.* **38**, 76–83 (2020).

20. Graf, N. & Altenbuchner, J. Genetic engineering of *Pseudomonas putida* KT2440 for rapid and high-yield production of vanillin from ferulic acid. *Appl. Microbiol. Biotechnol.* **98**, 137–149 (2014).

21. Fuchino, K., Kalnenieks, U., Rutkis, R., Grube, M. & Bruheim, P. Metabolic profiling of glucose-fed metabolically active resting *Zymomonas mobilis* strains. *Metabolites* **10**, 81 (2020).

22. Gasson, M. J. Plasmid complements of *Streptococcus lactis* NCDO712 and other

lactic streptococci after protoplast-induced curing. *J. Bacteriol.* **154**, 1–9 (1983).

23. Wegmann, U. *et al.* Complete genome sequence of the prototype lactic acid bacterium *Lactococcus lactis* subsp. *cremoris* MG1363. *J. Bacteriol.* **189**, 3256–3270 (2007).
24. Koebmann, B. J., Solem, C., Pedersen, M. B., Nilsson, D. & Jensen, P. R. Expression of genes encoding F1-ATPase results in uncoupling of glycolysis from biomass production in *Lactococcus lactis*. *Appl. Environ. Microbiol.* **68**, 4274–4282 (2002).
25. Price, C. E. *et al.* Adaption to glucose limitation is modulated by the pleotropic regulator CcpA, independent of selection pressure strength. *BMC Evol. Biol.* **19**, 15 (2019).
26. Chen, Y. *et al.* Proteome constraints reveal targets for improving microbial fitness in nutrient-rich environments. *Mol. Syst. Biol.* **17**, e10093 (2021).
27. Vizcaíno, J. A. *et al.* 2016 update of the PRIDE database and its related tools. *Nucleic Acids Res.* **44**, D447–D456 (2016).
28. Nugroho, A. D. W., Kleerebezem, M. & Bachmann, H. A novel method for long-term analysis of lactic acid and ammonium production in non-growing *Lactococcus lactis* reveals pre-culture and strain dependence. *Front. Bioeng. Biotechnol.* **8**, 1170 (2020).
29. Bachmann, H., Kleerebezem, M. & Van Hylckama Vlieg, J. E. T. High-throughput identification and validation of *in situ*-expressed genes of *Lactococcus lactis*. *Appl. Environ. Microbiol.* **74**, 4727–4736 (2008).
30. Molenaar, D., Van Berlo, R., De Ridder, D. & Teusink, B. Shifts in growth strategies reflect tradeoffs in cellular economics. *Mol. Syst. Biol.* **5**, 323 (2009).
31. Basan, M. *et al.* Overflow metabolism in *Escherichia coli* results from efficient proteome allocation. *Nature* **528**, 99–104 (2015).
32. Goel, A. *et al.* Protein costs do not explain evolution of metabolic strategies and regulation of ribosomal content: Does protein investment explain an anaerobic bacterial Crabtree effect? *Mol. Microbiol.* **97**, 77–92 (2015).
33. Koebmann, B. J. *et al.* The extent to which ATP demand controls the glycolytic flux depends strongly on the organism and conditions for growth. *Mol. Biol. Rep.* **29**, 41–45 (2002).
34. Garrigues, C., Loubiere, P., Lindley, N. D. & Cocaign-Bousquet, M. Control of the shift from homolactic acid to mixed-acid fermentation in *Lactococcus lactis*: predominant role of the NADH/NAD+ ratio. *J. Bacteriol.* **179**, 5282–5287 (1997).
35. Weissbach, H. *et al.* Peptide methionine sulfoxide reductase: structure, mechanism of action, and biological function. *Arch. Biochem. Biophys.* **397**, 172–178 (2002).
36. Ganesan, B., Stuart, M. R. & Weimer, B. C. Carbohydrate starvation causes a metabolically active but nonculturable state in *Lactococcus lactis*. *Appl. Environ. Microbiol.* **73**, 2498–2512 (2007).
37. Bachmann, H., Santos, F., Kleerebezem, M. & Van Hylckama Vlieg, J. E. T. Luciferase detection during stationary phase in *Lactococcus lactis*. *Appl. Environ. Microbiol.* **73**, 4704–4706 (2007).
38. Goel, A., Santos, F., de Vos, W. M., Teusink, B. & Molenaar, D. Standardized assay

medium to measure *Lactococcus lactis* enzyme activities while mimicking intracellular conditions. *Appl. Environ. Microbiol.* **78**, 134–143 (2012).

39. Tong, Y. *et al.* System-wide analysis of manganese starvation-induced metabolism in key elements of *Lactobacillus plantarum*. *RSC Adv.* **7**, 12959–12968 (2017).

40. Archibald, F. S. & Fridovich, I. Manganese and defenses against oxygen toxicity in *Lactobacillus plantarum*. *J. Bacteriol.* **145**, 442–451 (1981).

41. Iyengar, G. V., Kasperek, K., Feinendegen, L. E., Wang, Y. X. & Weese, H. Determination of Co, Cu, Fe, Hg, Mn, Sb, Se and Zn in milk samples. *Sci. Total Environ.* **24**, 267–274 (1982).

42. Mendil, D. Mineral and trace metal levels in some cheese collected from Turkey. *Food Chem.* **96**, 532–537 (2006).

43. John, D. & Leventhal, J. Bioavailability of metals. In *Preliminary compilation of descriptive geoenvironmental mineral deposit models* (U.S. Geological Survey, 1995).

44. Crow, V. L. & Pritchard, G. G. Fructose 1,6 diphosphate activated L-lactate dehydrogenease from *Streptococcus lactis*: kinetic properties and factors affecting activation. *J. Bacteriol.* **131**, 82–91 (1977).

45. Koebmann, B. J., Westerhoff, H. V., Snoep, J. L., Nilsson, D. & Jensen, P. R. The glycolytic flux in *Escherichia coli* is controlled by the demand for ATP. *J. Bacteriol.* **184**, 3909–3916 (2002).

46. Park, H. & Hwang, Y. S. Genome-wide transcriptional responses to sulfite in Saccharomyces cerevisiae. *J. Microbiol.* **46**, 542–548 (2008).

47. Serpaggi, V. *et al.* Characterization of the ' viable but nonculturable' (VBNC) state in the wine spoilage yeast *Brettanomyces*. *Food Microbiol.* **30**, 438–447 (2012).

48. van Mastrigt, O., Abee, T., Lillevang, S. K. & Smid, E. J. Quantitative physiology and aroma formation of a dairy *Lactococcus lactis* at near-zero growth rates. *Food Microbiol.* **73**, 216–226 (2018).

49. van Mastrigt, O., Gallegos Tejeda, D., Kristensen, M. N., Abee, T. & Smid, E. J. Aroma formation during cheese ripening is best resembled by *Lactococcus lactis* retentostat cultures. *Microb. Cell Fact.* **17**, 1–8 (2018).

50. Smit, G., Smit, B. A. & Engels, W. J. M. Flavour formation by lactic acid bacteria and biochemical flavour profiling of cheese products. *FEMS Microbiol. Rev.* **29**, 591–610 (2005).

Chapter 4

Supplementary Material

Supplementary Methods

SM4.1 Construction of *Lactococcus cremoris* MG1363 (pNZ5519)

Plasmid-encoded luciferase (*luxAB*) of *Vibrio harveyi* was used as a reporter of NADH availability in *L. cremoris*. Plasmid isolation and electro-transformation were performed as described previously[1,2]. Plasmid pNZ5519 that contains the constitutive *usp45* promoter upstream of the *cre-luxAB* cassette was isolated from its cloning host *L. cremoris* NZ5500[2] and introduced to strain MG1363[3].

SM4.2 Composition of chemically-defined medium for prolonged cultivation (CDMPC) as described previously[4]

Buffer	MW	CAS	mg/L	mM
Potassium phosphate monobasic	136.09	7778-77-0	2750.00	20.207
Sodium chloride	58.44	7647-14-5	2900.00	49.624
Sodium phosphate dibasic	141.96	7558-79-4	2850.00	20.076
Vitamins	**MW**	**CAS**	**mg/L**	**μM**
(±)-α-Lipoic acid or DL-6,8-Thioctic acid	206.33	1077-28-7	2.00	9.69
D-Pantothenic acid hemicalcium salt	238.27	137-08-6	0.50	2.10
Biotin	244.31	58-85-5	0.10	0.41
Nicotinic acid	123.11	59-67-6	1.00	8.12
Pyridoxal hydrochloride	203.62	65-22-5	1.00	4.91
Pyridoxine (pyridoxol) hydrochloride	205.64	58-56-0	1.00	4.86
Thiamine hydrochloride	337.27	67-03-8	1.00	2.96
Metals	**MW**	**CAS**	**mg/L**	**μM**
Ammonium molybdate tetrahydrate	1235.86	12054-85-2	0.30	0.24
Calcium chloride dihydrate	147.02	10035-04-8	3.00	20.41
Cobalt(II) sulphate heptahydrate	281.10	10026-24-1	0.30	1.07
Copper(II) sulphate pentahydrate	249.68	7758-99-8	0.30	1.20
Iron(II) chloride tetrahydrate	198.81	13478-10-9	4.00	20.12
Magnesium chloride hexahydrate	203.30	7791-18-6	200.00	983.76
Manganese chloride tetrahydrate	197.91	13446-34-9	4.00	20.21

Zinc sulphate heptahydrate	287.56	7446-20-0	0.30	1.04
Amino acids	MW	CAS	mg/L	mM
L-Alanine	89.09	56-41-7	130	1.4592
L-Arginine	174.20	74-79-3	244	1.4007
L-Asparagine	132.12	70-47-3	80	0.6055
L-Aspartic acid	133.10	56-84-8	137	1.0293
L-Cysteine hydrochloride monohydrate	175.63	7048-04-6	61	0.3473
L-Glutamic acid	147.13	56-86-0	97	0.6593
L-Glutamine	146.14	56-85-9	96	0.6569
Glycine	75.07	56-40-6	29	0.3863
L-Histidine	155.15	71-00-1	24	0.1547
L-Isoleucine	131.17	73-32-5	82	0.6251
L-Leucine	131.17	61-90-5	117	0.8920
L-Lysine monohydrochloride	182.65	657-27-2	187	1.0238
L-Methionine	149.21	63-68-3	38	0.2547
L-Phenylalanine	165.19	63-91-2	64	0.3874
L-Proline	115.13	147-85-3	412	3.5786
L-Serine	105.09	56-45-1	172	1.6367
L-Threonine	119.12	72-19-5	68	0.5709
L-Tryptophan	204.23	73-22-3	36	0.1763
L-Tyrosine	181.19	60-18-4	50	0.27595
L-Valine	117.15	72-18-4	86	0.7341

SM4.3 Strain-specific cultivation condition

CDMPC was supplemented with lactose 30 mM for strain NCDO712 and glucose 55 mM for the derivatives of strain MG1363. Chloramphenicol at final concentration of 5 μg/mL and riboflavin 10 mg/L was additionally supplemented for MG1363 harbouring the luciferase encoding pNZ5519. Erythromycin at final concentration of 5 μg/mL was additionally supplemented for MG1363 harbouring empty vector of pAK80 and MG1363 harbouring F1-ATPase encoding pCPC75::atpAGD. A stock of manganese chloride (2 mM) was prepared separately from the CDMPC metal supplement (in which manganese was omitted) and added into the medium to a final concentration of 20 μM

when indicated. Glycerol stocks of 25-generation precultured strains were used for subsequent proteome and non-growing TB-cell suspension fermentation studies.

SM4.4 Growth rate measurements

Aliquots (75 µL) of *Lactococcus cremoris* NCDO712 from each serial propagation was transferred to a 384-well microtiter plate (clear). Optical density at 600 nm (OD_{600}) was measured every 30 minutes until cultures reached stationary phase. Raw data files from the microplate reader were analysed and plotted with R (v 3.6.1). Maximum specific growth rates were calculated by determining the slope of the ln-transformed linear part of the growth curve.

SM4.5 Proteome sample preparation and analysis

Cells were harvested by centrifugation at maximum speed for 3 minutes at 4°C, dissolved in 100 mM TRIS pH 8 to an approximate concentration of 7.5E+08 cells/mL and flash frozen. Protein isolation was performed using a modified version of the In-StageTip procedure[5]. Cell suspensions were defrosted on ice and 100 µL was lysed in a water bath sonicator (Branson2510) for 5 minutes with cooling on ice in between. The lysed culture (40 µL) was loaded on StageTips containing a double Empore C18 membrane. Protein lysates were washed with 100 µL 50 mM ammonium bicarbonate (ABC), reduced with 20 µL 20 mM dithiothreitol for 45 minutes at 60°C and subsequently alkylated with 20 µL 20 mM acrylamide for 30 minutes at room temperature. The alkylated sample was washed with 100 µL ABC and 100 µL 95% ABC/5% acetonitrile. Proteins were digested overnight with 20 µL 5 ng/µL trypsin (Roche) at room temperature. Peptides were eluted and the membranes were washed with 70 µL 1 mL/L formic acid in water and with 5 µL 50% acetonitrile/50% 1 mL/L formic acid in water.

Mass spectra analysis was performed as described previously[6]. Raw datafiles were analysed using MaxQuant (version 1.6.1.0) and searched against the *L. cremoris* MG1363 database (Uniprot) supplemented with NCDO712 plasmid data[7] and frequently observed contaminants. In addition to the standard settings, Trypsin/P with a maximum of two missed cleavages was set as the digestion mode, acrylamide modifications on the cysteines were set as a fixed modification, and methionine oxidation, protein N-terminal acetylation and asparagine or glutamine deamidation were set as variable modifications. A false discovery rate of 1% at protein level was allowed and the minimum required peptide length was set at 7 amino acids. At least two peptides were required to allow protein identification and quantification with at least one peptide being unique in the database.

Statistical analysis on the MaxQuant output was performed with Perseus version 1.6.2.1. Proteins were accepted when it was measured in at least 3 of the 4 replicates. For statistical analysis log10 transformed LFQ values were used and zero values were replaced by taking random values from a normal distribution with mean (measured values per biological sample -1.8) and variation (0.3 x standard deviation of the measured values per biological replicate) to enable comparative quantifications. We then performed a 2-sided two sample t-tests using the log10 normalised LFQ intensity between manganese addition and omission with an FDR threshold of 0.05 and $S_0 = 0.01$[8]. Fold changes of Mn addition over Mn omission condition were calculated by dividing the log10 normalised LFQ intensity columns.

SM4.6 Fermentation end-product analysis

The concentrations of fermentation end-products in the growth media (lactic acid, formic acid, acetic acid, and ethanol) produced by strain NCDO712 were determined by high performance anion exchange chromatography (HPAEC) with UV and refractive index (RI) detection as previously described[9].

Culture supernatant samples were collected and filtered using 0.20 µm polyethersulfone (PES) membranes and stored at -20°C before analysis.

To determine the volatile compounds formed during incubation of cell suspensions in different media, a headspace solid phase microextraction (HS-SPME) was carried out in combination with gas chromatography/mass spectrometry (Fisons, USA) as previously described[10] with a few modifications. The solid phase extraction was carried out with a grey SPME fibre (Carboxen/PDMS/Divinylbenzene; Supleco, USA) for 15 minutes at 40°C. Subsequently, the fibre was desorbed for 3 minutes at 250°C in a splitless mode. The extracted compounds were refocused at the beginning of the column by cold trapping at -110°C. Subsequently the trap was heated to 250°C at a rate of 50°C/sec and the compounds were separated on a VF-Wax ms (30 m × 0.25 mm, df = 0.5 µm) capillary column (Varian, USA). The GC separation started at 40°C for 2 min, thereafter the temperature was raised with 10°C/min till 250°C and kept at 250°C for 5 min. Mass spectral data was recorded in Full Scan mode over a range of m/z 25-250.

SM4.7 Viable cell enumeration and membrane integrity analysis

Measurements of culturable cells of NCDO712 during TB assay were performed through plating on CDMPC supplemented with 1% glucose and 0.5% UltraPure agarose (Invitrogen 16500500). Serial dilutions were prepared in PBS and 100 µL of the diluted cultures were plated on agar plates. Plates were incubated at 30°C for 24-48 hours and colonies were enumerated.

Membrane integrity of cells during prolonged incubation was analysed using Live/Dead® BacLightTM Bacterial viability and counting kit (Invitrogen L34856) and a BD LSR Fortessa Flow Cytometry instrument (BD Biosciences), according to manufacturer instructions. A staining mixture was prepared with 1.5 µL of PI (λex/em: 535/617 nm), 1.5 µL of SYTO 9 (λex/em: 485/498 nm) stock-solutions, 5 µL microsphere standard (1E+08 beads/mL), 892 µL of

running buffer (FACS Flow), and 100 μL of sample resulting in a total of 1 mL assay reaction. Fluorescence signals were measured with FITC (bandpass filter 530/30 nm) and PE-Texas Red (bandpass filter 610/20 nm) detectors. Gating was performed on the basis of fresh overnight culture (live) and cells incubated in 60% ethanol (dead). Live cells were characterised as population with high signal in FITC detector, but low signal in PE-Texas Red detector. Dead cells were characterised as the population with low signal in FITC detector, but high signal in PE-Texas Red detector. The third population of cells that was recognized displays high signal in both detectors, thereby placing these cells intermediately between the "live" and "dead" populations. Although the viability status and physiology of these cells is not entirely clear, we classified this population as "damaged cells" based on their staining characteristics.

Supplementary Data

SD4.1 Growth characteristics of *L. cremoris* NCDO712 in the presence or absence of Mn

The effect of manganese omission on the growth of our model strain NCDO712 was monitored throughout 4 subcultures (Figure SD4.1). Growth rate, final optical density (OD_{600}) and final pH were measured every subculture, while organic acid composition was characterised at the end of the first and the third subculture. Growth rate of the 4^{th} subculture and organic acid composition of the 3^{rd} subculture was shown in Figure 4.1.

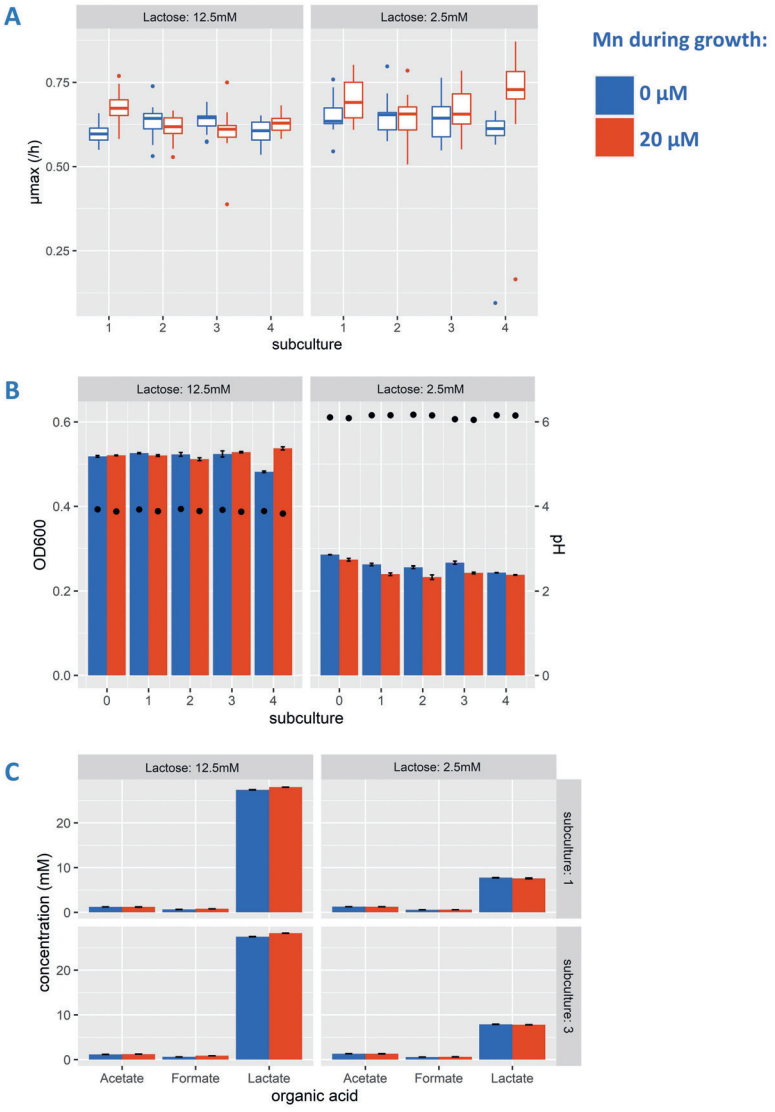

Figure SD4.1 Lactococcus cremoris *NCDO712 was serially propagated 4 times in defined medium supplemented with lactose at excess (12.5 mM – growth stops due to acid accumulation) or limited (2.5 mM – growth stops due to carbon depletion) concentration in the presence (red) and absence (blue) of manganese (20 µM). Maximum specific growth rate (panel A) and maximum* OD_{600} *and minimum pH (panel B) were measured throughout the subcultures. Concentrations of organic acids (panel C) were measured after the* 1^{st} *and the* 3^{rd} *subculture step. Roughly 5 generations of growth occur in every subculture. Error bars indicate the standard deviation from 3 biological replicates, except for organic acids measurement where 2 biological replicates were analysed.*

SD4.2 Acidification profile of translationally-blocked *L. cremoris* NCDO712 in the presence or absence of Mn

Organic acids were measured from translationally-blocked cells of strain NCDO712. Next to lactic acid, which is shown in panel A of Figure 4.2, formic acid and acetic acid were quantified as well. In all samples, lactic acid makes up at minimum 85% of the total acid concentrations in Cmol.

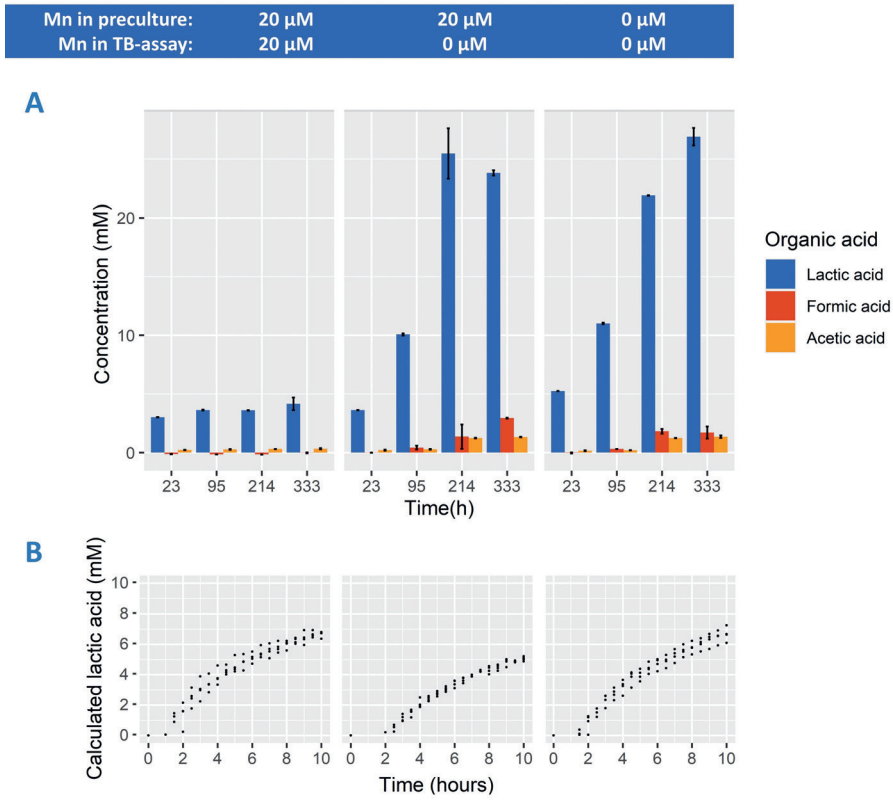

Figure SD4.2 Lactococcus cremoris *NCDO712 was subcultured 4 times in defined medium supplemented with lactose in the presence (left and middle panel) and absence (right panel) of manganese (20 µM). Cells were transferred at approximately 2.5E+07 cells/mL into fresh medium containing 5 µg/mL erythromycin, 30 mM lactose, and when indicated 20 µM manganese (left panel). Concentration of organic acids (panel A) was measured for lactic acid (blue), formic acid (red), and acetic acid (orange) throughout incubation at 30°C. Continuous measurement of medium pH to calculate lactic acid production for the first 10 hours can be seen in panel B. Error bars indicate the standard deviation from 3 biological replicates.*

SD4.3 Superoxide dismutase or oxidative stress plays no role in stagnated acidification of translationally-blocked cells in the presence of Mn

To investigate the role of oxidative stress in relation to manganese, we employed strain NZ9000Δ*sodA*[11] that is deficient of superoxide dismutase (SOD) and thereby more sensitive to oxidative stress. As a control, we utilised the wildtype strain NZ9000, which is the host strain for the nisin controlled gene expression (NICE) system[12] and a close derivative of strain MG1363. Cells were precultured in the presence of manganese and translationally-blocked assay was performed as described in the Methods section at a cell density of 2.5E+07 with glucose (55 mM) as the carbon source. Acidification of SOD-deficient mutant (Figure SD4.3) was lower than its wildtype likely due to exposure to oxygen following harvesting and assay preparation. Nonetheless, the phenotypes observed in our model strain were reproducible. Stagnated acidification was observed in the presence of manganese and cells continued to acidify in the absence of manganese. This suggest that superoxide dismutase is unlikely to be the underlying mechanism of the phenomenon described in the present study. Moreover, throughout the experiments, *L. cremoris* was incubated without aeration and with limited headspace. With different Mn supplementation, the remaining dissolved oxygen in the medium did not lead to a significant differential expression of oxidative stress response, e.g., superoxide dismutase (SodA) in our proteomics data. LFQ intensity of SodA ranged between 7.1 and 7.4 in the absence of Mn, which is a slightly lower range than between 7.3 and 7.85 when manganese is present.

While we do not consider oxidative stress to be a major threat in our setup, we still tried to consider the contribution of other factors that lead to oxidative stress. In *L. cremoris*, iron can be imported by MntH and was found to be more accumulated with higher extracellular manganese concentration, resulting in higher oxidative stress due to Fenton-type reaction[13]. Among other

glycolytic enzymes, GAPDH was found to be the most sensitive to radical oxygen species (ROS)[14,15]. In this scenario, the lack of manganese would reduce iron import and the subsequent formation of ROS by Fenton-type reactions. This potentially prevents GAPDH inactivation, the eventual stagnated acidification and NADH depletion. However, our experiments with strain MG1363 showed that the absence of a plasmid-encoded $MntH_p$ did not seem to delay the occurrence of stagnated acidification. It also has to be noted that the concentration of manganese and iron in the present study is 50- and 5-fold respectively lower than in Turner et al. (2007). In combination with the absence of oxidising agents and aeration, we consider the oxidative stress explanation to be very unlikely.

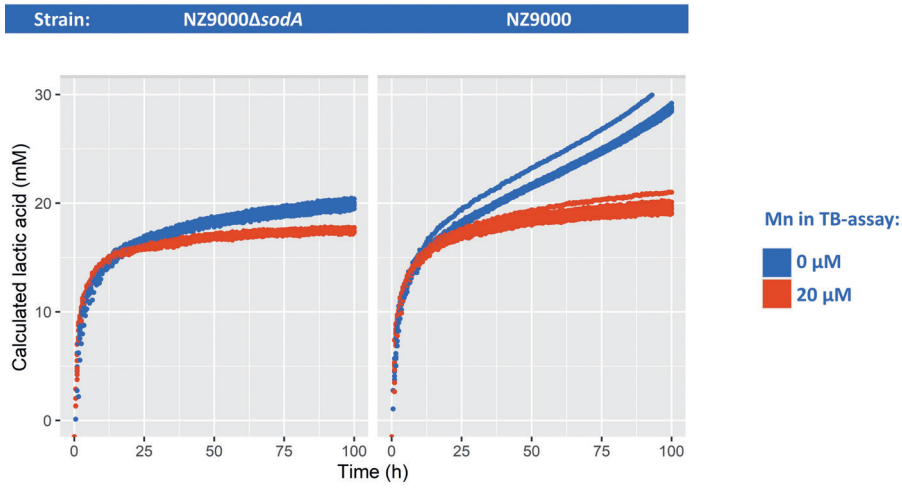

Figure SD4.3 Lactococcus cremoris *NZ9000 (right panel) and its derivative that contains deletion of superoxide dismutase (*sodA*) was precultured in the presence of manganese (20 µM). Cells (2.5E+07 cells/mL) were transferred into fresh medium containing translational blocker erythromycin (5 µg/mL) and 20 µM manganese (red) or 0 µM manganese (blue). Continuous measurement of medium pH to calculate lactic acid production overtime is shown. Experiment was carried out with 3 biological replicates.*

References

1. Bachmann, H., Santos, F., Kleerebezem, M. & Van Hylckama Vlieg, J. E. T. Luciferase detection during stationary phase in *Lactococcus lactis*. *Appl. Environ. Microbiol.* **73**, 4704–4706 (2007).
2. Bachmann, H., Kleerebezem, M. & Van Hylckama Vlieg, J. E. T. High-throughput identification and validation of *in situ*-expressed genes of *Lactococcus lactis*. *Appl. Environ. Microbiol.* **74**, 4727–4736 (2008).
3. Wegmann, U. *et al.* Complete genome sequence of the prototype lactic acid bacterium *Lactococcus lactis* subsp. *cremoris* MG1363. *J. Bacteriol.* **189**, 3256–3270 (2007).
4. Price, C. E. *et al.* Adaption to glucose limitation is modulated by the pleotropic regulator CcpA, independent of selection pressure strength. *BMC Evol. Biol.* **19**, 1-15 (2019).
5. Kulak, N. A., Pichler, G., Paron, I., Nagaraj, N. & Mann, M. Minimal, encapsulated proteomic-sample processing applied to copy-number estimation in eukaryotic cells. *Nat. Methods* **11**, 319–324 (2014).
6. Sotoca, A. M. *et al.* Quantitative proteomics and transcriptomics addressing the estrogen receptor subtype-mediated effects in T47D breast cancer cells exposed to the phytoestrogen genistein. *Mol. Cell. Proteomics* **10**, (2011).
7. Tarazanova, M. *et al.* Plasmid complement of *Lactococcus lactis* NCDO712 reveals a novel pilus gene cluster. *PLoS One* **11**, e0167970 (2016).
8. Tusher, V. G., Tibshirani, R. & Chu, G. Significance analysis of microarrays applied to the ionizing radiation response. *Proc. Natl. Acad. Sci. U. S. A.* **98**, 5116–5121 (2001).
9. Hugenholtz, J. & Starrenburg, M. J. C. Diacetyl production by different strains of *Lactococcus lactis* subsp. *lactis* var. *diacetylactis* and *Leuconostoc* spp. *Appl. Microbiol. Biotechnol.* **38**, 17–22 (1992).
10. Gamero, A., Wesselink, W. & de Jong, C. Comparison of the sensitivity of different aroma extraction techniques in combination with gas chromatography-mass spectrometry to detect minor aroma compounds in wine. *J. Chromatogr. A* **1272**, 1–7 (2013).
11. Fu, R. Y. *et al.* Introducing glutathione biosynthetic capability into *Lactococcus lactis* subsp. *cremoris* NZ9000 improves the oxidative-stress resistance of the host. *Metab. Eng.* **8**, 662–671 (2006).
12. Kuipers, O. P., De Ruyter, P. G. G. A., Kleerebezem, M. & De Vos, W. M. Quorum sensing-controlled gene expression in lactic acid bacteria. *Journal of Biotechnology* vol. 64 15–21 (1998).
13. Turner, M. S., Yu, P. T. & Giffard, P. M. Inactivation of an iron transporter in *Lactococcus lactis* results in resistance to tellurite and oxidative stress. *Appl. Environ. Microbiol.* **73**, 6144–6149 (2007).
14. Cesselin, B. *et al.* Responses of lactic acid bacteria to oxidative stress. in *Stress Responses of Lactic Acid Bacteria* 111–127 (Springer US, 2011).
15. Weber, H., Engelmann, S., Becher, D. & Hecker, M. Oxidative stress triggers thiol oxidation in the glyceraldehyde-3-phosphate dehydrogenase of *Staphylococcus aureus*. *Mol. Microbiol.* **52**, 133–140 (2004).


5

Chapter 5

Glycolytic Flux Increase in *Lactococcus cremoris* Accelerates Pathway Decay and Reduces Cumulative Product Yield

Nugroho, A. D. W., Kleerebezem, M. & Bachmann, H.

Manuscript submitted for publication (Letter format)

Abstract

Non-growing cells are commonly encountered and often desired in biotechnological applications to maximise product yields. Such cells exhibit limited protein synthesis, and their metabolic functionality relies on the long-term stability and repair of enzymes to sustain metabolic activity. However, knowledge of the factors that influence prolonged metabolism is lacking. An example is the production of lactic acid (LA)[1–3]. Here we show that prolonged LA formation in translationally-blocked (TB) cells is not constrained by the number of catalytic cycles, as commonly assumed, but by the metabolic flux. We found that faster conversion leads to faster pathway decay and most importantly lower cumulative yield, and vice versa. This behaviour is consistent irrespective of whether the flux is altered through manganese addition, changing the cellular ATP demand, or enzyme expression levels. Our results imply that *in vivo* functional life-span, rate, and cumulative yield of enzymes can be modulated through a non-engineering approach, i.e., by preculture conditions.

5.1 Faster glycolysis accelerates pathway decay and reduces cumulative product yield

Improving prolonged metabolite formation is of significant industrial interest since it increases production efficiency and thereby the overall yield. In various processes, long-term suboptimal conditions induce microbial cells to enter a non-growing but metabolically active state. For example, to minimise bioprocess and refinery costs, LA is produced with cells supplied solely with glucose without other nutrients, thereby rendering them non-growing[4]. Similarly, valorisation of side streams as raw materials that contain inhibitory compounds[1] may result in growth arrest. In the absence of growth, whole-cell metabolic conversions depend on the flux stability that is dependent on initial expression level in combination with deactivation and/or degradation kinetics of active enzymes. These factors vary significantly under different environmental conditions[5]. Moreover, during growth or biomass production, the preculture conditions could influence cellular fitness through "cell-memory" and the expression of proteins related to stress response or repair[6]. Altogether, the final metabolite yield of processes that (in part) involve non-growing metabolically active cells relies on the stability of cellular metabolism, which is still poorly understood.

At present, there is a lack of a parameter to represent stability and yield of metabolism, especially *in vivo*. TTN (total turnover number) is often used, which is a dimensionless number, defined as the number of catalytic events performed by one active site of one molecule of the enzyme during its lifespan[7]. While various factors can deactivate an enzyme (pH, oxygen radicals, or chaotropes)[8], TTN is typically determined in relation to temperatures. However, TTN does not necessarily reflect the kinetic profile or behaviour of the decay over time of biocatalysis. In whole-cell biocatalysis, the modelling of metabolic stability is even more challenging since product formation involves a number of enzymes and further depends on substrate import as well as enzyme-interactions with other intracellular components, like molecular chaperones[9]. With the advancement of 'omics technology, several parameters to represent *in vivo* protein stability were proposed, such as mRNA/protein

ratio between 2 growth rates[10] or CCR (Catalytic Cycles until Replacement), which is a ratio between flux and protein turnover rate[11]. However, both calculations are confounded by growth or flux predictions that do not always accurately reflect *in vivo* enzyme or protein lifetime, and thus experimental approaches are still required for their validation.

In this study, we define yield as the cumulative amount of a metabolite, in our particular case lactate, produced by a cell before metabolite production seizes. We used translationally-blocked cells of *L. cremoris (*previously *L. lactis* subsp*. cremoris)* as a model organism[12] to investigate prolonged biocatalysis in non-growing cells. With a previously established method that allows to follow LA formation over weeks[12], we examined the effect of the carbon source in the preculture of cells followed by a transition to the same or a different sugar. In short, acidification is monitored via a fluorescent pH indicator continuously in a sugar containing buffer. The buffer concentration and cell density are tailored to allow acidification without product inhibition for weeks while no new protein is made due to the addition of a translational inhibitor. In *L. cremoris* strain NCDO712, the sugar preculture determines the expression level of the Le Loir and Tagatose pathway for the utilisation of galactose and lactose, respectively. In glucose-precultured cells, both pathways are repressed but limited utilisation of galactose[13] or lactose[14] is facilitated by promiscuous activities or by the low levels of existing transporters or glycosyl hydrolase. Following the different precultures, translational blocking and transitioning to different sugars we expectedly found that acidification rates varied between conditions. Glucose-utilisation was overall the fastest during the first week after the transition (Figure 5.1A). In glucose-precultured cells (middle panel, Figure 5.1A), galactose and lactose utilisation were significantly slower than glucose-utilisation. After glucose transition, 10 mM of LA was produced within 1 day while it took 3 and 4 days to produce the same amount of LA on galactose and lactose, respectively. However, following 10 mM LA production, the performance of glucose-transitioned cells declined at a faster rate than its galactose or lactose counterpart. The LA production-rate in glucose was subsequently surpassed by the production-rate in galactose and lactose after about two weeks following the initiation of the conversion. By the end of the

assay (approximately 3 weeks), the highest amount of LA was achieved by cells converting lactose, which formed a total of approximately 20 mM of LA. This amount is 33% higher than the 15 mM of LA produced by cells converting glucose.

The difference in the decline of prolonged acidification is therefore not related to the number of catalytic cycles because in our system no new enzymes could be synthesized due to the continuous presence of a translation inhibitor[12]. To demonstrate this, we calculated the production rate as the first-order of time-derivative and visualised it as a function of the LA produced (Figure 5.1B). If the number of catalytic cycles influences the decay, parallel lines would have been observed, which is not the case in our analysis. The decay of production rates varies between conditions and is not solely explained by the preculture or the type of sugar during the translationally-blocked cell assay. We hypothesized that such differences in the decline of prolonged acidification mainly originates from the kinetic differences, rather than other possible factors, i.e., proteome differences. Therefore, we calculated the decay constant and initial (maximum) production rate based on the second derivative and the intercept of the lines in Figure 5.1B, respectively. We found a linear correlation (R-squared of 0.93) between the decay constant and the initial production rate (Figure 5.1B). This indicates a trade-off between flux and the cumulative yield of LA.

The strong correlation between the maximum acidification rate and decay rate observed with different sugar precultures and transitions led us to question whether the same relation is found when using other means of modulating the LA production rate. This was done to exclude that the distinct decline of LA production observed following transition could be specifically caused by metabolic feedback mechanisms. To investigate whether the cumulative LA yields of acidification vary with other treatments, we employed (1) a titration of manganese into the medium and (2) strains that overexpress the F1-ATPase at different levels. Both approaches modulate the acidification rate through different mechanisms. Manganese titration was found to influence the acidification rate through activation of enzymes and/or NADH availability[15].

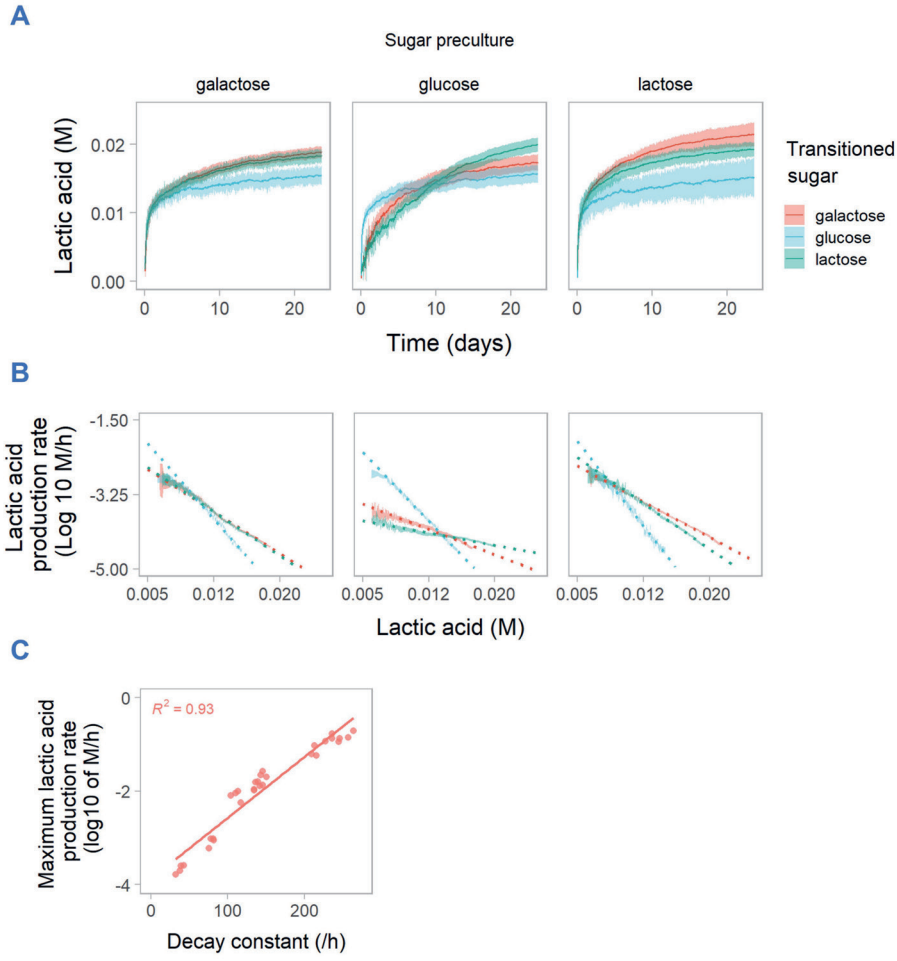

Figure 5.1 *Prolonged acidification of* L. cremoris *NCDO712 (1E+07 cells/mL) prepared in three different precultures and transitioned to three sugars (differentiated by colour). (A) The accumulation of lactic acid overtime. Solid lines indicate the average four biological replicates. (B) Production rate (1st time-derivative) as a function of LA produced. Column label indicates the sugar of the preculture. Dashed lines indicate data projection based on a linear fit. In both figures, shaded ribbons indicate the 95% confidence interval. (C) Based on curve fits, kinetic parameters are obtained. Maximum production rate (intercept of production rate in 5.1B) shows a good linear correlation (solid red line) with decay constants (slope of production rate in 5.1B). Averages of the kinetic parameters are provided in Supplementary Data Table SD5.1.*

In contrast, F1-ATPase overexpression modulates acidification rate through increased ATP demand, which drives higher glycolytic flux, especially in non-growing cells in *L. cremoris*[16]. Both approaches allow us to tune acidification rate in a finer manner compared to the different sugar precultures. Additionally, we compared different closely-related strains to investigate whether the previous observation is strain-dependent. We would also like to note that all the conditions tested have comparable metabolite profiles with LA as the main metabolic end product[12,15,17].

In line with previous observations[15], the addition of manganese to glucose-precultured cells increased the initial rate of acidification, which gradually decreased. The decrease was faster (steeper slope in Figure 5.2A) for cultures with a high initial LA production rate (leftmost data points on the y-axis in Figure 5.2A). We observed that strain MG1363 (plasmid-deficient, prophage-cured derivative of NCDO712) was more sensitive to manganese-induced acidification decay than strain NCDO712, which led to fewer conditions (Mn <1.5 mM) feasible for rate analysis. However, the correlation between rate and decay (Figure 5.2B) remain strong for both strains (R-squared >0.90). Remarkably, this trade-off was still observed when the modulation of acidification rate was achieved by using 9 engineered strains (Figure 5.2C) that constitutively overexpress various levels of the lactococcal F1-ATPase enzymes[16]. The results demonstrated that these acidification rate modulations also showed that faster initial acidification rate leads to a higher decay constant (R-squared 0.72, Figure 5.2D). Taken together, we show that irrespective of the approach employed to modify the acidification rate in lactococci, there is a consistent trade-off between the initial acidification rate and the decay constant as well as the cumulative LA yield.

To understand whether the degree of flux-dependent decay varies with different acidification rate modulations, we sought to calculate a global correlation coefficient. Previous modulations were done in different strains and preparations, which consequently shows a slightly different equation of the correlation between maximum rate and decay constant. The calculated slopes of the correlation vary between 0.0080 and 0.0131 for the earlier presented

modulations. In addition, it is unknown how different modulations interact and whether the effect will be additive or multiplicative. Hence, we further modulated the acidification rate of ATPase mutants with manganese titrations. Altogether, we achieved a more than 300-fold increase in the maximum acidification-rate across conditions (2.5-fold difference on the log scale in Supplementary Data Figure SD5.1). While we did not detect an interaction between modulations, a more pronounced rate increase (approximately 4-fold higher on a linear scale) due to manganese titration was found in strains with F1-ATPase activity above 95 Miller units. The total dataset (Figure 5.3) results in a Pearson correlation with an R-squared of 0.92, indicating a generic observation and demonstrating the inherent influence of rate increase on activity decay irrespective of other experimental variables. A 10-fold increase in the initial acidification rate corresponds with a 1.8 times faster decay of the enzyme activity. If extrapolated to the point where production rate drops under 1E-05 M/h this would result in a 25.7% lower cumulative LA yield.

To our knowledge, this is the first demonstration of the trade-off between conversion rate and cumulative product yield. Our result challenges the common view that enzymes under a non-stress condition catalyse a similar number of reactions in their lifespans, which might be confounded by the fact that studies typically do not measure conversion rates for prolonged periods. This research shows that the decline of *in vivo* enzyme performance in translationally-blocked non-growing cells is exacerbated by a fast catalytic rate, which bears a direct consequence on its cumulative yield. A trade-off between activity and stability have been described earlier. However, such correlations originate from sequence variations of the proteins studied, which may affect their molecular integrity in addition to activity or conversion rates[18]. Next to that, activity-stability trade-offs are often assessed in relation to temperatures particularly in the range that is considered as stress and typically determined within less than 1 hour[19]. We measured enzyme activity within intact cells up to a period of 3 weeks, which was done with a dedicated assay to avoid substrate limitation or product inhibition[12]. Altogether, the presented approach fills the missing gap of *in vivo* determination of enzyme lifetime.

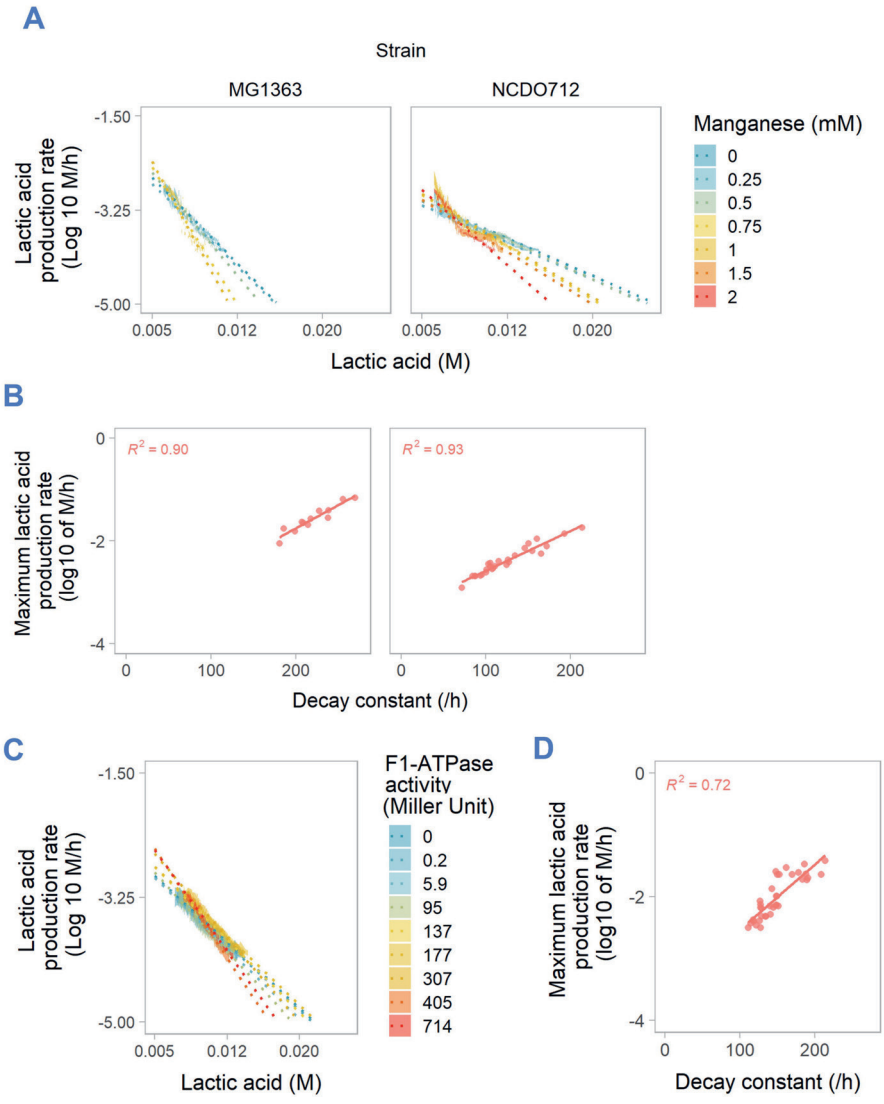

Figure 5.2 *Prolonged acidification of* L. cremoris *(2E+07 cells/mL) modulated through (A & B) manganese addition in strain MG1363 and NCDO712 (left and right column) or (C & D) varying F1-ATPase overexpression levels. (A & C) Production rate (1st time-derivative) based on lactic acid accumulation as a function yield. F1-ATPase activity[16] (expressed in Miller unit) and manganese supplementation are indicated by the colour. (B & D) Based on curve fits, kinetic parameters are obtained, and linear correlations (solid red lines) of maximum rate and decay constant are shown. For both production rate graphs, average of four biological replicates is shown with shaded ribbon indicates 95% confidence interval, and dashed line indicates data projection based on linear fit. Averages of the data are provided in Supplementary Data Table. SD5.2 and SD5.3.*

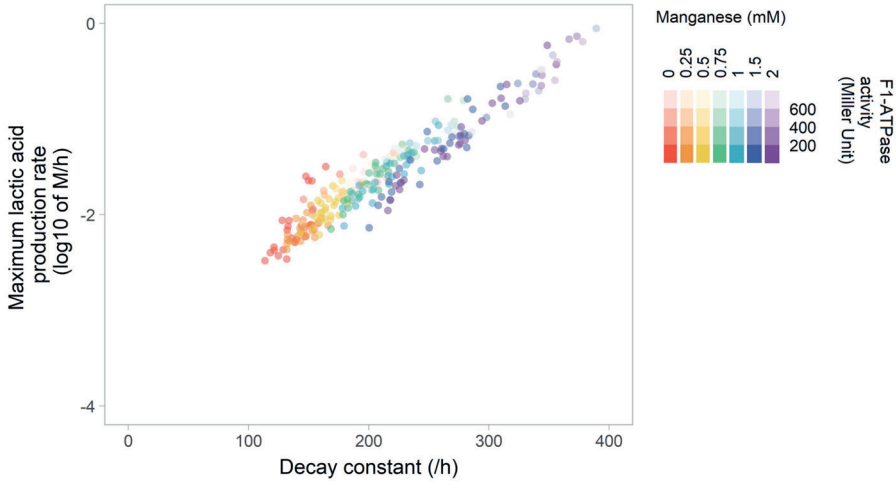

Figure 5.3 *Prolonged acidification of* L. cremoris *(2E+07 cells/mL) modulated through both manganese and F1-ATPase overexpression. Manganese supplementation is differentiated by colour, while F1-ATPase activity is differentiated by colour saturation. The formula of the linear model is y= 0.00791x – 3.26. A detailed figure and averages of the data are provided in Supplementary Data Figure SD5.1 and Table SD5.4.*

Given that our model system measures the catabolic pathway from carbon import to LA production, the global correlation coefficient of rate and decay potentially reflects the least stable protein of this pathway, or "the weakest link". This suggests that an improvement of prolonged activity might be achieved either through protein engineering of the most sensitive protein, or through a better selection of the operating regime. While processes typically operate at temperatures optimised for production rate, our data suggest that under such conditions rapid deactivation can lead to shorter process operating time and more frequent downtimes. Alternatively, a biocatalysis regime might be optimised for the overall product yield, but that optimisation might come with longer conversion times. Conversely, processes that aim for a specific product yield may benefit from conditions that allow maximal rate with the concomitant production decline due to pathway decay in order to prevent further product formation after the desired level of metabolic product is reached. Such scenario may be worked out to prevent the undesired post-production acidification in products like yoghurt. Hence, understanding conversion decay in non-growing cells is needed not only for production

efficiency but also product stability. From an ecological point of view this finding opens questions on the role of metabolic fluxes in growth arrested organisms. It remains to be seen if the described trade-off impacts the fitness of organisms that compete either through rate-determined substrate competition or through cumulative-yield-determined environmental changes such as increased organic acid concentrations. Finally, the production of LA makes use of central carbon metabolism, which is highly conserved across all domains of life[2], suggesting that similar rate-yield trade-offs may be applicable to the central metabolism of other organisms and eventually also other (biotechnologically - relevant) enzymatic pathways. In all cases, the demonstrated trade-off implies the potential role that catalytic rate might have on enzyme decay and this knowledge could provide alternative avenues to optimise biocatalysis process design and open different perspectives on metabolic activities of growth arrested environmental microorganisms.

5.2 Materials and methods

5.2.1 Strain and cultivation conditions

Lactococcus cremoris NCDO712[20] or MG1363[21] was grown on a chemically defined medium for prolonged cultivation (CDMPC)[22]. The medium was supplemented with either lactose 30 mM, galactose 55 mM, or glucose 55 mM depending on the strain and experimental design. *L. cremoris* MG1363 derivatives with uncoupled F1-ATPase activity (0-714 Miller unit)[17] were kindly provided by Peter Ruhdal Jensen from the National Food Institute of Technical University of Denmark. For these overexpression strains, cultivation was done in M17 (supplemented with 0.5% glucose and erythromycin 5 µg/mL). For each experiment, overnight cultures were prepared by inoculating from a frozen glycerol stock into a 10 mL medium with a 1,000-fold dilution factor. This resulted in a minimum of 10 generations growth in the preculture. The overnight culture was transferred to the corresponding fresh medium (50 mL) with 40-fold dilution factor and harvested at OD_{600} 0.1-0.2 (CDMPC) or 0.3-0.5 (M17). Incubation was done at 30°C.

5.2.2 The standard measurement of activity decay in intact cells

Long-term analysis of metabolite production was performed as described earlier[12]. For strains harbouring an erythromycin resistance gene, chloramphenicol (50 μg/mL) was used for translation inhibition in place of erythromycin. For manganese-modulated acidification, a separate working stock of manganese (400 g/L) was prepared to be added to the medium at a desired concentration. Sugar was provided depending on experimental design at excess final concentration of 30 mM (lactose) or 55 mM (glucose or galactose). All measurements were done with 4 biological replicates in 384-well plate for each treatment. Raw data files were analysed and plotted with RStudio (v 1.1.463).

5.3 Acknowledgments

The authors would like to thank Peter Ruhdal Jensen who kindly provided F1-ATPase overexpressing strains, as well as Saskia van Schalkwijk for technical assistance.

References

1. de la Torre, I., Ladero, M. & Santos, V. E. D-lactic acid production from orange waste enzymatic hydrolysates with *L. delbrueckii* cells in growing and resting state. *Ind. Crops Prod.* **146**, 112176 (2020).
2. Court, S. J., Waclaw, B. & Allen, R. J. Lower glycolysis carries a higher flux than any biochemically possible alternative. *Nat. Commun. 2015 61* **6**, 1–8 (2015).
3. Castillo Martinez, F. A. *et al.* Lactic acid properties, applications and production: a review. *Trends Food Sci. Technol.* **30**, 70–83 (2013).
4. Hujanen, M., Linko, S., Linko, Y. Y. & Leisola, M. Optimisation of media and cultivation conditions for L(+)(S)-lactic acid production by *Lactobacillus casei* NRRL B-441. *Appl. Microbiol. Biotechnol. 2001 561* **56**, 126–130 (2001).
5. Helbig, A. O. *et al.* The diversity of protein turnover and abundance under nitrogen -limited steady-state conditions in *Saccharomyces cerevisiae*. *Mol. Biosyst.* **7**, 3316–3326 (2011).
6. Wolff, S., Weissman, J. S. & Dillin, A. Differential scales of protein quality control. *Cell* **157**, 52–64 (2014).
7. Rogers, T. A. & Bommarius, A. S. Utilizing simple biochemical measurements to predict lifetime output of biocatalysts in continuous isothermal processes. *Chem. Eng. Sci.* **65**, 2118-2124 (2010).
8. Gibbs, P. R., Uehara, C. S., Neunert, U. & Bommarius, A. S. Accelerated biocatalyst

stability testing for process optimization. *Biotechnol. Prog.* **21**, 762–774 (2005).

9. Schramm, F. D., Schroeder, K. & Jonas, K. Protein aggregation in bacteria. *FEMS Microbiol. Rev.* **44**, 54–72 (2019).
10. Dressaire, C. *et al.* Transcriptome and proteome exploration to model translation efficiency and protein stability in *Lactococcus lactis*. *PLoS Comput. Biol.* **5**, 1000606 (2009).
11. Hanson, A. D. *et al.* The number of catalytic cycles in an enzyme's lifetime and why it matters to metabolic engineering. *Proc. Natl. Acad. Sci.* **118**, e2023348118 (2021).
12. Nugroho, A. D. W., Kleerebezem, M. & Bachmann, H. A novel method for long-term analysis of lactic acid and ammonium production in non-growing *Lactococcus lactis* reveals pre-culture and strain dependence. *Front. Bioeng. Biotechnol.* **8**, 580090 (2020).
13. Solopova, A., Bachmann, H., Teusink, B., Kok, J. & Kuipers, O. P. Further elucidation of galactose utilization in *Lactococcus lactis* MG1363. *Front. Microbiol.* **9**, 1–9 (2018).
14. Solopova, A. *et al.* A specific mutation in the promoter region of the silent cel cluster accounts for the appearance of lactose-utilizing *Lactococcus lactis* MG1363. *Appl. Environ. Microbiol.* **78**, 5612–5621 (2012).
15. Nugroho, A. D. W. *et al.* Manganese modulates metabolic activity and redox homeostasis in translationally-blocked *Lactococcus cremoris*, impacting metabolic persistence, cell-culturability, and flavor formation. *Microbiol. Spectr.* **10**, e02708-21 (2021).
16. Koebmann, B. J., Andersen, H. W., Solem, C. & Jensen, P. R. Experimental determination of control of glycolysis in *Lactococcus lactis*. *Antonie Van Leeuwenhoek* **82**, 237–248 (2002).
17. Koebmann, B. J., Solem, C., Pedersen, M. B., Nilsson, D. & Jensen, P. R. Expression of genes encoding F(1)-ATPase results in uncoupling of glycolysis from biomass production in *Lactococcus lactis*. *Appl. Environ. Microbiol.* **68**, 4274–4282 (2002).
18. Studer, R. A., Christin, P. A., Williams, M. A. & Orengo, C. A. Stability-activity tradeoffs constrain the adaptive evolution of RubisCO. *Proc. Natl. Acad. Sci. U. S. A.* **111**, 2223–2228 (2014).
19. Maenpuen, S. *et al.* Creating flavin reductase variants with thermostable and solvent-tolerant properties by rational-design engineering. *ChemBioChem* **21**, 1481–1491 (2020).
20. Gasson, M. J. Plasmid complements of *Streptococcus lactis* NCDO712 and other lactic streptococci after protoplast-induced curing. *J. Bacteriol.* **154**, 1–9 (1983).
21. Wegmann, U. *et al.* Complete genome sequence of the prototype lactic acid bacterium *Lactococcus lactis* subsp. *cremoris* MG1363. *J. Bacteriol.* **189**, 3256–3270 (2007).
22. Price, C. E. *et al.* Adaption to glucose limitation is modulated by the pleotropic regulator CcpA, independent of selection pressure strength. *BMC Evol. Biol.* **19**, 1-15 (2019).

Chapter 5

Supplementary Material

Supplementary Data

Table SD5.1 *Calculated kinetic parameters of the decay of lactic acid production rate modulated by sugar precultures*

Preculture	Addition	Max. LA production rate (log10 of M/h)		Decay constant (/h)	
		Average	Std.error	Average	Std.error
Galactose	Galactose	-2.107	0.007	124.590	0.440
Galactose	Glucose	-1.271	0.016	209.415	1.166
Galactose	Lactose	-1.969	0.007	136.054	0.439
Glucose	Galactose	-3.261	0.007	67.118	0.448
Glucose	Glucose	-1.622	0.016	183.262	1.167
Glucose	Lactose	-3.588	0.004	42.934	0.271
Lactose	Galactose	-2.113	0.005	105.738	0.273
Lactose	Glucose	-1.514	0.025	197.617	1.794
Lactose	Lactose	-1.771	0.007	137.532	0.420

Table SD5.2 *Calculated kinetic parameters of the decay of lactic acid production rate modulated by manganese titrations*

Manganese (µM)	Strain	Max. LA production rate (log10 of M/h)		Decay constant (/h)	
		Average	Std.error	Average	Std.error
0	MG1363	-1.623	0.017	208.154	1.672
0.25	MG1363	-1.860	0.019	192.322	1.898
0.5	MG1363	-1.490	0.024	232.694	2.440
0.75	MG1363	-1.346	0.048	273.164	5.274
1	MG1363	-0.931	0.063	328.439	7.050
0	NCDO712	-2.506	0.015	101.001	1.258
0.25	NCDO712	-2.601	0.014	99.783	1.153
0.5	NCDO712	-2.455	0.019	107.608	1.562
0.75	NCDO712	-2.267	0.022	132.925	1.952
1	NCDO712	-2.291	0.022	128.762	1.915
1.5	NCDO712	-2.279	0.027	141.388	2.492
2	NCDO712	-2.105	0.027	165.993	2.631
20	NCDO712	-1.619	0.038	227.767	3.922

Table SD5.3 *Calculated kinetic parameters of the decay of lactic acid production rate modulated by overexpressed F1-ATPase activities*

F1-ATPase (Miller unit)	Max. LA production rate (log10 of M/h)		Decay constant (/h)	
	Average	Std.error	Average	Std.error
0	-2.785	0.030	80.866	2.490
0.2	-2.816	0.029	80.038	2.478
5.9	-2.722	0.026	93.654	2.324
95	-2.890	0.034	76.298	2.948
137	-2.809	0.034	76.432	2.762
173	-2.966	0.038	63.813	3.105
177	-2.341	0.020	115.044	1.654
307	-2.342	0.029	116.772	2.441
405	-2.253	0.039	137.397	3.513
714	-1.910	0.027	163.800	2.372

Table SD5.4 *Calculated kinetic parameters of the decay of lactic acid production rate modulated by the combination of manganese titrations and overexpressed F1-ATPase activities*

Manganese (μM)	F1-ATPase (Miller unit)	Max. LA production rate (log10 of M/h)		Decay constant (/h)	
		Average	Std.error	Average	Std.error
0	0	-2.855	0.031	73.779	2.617
0	0.2	-2.883	0.031	73.141	2.642
0	5.9	-2.747	0.029	90.522	2.632
0	95	-2.964	0.035	68.209	3.095
0	137	-2.882	0.034	69.065	2.792
0	177	-2.356	0.022	113.551	1.845
0	307	-2.375	0.032	113.417	2.736
0	405	-2.304	0.042	131.185	3.879
0	714	-1.886	0.031	165.824	2.760
0.25	0	-2.255	0.018	132.657	1.584
0.25	0.2	-2.341	0.016	130.721	1.458
0.25	5.9	-2.395	0.018	130.860	1.688
0.25	95	-2.330	0.020	135.195	1.937
0.25	137	-2.271	0.020	134.719	1.822
0.25	177	-2.220	0.022	129.092	1.920
0.25	307	-2.031	0.024	146.416	2.093
0.25	405	-1.972	0.028	166.066	2.617
0.25	714	-2.238	0.028	137.205	2.516
0.5	0	-2.041	0.019	153.097	1.672
0.5	0.2	-2.154	0.016	148.862	1.494
0.5	5.9	-2.171	0.019	155.656	1.854
0.5	95	-2.129	0.022	155.072	2.148
0.5	137	-1.918	0.019	169.393	1.787
0.5	177	-2.028	0.024	147.698	2.102
0.5	307	-1.962	0.026	157.019	2.352
0.5	405	-1.542	0.029	208.267	2.788

0.5	714	-1.613	0.023	192.739	2.127
0.75	0	-1.869	0.027	178.056	2.521
0.75	0.2	-2.034	0.028	168.243	2.705
0.75	5.9	-2.045	0.026	171.432	2.626
0.75	95	-1.860	0.032	185.573	3.132
0.75	137	-1.476	0.031	219.773	2.967
0.75	177	-1.660	0.030	193.285	2.809
0.75	307	-1.481	0.035	209.776	3.283
0.75	405	-1.391	0.047	233.143	4.678
0.75	714	-1.658	0.030	196.002	2.852
1	0	-2.056	0.034	165.426	3.289
1	0.2	-1.850	0.026	190.384	2.633
1	5.9	-2.274	0.037	151.985	3.791
1	95	-1.776	0.038	201.244	3.902
1	137	-2.022	0.051	173.278	5.172
1	177	-1.635	0.035	204.103	3.417
1	307	-1.625	0.046	205.503	4.490
1	405	-1.751	0.054	203.476	5.547
1	714	-1.668	0.038	196.294	3.569
1.5	0	-2.140	0.051	165.362	5.263
1.5	0.2	-2.223	0.050	161.845	5.308
1.5	5.9	-2.838	0.050	98.208	5.414
1.5	95	-1.914	0.060	201.644	6.559
1.5	137	-1.528	0.073	242.832	7.993
1.5	177	-1.706	0.070	212.393	7.284
1.5	307	-0.933	0.077	298.975	8.206
1.5	405	-1.528	0.097	238.667	10.524
1.5	714	-1.679	0.071	215.543	7.402
2	0	-1.774	0.052	207.007	5.488
2	0.2	-1.688	0.053	225.112	5.739
2	5.9	-2.027	0.053	195.992	6.051
2	95	-1.527	0.066	239.954	7.149
2	137	-1.198	0.083	274.231	8.969
2	177	-1.655	0.083	215.753	8.649
2	307	-1.292	0.102	259.180	10.834
2	405	-1.098	0.117	287.448	12.800
2	714	-1.827	0.095	201.574	10.078

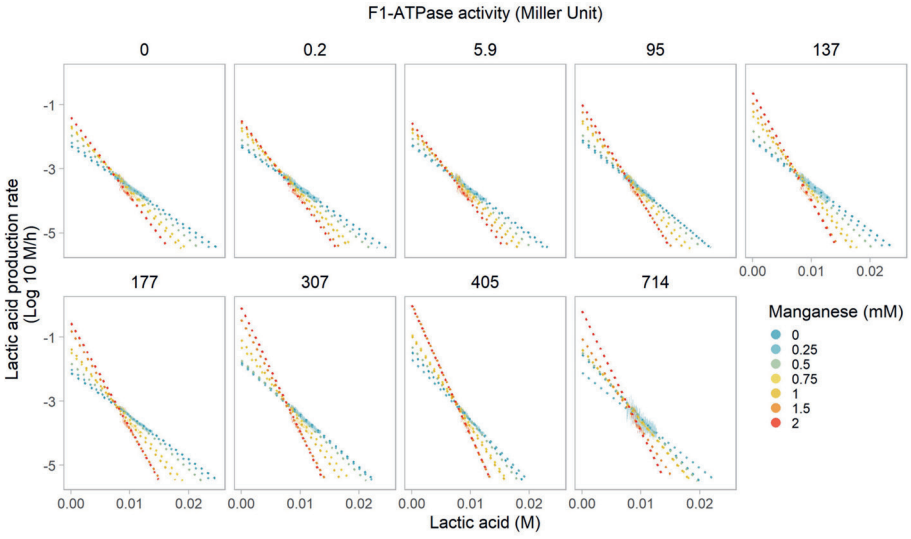

Figure SD5.1 *Lactic acid production rate as a function yield from the combined modulations of manganese titrations (distinguished by colour) and overexpressed F1-ATPase activities (shown in separate panels). Solid lines indicate the averages (n=4), shaded ribbons indicate 95% confidence intervals, and dashed lines indicate data projection based on linear fit.*

Chapter 6

Trade-Offs in Growth and Metabolite Formation in Dairy Lactococci

Nugroho, A. D. W., van Olst, B., Molenaar, D., Li, S.,
Guiso, A., Kleerebezem, M. & Bachmann, H.

Manuscript in preparation

Abstract

In the dairy industry starter cultures are commonly used. These cultures are often optimised for acidification rate to maximise production efficiency and food-safety. In several organisms, fast growth was correlated with higher levels of ribosomal proteins, which came at the expense of metabolic proteins. However, it is unknown whether such trade-off occurs in the important dairy starter *Lactococcus cremoris* and to what extent it influences secondary metabolite formation during food fermentation. Here, we modulated the growth rate of *L. cremoris* NCDO712 by erythromycin-mediated translation inhibition and by growing the cultures at different temperatures in a defined medium and/or milk. Proteome analyses identified 3 separate clusters of proteins that displayed co-regulation and responded to growth rate: (1) Cluster A (ribosome-related) (2) Cluster B (metabolic-related) and (3) Cluster Core (non-regulated). While up to a 3-fold difference in growth rate was achieved by our interventions, we saw that the ribosome-related fraction did not always correlate with growth rate. Translation inhibition using erythromycin in defined medium grown cells led to an approximate 10% and 15% increase in Cluster A in glucose and galactose growing cultures, respectively. The increased proteome allocation towards translation was accompanied by a decrease in the proteome fraction associated with amino acid metabolism, including the enzymes involved in the 3-methylbutanal formation pathway. Less than 10% increase of the ribosome-related fraction was observed when the growth rate was modulated through temperature in defined medium, or by erythromycin-mediated translation inhibition in milk. In the latter conditions, no changes in the fraction of amino acid metabolism were detected. Strikingly, reduced growth rates led to reduced production levels of various key-flavours (up to 30-fold) compared to the corresponding fastest growth conditions. Our data shows fast growth does not always come at the expense of metabolic proteins and that growth rate correlates to secondary metabolite formation independent of the levels of the enzymes involved. This knowledge is important for both starter preparation and industrial production of food or ingredients.

6.1 Introduction

A starter culture is a preparation of living microbes that is added to raw food material to accelerate, steer, and ensure consistent characteristics of the resulting fermentation product, which is often characterised by the timely production of desired microbial metabolites. Lactic Acid Bacteria are widely prevalent as starter cultures in fermented dairy, sausage, vegetables, soy sauce, sourdough, and wine[1]. For higher industrial productivity, a starter culture is typically optimised to perform certain conversions. While various traits, e.g., stress tolerance, adaptation to technological parameters, and key-metabolite production can be optimised, growth and acidification rate remain as one of the predominant selection criteria across products and organisms[2].

Growth rate is indeed a fundamental property that reflects fitness and is highly optimised in unicellular organisms[3]. In applications, the selection of starter cultures toward a faster growth rate under industrially relevant conditions ensures economical production. The corresponding faster acidification ensures that the starter culture outcompetes spoilage or pathogenic microorganisms through depletion of carbon source and pH inhibition. However, several disadvantages are seen with growth and acidification optimisation. One common example is the loss of plasmid-encoded traits due to the cellular burden of plasmid maintenance[4,5]. Additionally, the rise and subsequent invasion of cheater subpopulations that exploit public-good producing subpopulations may occur and lead to lower product formation and population collapse at worst[5–7]. In the case of dairy fermentations, a plasmid-encoded membrane bound protease (PrtP) is a burden to the cell and often lost upon propagation, which leads to the emergence of faster growing prt^- mutants that invade the slower growing prt^+ population[5].

Adaptation to environmental conditions can lead to growth rate dependent switching in metabolic strategies, which is suggested to occur due to trade-offs in cellular economy and resource allocation to maximise fitness[7]. In LAB, this manifests in overflow metabolism, particularly lactic acid fermentation. Pyruvate conversion to lactic acid is highly predominating during higher growth rates despite yielding 1 ATP less as compared to its conversion

to acetic acid. This may be counterintuitive since it seems a waste of energy. However, lactic acid fermentation requires fewer enzymes to be synthesized[8] and allows the maintenance of a high glycolytic flux, whereby it supports higher growth rates. The difference in enzymes required for the two strategies relates to constraints in the cytoplasmic proteome, which is conceptualised as "bacterial growth law"[9]. This law describes that a high ribosome abundance (ribosomal proteins constitute a larger fraction of the cellular proteome) correlates with fast growth, which effectively decreases the proteome fraction that is allocated to metabolic proteins[9]. The underlying reason is described to be constraints on protein content and cell size, which cannot increase indefinitely. This suggests that a high ribosomal fraction during fast growth of a dairy starter could come at the expense of starter functionality. These growth-law-dependent trade-offs in proteome allocation have initially been demonstrated in *E. coli* and were confirmed to also apply to *Bacillus subtilis*[10], *Aerobacter aerogenes*, various yeasts[11,12], fungi, and *Euglena gracilis*[9]. However, despite these consistent findings in these heterotrophic organisms, the same observation could not be replicated in *Methanococcus maripaludis*, which is a slow-growing chemolithoautotrophic archaeon that is highly adapted to energy-limiting environments[13]. In this organism, ribosome numbers were largely invariant with growth rate, and protein synthesis rates were altered through modulation of ribosomal activity rather than ribosomal abundance. This suggests that adaptation to different lifestyles and habitats may coincide with the evolution of alternative resource allocation strategies.

In the case of dairy LAB, cells evolved to the lactose-abundant and nutrient-rich environments that are possibly different to the typical feast-and-famine environments of *E. coli*. For lactococci, "chemical warfare" is considered to be a competitive strategy, which is facilitated by rapid acidification to create unsuitable environment for competitors[14]. In this organism, it has been reported that the proteome hardly changed with growth rate[15]. To assess whether such a bacterial growth law applies in lactococci and if it influences starter culture performance in particular flavour formation in a dairy environment, we analysed the proteome of *L. cremoris* NCDO712 cultured at

different growth rates. Growth-rate modulations were achieved by using either a defined medium or milk supplemented with subinhibitory concentrations of a translation inhibitor or by varying the growth temperature. Furthermore, we also quantified the ability to accumulate flavour volatiles in these cultures in a non-growing bacterial-suspension model[16] and during cheesemaking and ripening using the microcheese model system[17].

6.2 Materials and methods

6.2.1 Strain and cultivation conditions

Lactococcus cremoris NCDO712[18] was grown on a chemically defined medium for prolonged cultivation (CDMPC)[19] or skimmed milk (Tritium). CDMPC was supplemented with either 55 mM galactose, or glucose. Cells were subsequently adapted for at least 15 generations to growth in the presence of subinhibitory concentrations of the translation inhibitor erythromycin or to growth at a suboptimal temperature. These conditions resulted in different growth rates. From these cultures, cells were harvested during the mid-exponential phase of growth, which corresponded to an optical density at 600 nm (OD_{600}) between 0.1 and 0.4 in CDMPC or a pH between 5.5 and 5.9 in milk. Except for the indicated temperature modulation, all growth experiments were performed at 30°C. Exponential growth rate measurements were performed as described previously[20] and were calculated through slope determination of exponentially linear range of the growth curves.

6.2.2 Proteome sample preparation and analysis

Proteome samples were harvested in independent biological duplicates. Protein extraction and analysis were performed as described previously[8,20] with modifications. After subculturing to mid-exponential growth, cells were pelleted and resuspended in ice-cold 100 mM TRIS pH8 approximately at a density of 8E+09 cells/mL. Cell solutions (100 µL) were subsequently lysed using a needle sonicator (MSE) for 3 cycles of 10 seconds at 22 microns amplitude with 5 seconds of intermittent cooling on ice. An aliquot of the cell lysate (60 µL) was reduced by dithiothreitol (15 mM) addition and thereafter shaken for 30 minutes at 45°C, 350 rpm in an Eppendorf

Thermomixer Comfort. Lysate leftover was used for determination of protein concentration using standard BCA assay (Thermo Pierce) and was centrifuged once more to minimise the presence of cell debris.

Afterward, the reduced lysate was subjected to denaturation and alkylation with 132 µL of 8M urea in 100 mM TRIS pH 8 and 20 mM acrylamide (final concentration) for 10 minutes at 21°C. The denatured and alkylated sample was transferred to an ethanol-washed Pall 3K Omega filter (Sigma-Aldrich). Following centrifugation (35 minutes at 13523 g, room temperature, unless specified), filter was washed using 130 µL of 50 mM ammonium bicarbonate. Another round of centrifugation was done at the same setting. Subsequently, on-filter protein digestion was performed by adding 100 µL of 5 ng/µL sequencing-grade trypsin (Roche) at room temperature, overnight. Initial elusion of the peptides was done by centrifugation (30 minutes). Additionally, 100 µL of 0.1% HCOOH in water was added into the filter and eluted by centrifugation (30 minutes). The pH of the final elute was adjusted to pH 3 using 10% trifluoroacetic acid and stored at -20°C until further processing. The resulting peptides were measured by a Q-Exactive HF-X (Thermo electron, San Jose, CA, USA). Proteome data is available on request.

6.2.3 Volatile analysis

To determine the volatile compounds formed during incubation of cell suspensions in different media, a headspace solid phase microextraction (HS-SPME) was carried out in combination with gas chromatography/mass spectrometry (Fisons, USA) as previously described[20,21]. Flavour accumulation was performed with long-incubation (7 days) of non-growing cells in defined medium (CDMPC)[16]. An exception to this approach were milk-grown cells that were inoculated into cheese milk (with 5 µg/mL erythromycin) and subsequently used for cheesemaking[17] and ripening (14 days) to determine flavour accumulation during this process.

6.2.4 Proteome data analysis

To compare between samples, iBAQ fractions were calculated as the ratio between iBAQ value of a protein and the total iBAQ values of all measured

proteins. Subsequently, the sample standard deviation was correlated as a function of the mean value of iBAQ fractions, which could be modelled by a smoothing spline fit, suggesting highly unequal sample variance (squared value of standard deviation). To create a dataset with equal standard deviation, variance stabilising transformation of iBAQ fractions was done. The variance stabilising function *g(x)* for an iBAQ fraction *x* was derived from the standard deviation *σ(μ)* as a function of the expected value *μ* of the iBAQ fraction, as follows:

$$g(x) = \int^{x} \frac{1}{\sigma(\mu)} d\mu \qquad (1)$$

The integral in Equation 1 was approximated by discrete summation of the area under the smoothing spline curve. The transformed data set shows equal standard deviation across the data, except at very low iBAQ fractions (below 1E-06). ANOVA was subsequently used to detect significantly regulated proteins with a p-value cut-off of 0.1, which leads to 76.4% of the observed proteins to be classified as regulated. Proteins that are not regulated but significantly expressed (iBAQ fraction >5E-07) belong to Cluster Core. Proteins that are not regulated and non-significantly expressed are classified as noisy proteins. Significantly regulated proteins were clustered and ordered based on Pearson correlation of coefficients calculated from the non-transformed iBAQ fractions. Enrichment analysis based on COG categories was done with FunRich 3.1.3[22]. For data visualisation, Rstudio (2022.07.1+554 with R version 4.2.1) was used.

6.3 Results

6.3.1 Various volatiles are correlated with growth rate

A variation of means can be employed to modulate microbial growth rates, including nutrient limitations, nutrient quality, translation inhibition, protein overexpression, enhanced energy dissipation, and temperature alterations[23–25]. In this study, we varied medium composition (chemically defined vs rich medium), carbohydrate quality (glucose vs galactose), translation inhibition (erythromycin) and growth-temperature modulations to

achieve different growth rates of *Lactococcus cremoris* NCDO712 ranging from 0.12 to 0.70 /h. These growth rate-modulating conditions were selected to enable comparison to existing proteome allocation studies[26,27] and to provide relevant insights on industrial applications of *L. cremoris* as a starter culture in dairy fermentation.

To measure the accumulation of volatiles, we used our standardised non-growing cell model[16]. The block of protein synthesis at the harvesting point of exponential growth allows us to correlate the corresponding proteome to their metabolite formation capacity. For milk-grown cells, casein carry-over was inevitable, therefore flavour formation was performed in a non-growing microcheese model[17]. In both models (defined and cheese), we mimic environmental conditions during cheese ripening where long-term metabolite accumulation is the result of enzyme stability, cell integrity, and metabolic maintenance such as NAD/NADH regeneration[16,20,28]. In the case of defined medium, free amino acids will be imported into the cell, whereas proteolysis of milk proteins is required for the cheese model. Figure 6.1 shows the peak area of various key-flavours in cheese[29] at the end of 7 and 14 days of incubation in the non-growing model and the cheese model, respectively. For each of the preculture conditions, the formation of various volatiles was remarkably decreased and corresponded with the preculture growth rates in a linear manner. This was particularly consistent in branched-chain amino acid derived aldehydes (2-methylbutanal, 3-methylbutanal, 2-methylpropanal) where an up to 10-fold reduction could be observed. Interestingly, the correlation of these volatiles with growth rate was more pronounced upon translation inhibition or temperature modulation in galactose-supplemented defined medium relative to translation inhibition in glucose-supplemented defined medium or milk. In the latter two conditions, formation of 2-methylbutanal and 2-methylpropanal remained relatively constant while the formation of 3-methylbutanal declined by 0.3 log10 (~2-fold) and 0.2 log10 (~1.6-fold). These reduced levels of 3-methylbutanal are exacerbated in galactose-supplemented defined medium, where an approximate 3-fold reduction was observed as a consequence of both translation inhibition and temperature-mediated growth rate modulation. This

implies that growth rate and the formation of flavour derived from branched-chain amino acids is correlated, but the slope of such correlation seems to be condition-dependent.

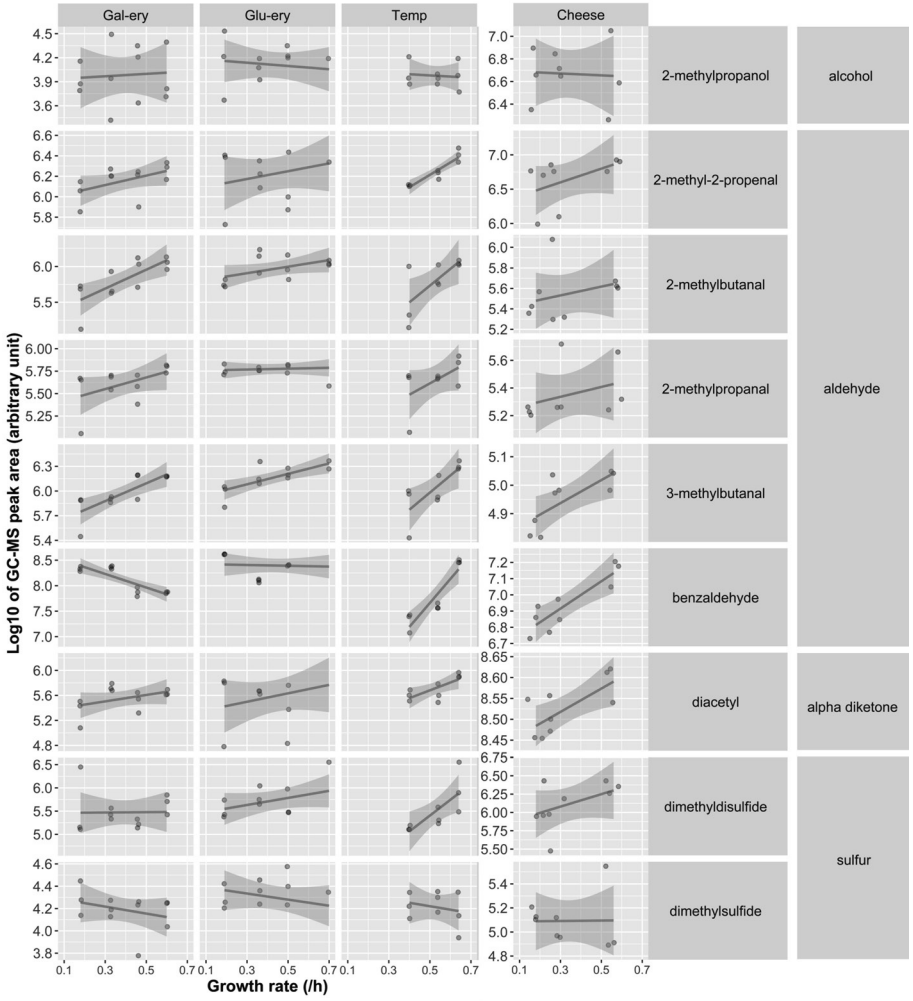

Figure 6.1 *GC-MS peak area of 3-methylbutanal formation following 1 week and 2 weeks in non-growing in defined medium (defined medium preculture) and cheese model (milk preculture), respectively. Values are individual biological replicates (n=3 per condition).*

6.3.2 General trade-off exists between translation and metabolism in varying degrees

The observed correlation between growth rate and flavour formation might potentially be a result of proteome constraints and reallocation, therefore we analysed the proteome of the cells used in these analyses, resulting in the detection and quantification of more than 1600 proteins (> 65% of the *in silico* proteome of NCDO712; Figure 6.2A). Hierarchical clustering analysis was performed using Pearson correlation distance and this resulted in a proteome-wide clustering of protein co-expression. Three main clusters were observed and referred to as Cluster A, Cluster B, and Cluster Core. Cluster Core was consistently found to be approximately 18% of the overall proteome irrespective of the growth condition or growth rate modulation (Figure 6.2B). Ribosomal proteins that belong to the Cluster Core fraction consistently contributed less than 3% of the total proteome (i.e., proteome fraction), which is approximately 10-fold lower than the proteome fraction encompassed by ribosomal proteins in Cluster A (Figure 6.2C). Cluster core was particularly enriched (Figure 6.2D) for proteins that belong to COG category K (Transcription) and encompassed specific transcriptional regulators that were apparently expressed at a comparable level under the employed growth conditions. Contrary to this Cluster Core, the relative fraction of the overall proteome occupied by Clusters A and B varied with growth rate. Taken together, clusters A and B encompass 1236 of the 1617 detected proteins, which highlights that the majority (76.4%) of the proteome is subject to adaptation by growth rate, whereas Cluster Core represents a stable proteome fraction.

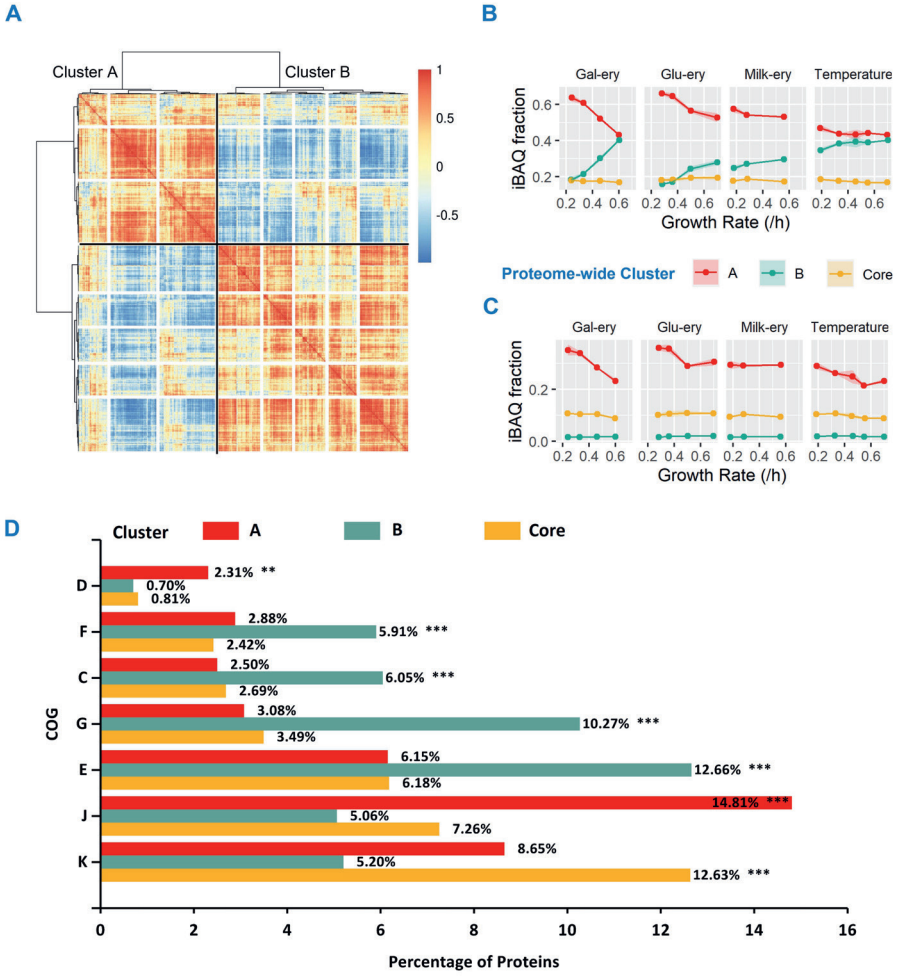

Figure 6.2 *Clustering analysis of protein co-expression. (A) A correlation matrix and hierarchical clustering reveals coregulated protein clusters (Cluster A and B) for proteins above noise level. Non-noisy proteins but non-coregulated proteins were grouped as Cluster Core (i.e., not represented in panel A). (B) Fraction of proteome (iBAQ) and (C) 30S and 50S ribosomal proteins based on the 3 clusters in different growth conditions. Translation inhibition modulation in different media (CDMPC-gal/glu and milk) and temperature modulation. (D) Enrichment analysis of proteins within each cluster based on COG categories: C (Energy production & conversion), D (Cell cycle control, cell division, and chromosome partitioning), E (Amino Acid metabolism & transport), F (Nucleotide metabolism & transport), G (Carbohydrate metabolism & transport), J (Translation, ribosomal structure & biogenesis), K (Transcription).*

The proteins in Cluster A and B negatively correlate with each other. Growth rate decrease due to increasing levels of translation inhibition or stepwise lowering of growth temperatures, associated with increasing and decreasing abundance of proteins in Cluster A and B, respectively. Cluster A encompasses 529 proteins and is enriched for functions that are mainly associated with the COG category J (Translation, ribosomal structure and biogenesis) and to a lesser extent the COG category D (Cell cycle control, cell division and chromosome partitioning). Within COG category J, Cluster A encompasses 34 out of the 52 ribosomal proteins detected (30S and 50S), and COG category D proteins in Cluster A contains 11 out of the 18 COG D proteins. Among the 11 proteins of COG D in Cluster A, cell division proteins (encoded by *ftsA, ftsE, ftsK, ftsW1, ftsX*) and plasmid partition proteins (*parA* encoded by pLP712 and pNZ712) were captured. Notably, under all conditions, the ribosomal proteins contributed approximately half of the total proteome fraction occupied by Cluster A proteins. Cluster B encompasses 718 proteins and is enriched for proteins associated with metabolic proteins of COG category C (Energy production and conversion), E (Amino Acid metabolism and transport), F (Nucleotide metabolism and transport), and G (Carbohydrate metabolism and transport). Interestingly, proteins belonging to COG category E displayed the strongest enrichment in Cluster B (12.66%) and includes various enzymes involved in flavour formation for instance Opp proteins, peptidases, aminotransferase (AraT and IlvE) as well as those belonging to arginine deiminase pathway. In general terms, these results demonstrate that increasing proteome allocation towards translation (ribosomal protein fraction) comes at the expense of various metabolic processes, which is particularly emphasized for amino acid metabolism. The observed negative correlation between protein abundances of proteins in clusters A and B seems to make sense if a growth rate decrease is caused by translation inhibition, where the cell increases its ribosomal capacity to (partially) compensate for the exerted translation inhibition. The reduced growth rate of these cells, requires less energy and building blocks for growth, allowing the cell to downregulate proteins involved in these processes. However, this argumentation may not be valid when growth rate decrease is caused by lower growth temperature, where one would expect

that proteome fractions would be relatively stable if one assumes that most enzyme and pathway or process efficiencies are equally affected by temperature changes.

Although the trade-off between translation and metabolism is in line with previous studies in *E. coli*[23–25], we observed that changes in the relative proteome fraction occupied by the Cluster A and B proteins is not always equally apparent in different growth rate modulations. For example, growth rate reductions induced by translation inhibition in milk or suboptimal growth temperatures were accompanied with much smaller proteome fraction changes for Cluster A and B as compared to similar growth rate reductions achieved by translation inhibition in defined medium. More specifically, the relative proteome fraction occupied by Cluster A proteins (enriched for COG category J; predominated by ribosomal proteins) seems to be approximately constant in growth rates exceeding 0.3 /h. This finding emphasizes that the extent of proteome reallocation as a function of growth rate varies significantly and depends on the specific growth rate modulation and growth medium employed.

6.3.3 Enzymes of 3-methylbutanal formation do not always correlate with growth rate

In light of the importance of flavour formation by *L. cremoris* during cheese manufacturing, we decided to further investigate the proteins included in COG category E (Amino acid metabolism and transport) that were enriched in Cluster B (see above). In particular, we focus on the formation of 3-methylbutanal, which shows the strongest correlation across conditions and subsequently allows correlation to the corresponding enzyme levels. The simplified higher level overview of the pathway[30] can be seen in Figure 3. In cheese, nitrogen is present mainly as casein and the acquisition of amino acids such as leucine requires proteolysis by the membrane-bound proteolytic system, import of the resulting oligopeptides, and peptidolysis to liberate amino acids. In defined medium, direct import of free extracellular leucine is required. Once intracellular free leucine is available, leucine can be transaminated to α-keto-iso-caproic acid (KICA). KICA is subsequently

converted through an additional step (direct route via ketoacid decarboxylase) to produce 3-methylbutanal. Alternatively, 3-methylbutanal can be formed via an indirect route where 3-methylbutanoic acid is formed as an intermediate before finally converted to 3-methylbutanal[31,32] by a carboxylic acid reductase(CAR)-like enzymes.

Overlapping with coarse-grain analysis, the majority of enzyme levels in the pathway of 3-methylbutanal formation declines when growth was reduced with translation inhibition in CDMPC (defined medium). In particular, proteolysis and peptidolysis mechanisms are reduced (Figure 6.3) and the biggest decrease (30- to 60-fold) was seen for several of the constiutuents of the oligopeptide import system (Opp). Strikingly, in milk, the expression of Opp proteins seem to be barely affected with growth rate reduction by translation inhoibition, which may reflect the crucial nature of this import function in nutrient acquisition during growth in milk. However, this difference between these media cannot be explained by the difference in nitrogen source alone since the proteome adjustments during temperature-mediated growth modulation in cells grown in CDMPC resembled the the translation inhibition effects in milk. In temperature modulated growth rates in CDMPC growing cells, the expression of many proteins belonging to proteolysis and peptidolysis was not correlated by growth rate. In fact, the level of PrtP, DppA, PepDA, and PepF (encoded by pLP712) appeared to be elevated at reduced growth rates and may be a response to compensate reduced enzyme activities at lower temperature. While the medium or growth-modulating agent does not seem to entirely explain the observed changes, the scale of the increase of Cluster A seem to fit better with the less pronounced changes at individual enzymes in milk (translation inhibition) and CDMPC (temperature). Both conditions show no increase of Cluster A at growth rate between 0.3 and 0.7 /h. For comparison, cells grown under translation inhibition in CDMPC-galactose and CDMPC-glucose showed an approximate 15% and 10% in Cluster A, respectively, at the same range of growth rate. This suggests that growth rate induced proteome changes identified only on galactose-supplemented defined medium seem to be

the consequence of differences in the ribosomal fraction that increased more significantly with translation inhibition than with temperature modulation.

In defined medium, amino acid import rather than peptidolysis is more relevant. We observed the decrease of the expression level of the leucine importer (BrnQ and, particularly, CtrA) under all conditions where growth was reduced through translation inhibition, and the strongest decrease was observed in defined medium. Similar to proteolytic and peptidolytic functions, the expression of leucine importers did not show a clear correlation with growth rate in cells grown in defined medium when growth was modulated by temperature. This observation seems to coincide once more with the lower impact on the ribosomal proteome fraction in temperature-modulated conditions.

The relative expression of proteins responsible for leucine transamination (downstream of leucine in Figure 6.3) displayed differential regulation depending on the growth medium and the means used to modulate growth rate. Growth rate modulation by temperature did not induce significant adjustments of any enzyme in the pathway while growth rate reduction by translation inhibition in milk elicited a reduction of expression of only branched-chain aminotransferase (IlvE) and acetate kinase (AckA). In contrast, all proteins of the transamination pathway (with exception of PanE) were significantly lower expressed in defined medium when growth rate was reduced by translation inhibition. Taken together, these results show that proteome reallocation can be seen at both global proteome clustering level and pathway specific level and (the extent of) the observed changes seem to be condition-dependent.

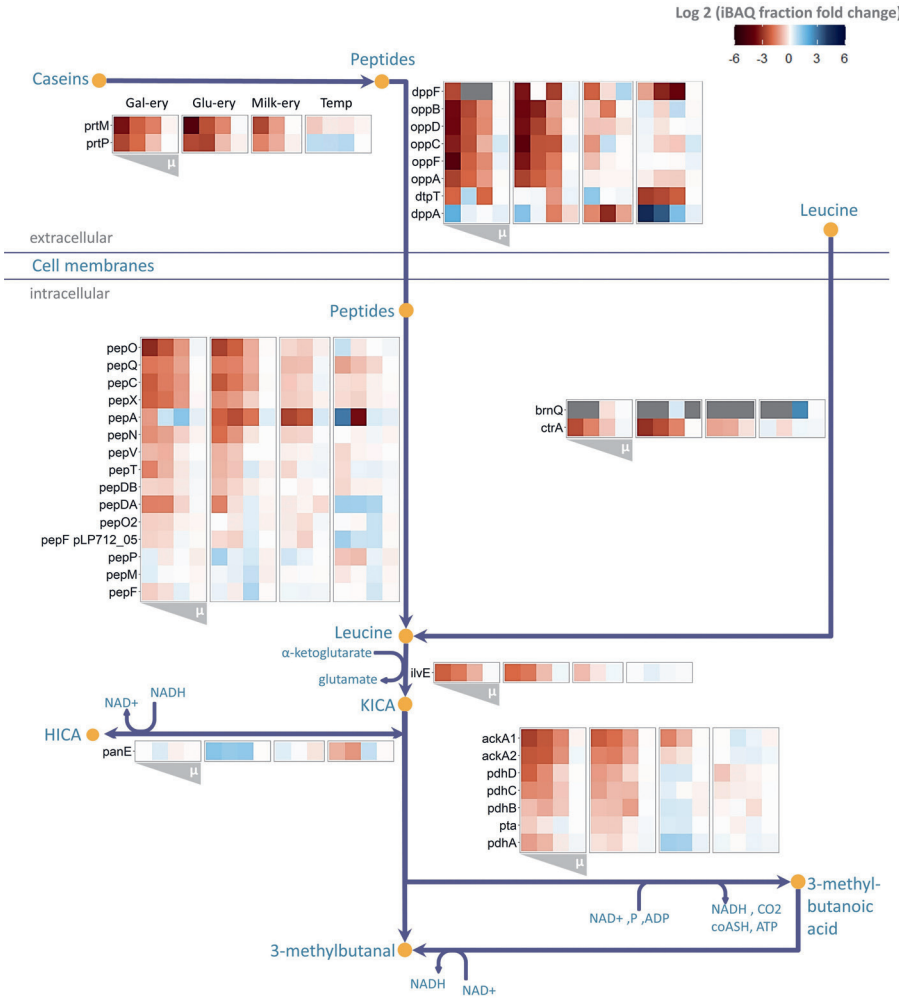

Figure 6.3 *Overview of relative expression level of proteins that are involved in 3-methylbutanal formation. Values represent the average of biological replicates and normalised to the level at the highest growth rate (rightmost column of the individual heatmaps). The heatmaps are sorted from left to right per conditions and growth rate (see top-left heatmaps for the order). Abbreviations: α-keto-isocaproic acid (KICA), hydroxy isocaproic acid (HICA), nicotinamine adenine dinucleotide (NAD⁺ and NADH for oxidised and reduced form, respectively), coenzyme A (coASH), and adenosine triphosphate (ATP).*

6.4 Discussion

The trade-off between growth and metabolism has been widely reported in microorganism, but few studies have investigated such phenomenon in food microorganisms[33–35]. Next to that, previous studies have predominantly focused on central carbon metabolism[13,36–39] or stress resistance[40–42]. Hence, our understanding of the implication of such trade-off on secondary metabolism under conditions relevant to applications remained limited. In this study, we investigated the influence of growth rate on amino acid metabolism, which is important for flavour formation. To exemplify this, we pay particular attention to the formation of 3-methylbutanal formation from the branched-chain amino acid leucine and place our findings in the context of proteome reallocation analyses in lactococci.

We demonstrated that a bacterial growth law as described for *E. coli*[9] seems to apply in *L. cremoris*, but the extent of proteome reallocation was found to be condition dependent. Similar to what was reported for *E. coli*, three differentially regulated clusters of proteins were identified in the *L. cremoris* proteome, which we designated as Cluster A, B and Core that respectively resembled the Ribosome, Metabolism, and Fixed fractions reported by Scott et al[9]. Using increasing levels of translation inhibiton and temperature reduction to reduce growth rate, we observed increasing allocation to the ribosomal-protein related fraction (Cluster A), albeit not necessarily following the linear relation with growth rate that was reported for *E. coli*[9]. Notably, when grown in milk (using translation inhibition) and in defined medium (using temperature reduction), the increase of Cluster A was only apparent at growth rates below 0.3 /h. This result is in agreement with a previous study that used a a closely related *L. cremoris* strain and showed that hardly any changes in ribosomal proteins were detected within a 3- to 4-fold increase in growth rate in fast growing cultures[15]. Despite variable changes in the ribosomal proteome fraction, we observed a reduction of 3-methylbutanal in slower growing cells irrespective of the growth rate reducing conditions or growth medium

employed. However, it remains to be determined whether this conclusion can be generalised to conditions beyond the scope of this study.

With respect to proteolysis, peptidolysis, and branched-chain amino acid catabolism, most of the corresponding proteins are regulated by the CodY repressor[43]. The data presented here demonstrate that proteolytic and peptidolytic proteins are expressed in defined medium where these functions are redundant based on the availability of non limiting free amino acids, suggesting that the CodY regulon is derepressed under these conditions, irrespctive of the amino acid availability. This finding is corroborating previous reports that describe that, in particular, dipeptides containing one of the branched-chain amino acids (leucine, isoleucine, or valine)[43] induce CodY repression rather than their free amino acid counterparts. Our findings demonstrate that growth in the presence of translation inhibiting antibiotics consistently decrease the expression level of proteins of the CodY regulon. Strikingly, growth in milk under similar conditions led to unaltered Opp proteins. This is in agreement with the relatively minor extent of proteome reallocation under these conditions, which may have prevented the detection of a potentially small reduction of Opp proteins. Additionally, the underlying mechanism that leads to the reduction of proteins of the CodY regulon might differ in milk relative to defined medium. During growth in milk, the regulatory dipeptides that affect CodY regulon expression may be more abundantly present at lower growth rate due to the longer time for the protease to digest proteins as generation time increases. Despite potentially distinct mechanisms, we demonstrate that growth rate reduction generally coincides with a reduction of enzymes relevant for flavor formation derived from amino acids, albeit to a highly variable extent depending on the growth medium and the means employed to reduce growth rate.

Among amino-acid derived flavors, 3-methylbutanal is a key-flavor compound in semi-hard cheeses with a low odor threshold (1 ppb in water[29]). It is mainly formed through whole-cell enzymatic conversion[28]. It is also typically higher in abundance compared to other branched-chain aldehydes like 2-

methylbutanal and 2-methylpropanal[32]. For the final step in the pathway, ketoacid decarboxylase (KDCA) and carboxylic acid reductase (CAR) are required. However, neither of these enzymes are found in strain NCDO712, whereas 3-methylbutanal spontaneous conversion has been reported to be negligible in previous studies[20,31]. Other studies[31,32] assumed aldehyde dehydrogenase (ALDH) to produce 3-methylbutanal from 3-methylbutanoic acid. However, ALDH only facilitates the reverse reaction from aldehydes to carboxylic acids[44], and it is not catalytically capable to activate a carboxylate substrate, unlike CARs[45,46]. Hence, we were unable to indicate corresponding enzymes for the last step of 3-methylbutanal formation but the data indicate the existence of such an enzyme in this strain. Considering the importance of the formation of 3-methylbutanal in various other fermented foods including wine, beer, bread, sausage, and soy sauce[47–51], the identification of the corresponding genes would be broadly relevant for food fermentation. The present study demonstrated a 2-fold reduction in 3-methylbutanal formation associated with lower growth rate. Although this seems a relatively small difference, such a reduction may substantially extend cheese ripening where it can take months to years to achieve a 2-fold increase of the 3-methyl butanal concentration[52,53].

To conclude, understanding the role of growth modulation in the context of starter preparation and its eventual non-growing cell metabolism is of interest from a scientific point of view as well as for industrial applications. The majority of microorganisms reside in a non-growing but metabolically active state in nature, and little is known of the impact of their cultivation history. Lactococci are highly interesting model microorganisms to study the relation betwen culture history and metabolite production under such non-growing states, since these microorganisms were shown to be capable to remain metabolically active in a viable but not culturable state for up to 3.5 years[54,55], and starter preparation (i.e., cultivation history) is an integral part of their applications. The proteomics knowledge of starter preparation allows a data-driven systems biology optimisation approach that should incorporate

multiple variables influencing flavor formation, which is heavily intertwined with other metabolic pathways in the cell.

6.5 Acknowledgment

The authors would like to thank Simon Jacobs who assisted with GC-MS analysis, Marjo Starrenburg who assisted with microcheese experiments, and Sjef Boeren who assisted with proteomics analysis.

References

1. Leroy, F. & De Vuyst, L. Lactic acid bacteria as functional starter cultures for the food fermentation industry. *Trends Food Sci. Technol.* **15**, 67–78 (2004).
2. Vinicius De Melo Pereira, G. *et al.* A Review of Selection Criteria for Starter Culture Development in the Food Fermentation Industry. *Food Rev. Int.* **36**, 135–167 (2019).
3. Molenaar, D., Van Berlo, R., De Ridder, D. & Teusink, B. Shifts in growth strategies reflect tradeoffs in cellular economics. *Mol. Syst. Biol.* **5**, 323 (2009).
4. Ow, D. S. W., Nissom, P. M., Philp, R., Oh, S. K. W. & Yap, M. G. S. Global transcriptional analysis of metabolic burden due to plasmid maintenance in *Escherichia coli* DH5α during batch fermentation. *Enzyme Microb. Technol.* **39**, 391–398 (2006).
5. Bachmann, H., Molenaar, D., Kleerebezem, M. & Van Hylckama Vlieg, J. E. High local substrate availability stabilizes a cooperative trait. *ISME J.* **5**, 929–932 (2011).
6. Smith, P. & Schuster, M. Public goods and cheating in microbes. *Curr. Biol.* **29**, R442–R447 (2019).
7. Bachmann, H., Bruggeman, F. J., Molenaar, D., Branco dos Santos, F. & Teusink, B. Public goods and metabolic strategies. *Curr. Opin. Microbiol.* **31**, 109–115 (2016).
8. Chen, Y. *et al.* Proteome constraints reveal targets for improving microbial fitness in nutrient-rich environments. *Mol. Syst. Biol.* **17**, e10093 (2021).
9. Scott, M., Gunderson, C. W., Mateescu, E. M., Zhang, Z. & Hwa, T. Interdependence of cell growth and gene expression: origins and consequences. *Science (80-.).* **330**, 1099–1102 (2010).
10. Reuß, D. R. *et al.* Large-scale reduction of the *Bacillus subtilis* genome: consequences for the transcriptional network, resource allocation, and metabolism. *Genome Res.* **27**, 289–299 (2017).
11. Elsemman, I. E. *et al.* Whole-cell modeling in yeast predicts compartment-specific proteome constraints that drive metabolic strategies. *Nat. Commun.* **13**, 1–12 (2022).
12. Xia, J. *et al.* Proteome allocations change linearly with the specific growth rate of *Saccharomyces cerevisiae* under glucose limitation. *Nat. Commun. 2022 131* **13**, 1–12 (2022).

13. Müller, A. L. *et al.* An alternative resource allocation strategy in the chemolithoautotrophic archaeon *Methanococcus maripaludis*. *Proc. Natl. Acad. Sci. U. S. A.* **118**, e2025854118 (2021).

14. Goel, A., Wortel, M. T., Molenaar, D. & Teusink, B. Metabolic shifts: A fitness perspective for microbial cell factories. *Biotechnol. Lett.* **34**, 2147–2160 (2012).

15. Goel, A. *et al.* Protein costs do not explain evolution of metabolic strategies and regulation of ribosomal content: Does protein investment explain an anaerobic bacterial Crabtree effect? *Mol. Microbiol.* **97**, 77–92 (2015).

16. Nugroho, A. D. W., Kleerebezem, M. & Bachmann, H. A novel method for long-term analysis of lactic acid and ammonium production in non-growing *Lactococcus lactis* reveals pre-culture and strain dependence. *Front. Bioeng. Biotechnol.* **8**, 580090 (2020).

17. Bachmann, H., Kruijswijk, Z., Molenaar, D., Kleerebezem, M. & van Hylckama Vlieg, J. E. T. A high-throughput cheese manufacturing model for effective cheese starter culture screening. *J. Dairy Sci.* **92**, 5868–5882 (2009).

18. Gasson, M. J. Plasmid complements of *Streptococcus lactis* NCDO712 and other lactic streptococci after protoplast-induced curing. *J. Bacteriol.* **154**, 1–9 (1983).

19. Price, C. E. *et al.* Adaption to glucose limitation is modulated by the pleotropic regulator CcpA, independent of selection pressure strength. *BMC Evol. Biol.* **19**, 1-15 (2019).

20. Nugroho, A. D. W. *et al.* Manganese modulates metabolic activity and redox homeostasis in translationally blocked *Lactococcus cremoris*, impacting metabolic persistence, cell-culturability, and flavor formation. *Microbiol. Spectr.* **10**, e02708-21 (2022).

21. Gamero, A., Wesselink, W. & de Jong, C. Comparison of the sensitivity of different aroma extraction techniques in combination with gas chromatography-mass spectrometry to detect minor aroma compounds in wine. *J. Chromatogr. A* **1272**, 1–7 (2013).

22. Pathan, M. *et al.* FunRich: an open access standalone functional enrichment and interaction network analysis tool. *Proteomics* **15**, 2597–2601 (2015).

23. Millet, V. & Lonvaud-Funel, A. The viable but non-culturable state of wine micro-organisms during storage. *Lett. Appl. Microbiol.* **30**, 136–141 (2000).

24. Teusink, B. & Molenaar, D. Systems biology of lactic acid bacteria: For food and thought. *Curr. Opin. Syst. Biol.* **6**, 7–13 (2017).

25. Mairet, F., Gouzé, J. L. & de Jong, H. Optimal proteome allocation and the temperature dependence of microbial growth laws. *npj Syst. Biol. Appl. 2021 71* **7**, 1–11 (2021).

26. Scott, M., Klumpp, S., Mateescu, E. M. & Hwa, T. Emergence of robust growth laws from optimal regulation of ribosome synthesis. *Mol. Syst. Biol.* **10**, 747 (2014).

27. Hui, S. *et al.* Quantitative proteomic analysis reveals a simple strategy of global resource allocation in bacteria. *Mol. Syst. Biol.* **11**, 784 (2015).

28. Nugroho, A. D. W., Kleerebezem, M. & Bachmann, H. Growth, dormancy and lysis: the complex relation of starter culture physiology and cheese flavour formation. *Curr. Opin. Food Sci.* **39**, 22–30 (2021).

29. Smit, G., Smit, B. A. & Engels, W. J. M. Flavour formation by lactic acid bacteria

and biochemical flavour profiling of cheese products. *FEMS Microbiol. Rev.* **29**, 591–610 (2005).

30. Liu, M., Nauta, A., Francke, C. & Siezen, R. J. Comparative genomics of enzymes in flavor-forming pathways from amino acids in lactic acid bacteria. *Appl. Environ. Microbiol.* **74**, 4590-4600 (2008).
31. Helinck, S., Le Bars, D., Moreau, D. & Yvon, M. Ability of thermophilic lactic acid bacteria to produce aroma compounds from amino acids. *Appl. Environ. Microbiol.* **70**, 3855-3861 (2004).
32. Afzal, M. I. *et al.* Biosynthesis and role of 3-methylbutanal in cheese by lactic acid bacteria: major metabolic pathways, enzymes involved, and strategies for control. Crit. Rev. Food Sci. Nutr. **57**, 399–406 (2016).
33. van Mastrigt, O., Egas, R. A., Lillevang, S. K., Abee, T. & Smid, E. J. Application of a partial cell recycling chemostat for continuous production of aroma compounds at near-zero growth rates. *BMC Res. Notes* **12**, 1-6 (2019).
34. Johanson, A., Goel, A., Olsson, L., Franzén, C. J. & Dudley, E. G. Respiratory physiology of *Lactococcus lactis* in chemostat cultures and its effect on cellular robustness in frozen and freeze-dried starter cultures. *Appl. Environ. Microbiol.* **86**, e02785-19 (2020)
35. Flahaut, N. A. L. *et al.* Genome-scale metabolic model for *Lactococcus lactis* MG1363 and its application to the analysis of flavor formation. *Appl. Microbiol. Biotechnol.* **97**, 8729–8739 (2013).
36. Basan, M. *et al.* Overflow metabolism in *Escherichia coli* results from efficient proteome allocation. *Nature* **528**, 99–104 (2015).
37. Castrillo, J. I. *et al.* Growth control of the eukaryote cell: a systems biology study in yeast. *J. Biol.* **6**, 1–25 (2007).
38. Ercan, O., Wels, M., Smid, E. J. & Kleerebezem, M. Molecular and metabolic adaptations of *Lactococcus lactis* at near-zero growth rates. *Appl. Environ. Microbiol.* **81**, 320–31 (2015).
39. Ercan, O. *et al.* Physiological and transcriptional responses of different industrial microbes at near-zero specific growth rates. *Applied and Environmental Microbiology* vol. 81 5662–5670 (2015).
40. Heunis, T., Deane, S., Smit, S. & Dicks, L. M. T. Proteomic profiling of the acid stress response in *Lactobacillus plantarum* 423. *J. Proteome Res.* **13**, 4028–4039 (2014).
41. Marques Da Silva, W. *et al.* Quantitative proteomic analysis of the response of probiotic putative *Lactococcus lactis* NCDO2118 strain to different oxygen availability under temperature variation. *Front. Microbiol.* **10**, 759 (2019).
42. Ercan, O., den Besten, H. M. W., Smid, E. J. & Kleerebezem, M. The growth-survival trade-off is hard-wired in the *Lactococcus lactis* gene regulation network. *Environ. Microbiol. Rep.* **14**, 632–636 (2022).
43. Guédon, E., Serror, P., Ehrlich, S. D., Renault, P. & Delorme, C. Pleiotropic transcriptional repressor CodY senses the intracellular pool of branched-chain amino acids in *Lactococcus lactis*. *Mol. Microbiol.* **40**, 1227–1239 (2001).
44. Terao, M., Garattini, E., Romão, M. J. & Leimkühler, S. Evolution, expression, and substrate specificities of aldehyde oxidase enzymes in eukaryotes. *J. Biol. Chem.* **295**, 5377–5389 (2020).

45. Strohmeier, G. A., Eiteljörg, I. C., Schwarz, A. & Winkler, M. Enzymatic one-step reduction of carboxylates to aldehydes with cell-free regeneration of ATP and NADPH. *Chem. – A Eur. J.* **25**, 6119–6123 (2019).

46. Winkler, M. Carboxylic acid reductase enzymes (CARs). *Curr. Opin. Chem. Biol.* **43**, 23–29 (2018).

47. Steinhaus, P. & Schieberle, P. Characterization of the key aroma compounds in soy sauce using approaches of molecular sensory science. *J. Agric. Food Chem.* **55**, 6262–6269 (2007).

48. Cho, I. H. & Peterson, D. G. Chemistry of bread aroma: a review. *Food Sci. Biotechnol.* **19**, 575–582 (2010).

49. Beck, H. C., Hansen, A. M. & Lauritsen, F. R. Metabolite production and kinetics of branched-chain aldehyde oxidation in *Staphylococcus xylosus*. *Enzyme Microb. Technol.* **31**, 94–101 (2002).

50. Huang, Y., Tippmann, J. & Becker, T. A kinetic study on the formation of 2- and 3-methylbutanal. *J. Food Process Eng.* **40**, e12375 (2017).

51. Culleré, L., Cacho, J. & Ferreira, V. An assessment of the role played by some oxidation-related aldehydes in wine aroma. *J. Agric. Food Chem.* **55**, 876–881 (2007).

52. Jo, Y., Benoist, D. M., Ameerally, A. & Drake, M. A. Sensory and chemical properties of Gouda cheese. *J. Dairy Sci.* **101**, 1967–1989 (2018).

53. Ayad, E. H. E., Verheul, A., Bruinenberg, P., Wouters, J. T. M. & Smit, G. Starter culture development for improving the flavour of Proosdij-type cheese. *Int. Dairy J.* **13**, 159–168 (2003).

54. Ganesan, B., Stuart, M. R. & Weimer, B. C. Carbohydrate starvation causes a metabolically active but nonculturable state in *Lactococcus lactis*. *Appl. Environ. Microbiol.* **73**, 2498–2512 (2007).

55. Ruggirello, M., Cocolin, L. & Dolci, P. Fate of *Lactococcus lactis* starter cultures during late ripening in cheese models. *Food Microbiol.* **59**, 112–118 (2016).

Chapter 7

General Discussion

Nugroho, A. D. W.

7.1 Introduction

Lactic acid bacteria (LAB) are key to many industrial and biotechnological processes. Its significance can be seen from the number of research publications on this group of organisms, which amounts to approximately one-third of those performed on the paradigm bacterial organism *Escherichia coli* (Figure 7.1). On the other hand, research publications specifically addressing lactococci amounts to substantially lower numbers (45-fold lower than *E. coli*) despite being the first species that was grown as a pure culture in a laboratory[1], approximately 12 years before pure cultures of *E. coli* were first reported in 1885[2]. Such difference in popularity of the lactococci (or the LAB in general) and *E. coli* can be associated with the versatility, minimum nutrient requirement, and ease of handling of *E. coli*[2]. The fast growth of *E. coli* was apparent from the start and its first (English language) publication described such characteristics as follows:

"Culturing them on gelatin plates is easily achieved."

"…shows a massive luxurious deep growth…"

Growth rate is undoubtedly an important trait in both research and application. In line with the high number of available publications, the generation time of *E. coli* is short and measures on average between 20 and 60 minutes[3]. In contrast, *L. cremoris* divides between 40 and 60 minutes[4], and generation times frequently are much longer under less favourable growth conditions, like 120 to 160 minutes when grown under amino acid limitations[5]. To further exemplify this difference, 1,000-fold diluted subcultures from a fresh stationary phase culture will become full-grown in less than 3.5 hours for *E. coli*, whereas at least 3 additional hours are required for lactococci to achieve the same when grown in rich, non-limiting conditions. As a consequence, *E. coli* has been considered as a model organism, despite its severely limited use in food and medical application due to its pathogenicity and toxicity[6,7]. On the

contrary, lactococci have a Generally-Recognized As Safe (GRAS) status[8]. In fact, it has become the first genetically-modified organism to be used as a live-biotherapeutic for a human disease treatment[9]. Next to its role in food fermentation and medical therapy, lactococci have emerged to be an effective microbial cell factory for the production of various industrial metabolites and (recombinant) proteins through the use of the NICE (nisin-controlled expression) system[10]. For a long time, lactococci have been the paradigm organism for LAB, which was driven by their genetic accessibility[11] and the early availability of genetic engineering tools based on plasmids[12], transposons[13], and phages[14]. A substantial amount of work has been done on lactococci, particularly where it differs with other model organisms[15]. The lactococcal metabolic potential includes facultative heterofermentation[16,17], facultative respiration[18] using an exogenous electron acceptor (e.g., heme), anaerobic but aerotolerant[19], and the production of natural secondary metabolites of industrial relevance, e.g., flavours[20] and nisin[21]. Recently, the increased popularity and strong research interest in probiotics[22] led to lactobacilli overshadowing the lactococci as paradigm representatives of the LAB. However, since lactococci are of particular interest with regards to non-growing metabolism and its role in cheese flavour formation, this area would deserve more attention than it currently receives.

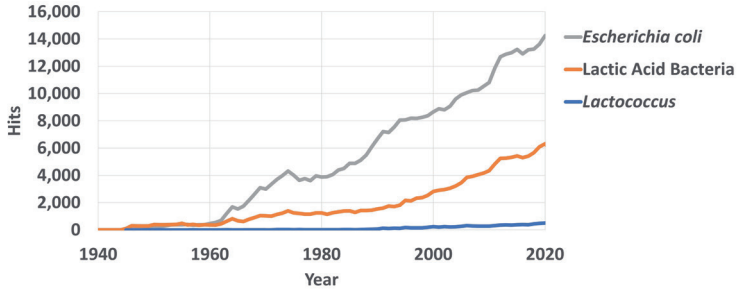

Figure 7.1 *PubMed search results using different keywords (shown by colours:* Escherichia coli *in grey, Lactic Acid Bacteria in orange, and* Lactococcus *in blue).* Lactococcus *search was repeated with the alternative terms "*Streptococcus lactis*" or "*Bacterium lactis*" and resulted in similar numbers.*

Moreover, most microorganisms spend the majority of their lifetime in a non-growing state, which further demonstrates the irony of fast-growing bacteria as a model organism. In this thesis, we aimed to investigate *Lactococcus cremoris* (previously *L. lactis* subsp*. cremoris*[23]) in the context of dairy fermentation and slow- or non-growing cells. We summarised various aspects important for its functionality from starter preparation to cheesemaking (**Chapter 2**). In line with its physiological state during cheese ripening, emphasis was given to its non-growing but metabolically-active characteristics. To facilitate the corresponding investigation, we developed a high-throughput method (**Chapter 3**) using bacteriostatic translation-blocking antibiotics to induce a non-growing state. Using this approach, we were able to compare different conditions, e.g., preculture conditions and mutants, in relation to their corresponding long-term stability of product formation. Previous experimental evolution experiments using serial propagation in emulsion[24] revealed a trade-off between growth rate and biomass yield and led to the isolation of a mutant that displayed a reduced growth rate due to lower glucose transporter activity, which coincided with mixed-acid fermentation and higher ATP yield. Through measurement of ammonia formation in the long-term metabolic model we developed, it could be established that arginine utilisation was activated in this mutant strain, which likely contributes to its higher biomass yield. The expression of the arginine utilisation pathway in relation to growth rate is relevant in dairy fermentation where arginine metabolism has been shown to contribute to the coping mechanisms that protect bacteria against acid stress. Moreover, **Chapter 3** provided the first examples for the trade-off between catalytic rate and cumulative product yield, which was further developed in **Chapter 6**.

This translation-blocked, non-growing cell model was further employed to measure other metabolites, e.g., 3-methylbutanal (**Chapter 4**). During the initial development, we tested different omissions of medium components in order to formulate a minimum assay medium. Omission of the

metal stock solution from the medium was found to severely influence acidification rate, which led to the discovery that the presence of manganese can accelerate the catalytic rate of the central pathway in carbon metabolism that leads to the production of lactic acid. This accelerated rate leads to draining of the NADH pools in the cell, which has important and pleiotropic consequences that are driven by this loss of redox balance, including reduced culturability, rapid declining acidification rates and adjusted profiles of flavour compounds (**Chapter 4**). Although the underlying mechanism of the impact of manganese was not identified, we argued that reduced glycolysis flux or LDH activity is associated with this phenomenon, and it is clear that manganese plays a crucial role in the non-growing metabolite formation. Using titration of manganese, F1-ATPase expression levels, and preculture conditions, we conducted further non-growing cell suspension experiments where we established a constant correlation between acidification rate, production decline, and its cumulative lactic acid yield (**Chapter 5**). Finally, we extended this study to the modulation of growth rate (**Chapter 6**) for the investigation of the trade-off between ribosomal and metabolic protein allocation. Through proteome analysis, we could establish that preculture growth rate is positively associated with downstream flavour formation, which contradicts the common assumption that slower growth leads to more flavours[25]. The way by which growth is adjusted determines the magnitude of the altered flavour formation, which may warrant further investigation to better harness this negative-correlation. The different findings described in this thesis are discussed in more depth in the following sections. A graphical summary of different concepts explained in this thesis can be seen in Figure 7.2.

7.2 Intracellular protein stability in relation to pathway activities

Functional *in vivo* lifespan of enzymes is an important performance indicator for the application of non-growing cells as well as their survival in nature. In this study, an increase of the maximum acidification flux in translationally-blocked cells of *L. cremoris* was surprisingly found to correlate with an accelerated decrease of activity over time. Because of the faster pathway-activity decay, a lower cumulative amount of product was formed. This trade-off is associated with overall reduced substrate conversion cycles per enzyme molecule over the lifespan of the pathway activity. This finding is consistent throughout various means by which we modulated the rate of acidification, but it remains to be seen how generic this phenomenon can be replicated for other metabolic pathways. In this context, the initial experiments that investigated arginine catabolism (in **Chapter 3**) provide an intriguing example of a similar phenomenon. The arginine catabolising capacity in lactococci was modulated by different preculture conditions (**Chapter 3**), which in subsequent non-growing cell suspension analysis demonstrated that accelerated catabolic rate of the arginine pathway coincided with a more rapid decay of its activity, which eventually led to a lower cumulative amount of product formed (using ammonium production as a proxy). Thereby this pathway confirms the proposed trade-off between pathway catalytic rate and the cumulative product formation capacity.

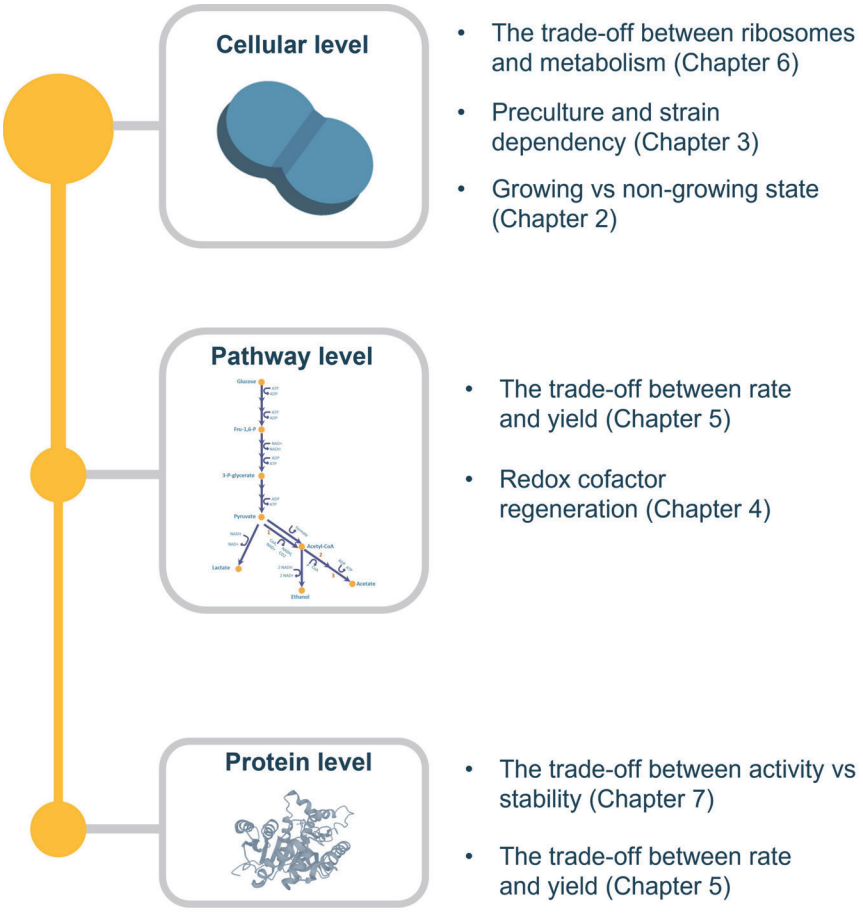

Figure 7.2 *Summary of various concepts investigated or addressed in this thesis. Different concepts apply at the level of protein, pathway or cellular. Notably, although hinted at in the experimental chapters, the establishment of the rate-yield trade-off at protein or enzyme level is predominantly discussed in* ***Chapter 7*** *and would require further experimental investigation.*

The arginine pathway experiments targeting the rate-yield trade-off may provide an excellent complement to the lactic acid formation pathway that was employed in **Chapter 5**. The Arginine deiminase (ADI) pathway involves a shorter sequence of reactions: (1) arginine/ornithine antiport, (2) conversion of arginine to ammonium and citrulline, (3) conversion of citrulline to ornithine, (4) conversion of citrulline to carbamoyl phosphate, (5) conversion

of carbamoyl phosphate and ADP to ATP, CO_2, and ammonium[26]. Compared to acidification, the ADI pathway is a simpler model for an ATP-generating pathway. Additionally, the exchanger function of arginine/ornithine transporter is highly attractive because it intrinsically avoids issues such as product inhibition. The formation of ammonium allows quantitative tracking using the method demonstrated in **Chapter 3** and minimum adjustment is required. The overall conversion requires no NAD(H), and it is thereby notably different from the ATP production by glycolysis and lactic acid formation. The formation of ATP is crucial since it potentially allows to prevent the use of translation-blocking antibiotics to prevent growth because the omission of fermentable carbon sources from the environment may achieve the same. Finally, since the initial extracellular pH in the arginine catabolism experiments was set at 5.5, these conditions resemble the general condition of cheese ripening more closely, which may allow better mimicking of cheese-like conditions in this assay system.

Albeit at reduced demand, ATP formation in non-growing cell is likely to be crucial to general survival (**Chapter 3-5**). Under acidic conditions, F1F0-ATPase can serve as a proton pump that aids in maintenance of intracellular pH at the cost of ATP[27]. The mechanisms that degrade, solubilise, or disaggregate deteriorated proteins, e.g., Clp and Lon proteases[28] require ATP. The role of Clp and Lon in non-growing cells is still disputed and studies reported either no importance[29,30] or importance[31–33]. Nevertheless, it is clear that they interact with major regulators such as the master regulators of stress response CtsR and HrcA[34] or the CodY transcriptional regulator[32,35]. Without such mechanisms of protein quality control, protein deterioration and aggregation become an aging factor that leads to loss of culturability and eventual cell death[36]. Such damage may occur due to “molecular wear and tear”, which may be caused by the binding of reactive species (substrate, intermediate, product, or cofactor) in the presence of damage-susceptible amino acid residues in the active site region[37]. The constant conformational changes of enzymes eventually lead to

detrimental covalent modifications, such as deamidation or oxidation[38,39]. Aggregated protein accumulates over time and seems to increase substantially during exponential growth[36], which coincides with high metabolic flux. This observation seems to overlap with our findings on the trade-off between rate and yield (**Chapter 5**). However, since the currently available information that supports this rate-yield trade-off is dominated by the lactic acid formation assays we performed, we are unable to conclusively decide whether pathway activity decline occurs due to deterioration at the level of enzyme decay (i.e., denaturation) or cellular function (i.e., metabolic dead end due to NADH depletion, as observed in **Chapter 4**). The preliminary results of ADI pathway suggest that the metabolic dead-end is not very likely and indirectly supports the alternative, which is pathway/enzyme decay. A multi-step non-growing assay, which investigates arginine catabolism in the described setup and subsequent transition to the acidification setup, and vice versa, may answer this question.

7.3 The remarkable longevity of metabolite formation in non-growing cells

The experiments in this thesis (**Chapter 3** and **5**) highlighted the remarkable stability of metabolite formation by cellular pathways. To demonstrate this further, we compared our results to the catalytic cycles until replacement (CCR) that represents the mole of substrate converted per mole of enzyme as defined by Hanson *et al*[37]. The CCR calculations are based on previously reported protein turnover rates (k_D) and the corresponding metabolite fluxes. In the case of *L. cremoris,* fluxes were calculated from genome scale metabolic models, which resulted in CCR values from 1E+03 to 1E+06. Similar calculation can be done based on the results described in **Chapter 3**, which demonstrated that 2.5E+0^7 translationally-blocked *L. cremoris* cells produce approximately 17.3 mM of lactate from glucose over a period of 264 hours (**Chapter 3**; Figure 3.2.)[40]. Given an estimated cell volume of 0.5 fL[24],

approximately 725 protein molecules per fL[41], and the known fraction of a given enzyme in the proteome pool of the cell (e.g., ~0.5% for lactate dehydrogenase)[16], one can calculate the CCR for the unique enzymes involved in glucose to lactate catabolism. Table 7.1 shows that the numbers of catalytic cycles for glycolytic enzymes based on our assay are 4.5-6.5 orders of magnitude higher compared to the values reported by Hanson *et al*. Since our estimated values of the numbers of enzymes per biomass (Table 7.1) are very similar to those used by Hanson *et al*.[37], the majority of the discrepancy between the CCR values is determined by the flux per protein estimation. Protein turnover data[42] used in the CCR calculation by Hanson *et al.* includes enzyme synthesis as a result of growth, which leads to an over-estimation of the real protein turnover and underestimations of *in vivo* enzyme lifespan. While the definition of CCR refers to the catalytic cycles until replacement, an enzyme might not likely be replaced while it is still functional, and inactivation-aggregation seems to be a main requirement. Our data shows that glycolytic enzymes of *L. cremoris* remain remarkably active for weeks. If the stagnation of pathway in our system would be caused by metabolic dead-end issues as opposed to enzyme decay, the calculated CCR based on our model may even be an underestimation of the real CCR. This implies that intracellular enzymes seem to execute their catalytic functions for very long periods.

Table 7.1 *Amount of enzyme per gram dry weight (DW) and CCR for 8 glycolytic enzymes as reported by Hansen et al. and calculations based on the data of Nugroho et al. The fraction of individual enzymes on the total proteome was taken as the iBAQ fraction of each enzyme in % of the total iBAQ values from* L. cremoris *MG163 as reported by Chen et al.[16]. For the calculations of the enzyme per gram, a dry weight of 150 fg per cell was assumed (based on the volume corrected dry weight as reported by Milo et al.[41]). For enzymes in upper glycolysis, the number of performed reactions was corrected by a factor two to account for the C6 vs C3 molecules measured as lactate.*

Enzyme	mmol enzyme per g of DW (Hanson et al.)	CCR (Hanson et al.)	Enzyme iBAQ fraction (Chen et al.)	mmol enzyme per g of DW	CCR (Nugroho et al.)	Log10 of CCR fold difference
Glucose-6-phosphate isomerase (EC 5.3.1.9)	2.1E-05	6.5E+05	0.16	2.6E-05	8.7E+10	5.13
6-phosphofructokinase (EC 2.7.1.11)	3.7E-06	2.4E+06	0.20	3.2E-05	7.1E+10	4.48
Fructose-bisphosphate aldolase class II (EC 4.1.2.13)	1.2E-04	4.1E+04	0.85	1.4E-04	3.4E+10	5.91
Triosephosphate isomerase (EC 5.3.1.1)	1.5E-04	2.8E+04	0.32	5.1E-05	9.1E+10	6.52
Phosphoglycerate kinase (EC 2.7.2.3)	2.1E-04	4.1E+04	0.42	6.7E-05	6.9E+10	6.22
Phosphoglycerate mutase (EC 5.4.2.11)	5.5E-05	2.3E+05	0.29	4.6E-05	1.0E+11	5.63
Pyruvate kinase (EC 2.7.1.40)	7.1E-05	1.6E+05	0.39	6.2E-05	7.4E+10	5.67
L-lactate dehydrogenase (EC 1.1.1.27)	8.3E-05	1.6E+05	0.48	7.7E-05	6.0E+10	5.57

7.4 The trade-off between activity, stability, and yield at the protein level

How to engineer enzymes to be fast, stable, and efficient is a key-question in Biotechnology and Biochemistry. Similar to our findings in **Chapter 5**, a trade-off between activity and stability is widely recognized in evolutionary biology. A great example is the evolution of RubisCo (ribulose-1,5-bisphosphate carboxylase) that is responsible for CO_2 fixation in plant photosynthesis[43]. The natural evolution of RubisCo is strongly constrained by the requirement to maintain enzyme (thermal) stability. Enhanced activity requires enhanced

flexibility of the active site that is inherently destabilising to the enzyme structure, therefore it is preceded and followed by the accumulation of structural mutations that stabilise the protein conformation[44]. These mutations alter the amino acid residues that maintain and hold the complex native 3D conformation of an enzyme in order to be catalytically active[45]. To understand the fundamental relation that explains the trade-off between activity and stability, we need to visit the activation thermodynamics of enzymes. Enzymes facilitate a non-spontaneous reaction by decreasing the barrier of activation free-energy ($\Delta G^{\#}$) between the ground state (substrate) and the transition state (intermediate, $[TS]^{\#}$) before the formation of a product (Figure 7.3).

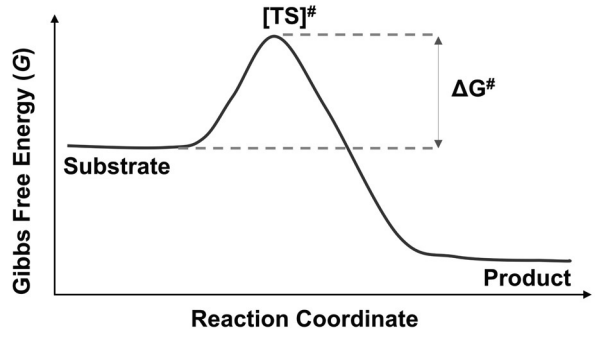

Figure 7.3 *The Gibbs free energy profile of a reaction*[46]

Activation free energy $\Delta G^{\#}$ is described by equation 1[47]:

$$\Delta G^{\#} = \Delta H^{\#} - T\Delta S^{\#} \qquad (1)$$

where $\Delta H^{\#}$ is the change in activation enthalpy, $\Delta S^{\#}$ is the change in activation entropy and T is the absolute temperature.

Additionally, these thermodynamic activation parameters(#) are related to catalytic constant k_{cat} by equation 2[48]:

$$k_{cat} = \left(\frac{k_B T}{h}\right) e^{-\Delta G^{\#}/RT} \qquad (2)$$

where k_B is the Boltzman constant (1.38E−23 J K^{-1}), h is the Planck constant (6.63E−34 J s), and R is the Gas constant (8.314 J K^{-1} mol^{-1}).

Solving Equation 1 and 2 will give us equation 3:

$$k_{cat} = \left(\frac{k_B T}{h}\right) e^{-\left(\frac{\Delta H^{\#}}{RT}\right)} e^{\left(\frac{\Delta S^{\#}}{R}\right)} \quad (3)$$

Based on equation 3, in order to increase k_{cat} (catalytic rate) at a constant temperature, either $\Delta S^{\#}$ (entropy of activation) has to increase or $\Delta H^{\#}$ (enthalpy of activation) has to decrease. Insight from studies with enzymes at lower temperatures suggests that the latter is more commonly encountered with a concomitant reduction in affinity (increase of Michaelis constant)[49]. This is achieved through structural mutations within the substrate binding pocket, which reduce the interactions that are required to be broken to go to the transition state[49,50]. These include hydrophobic or electrostatic (H-bonds, amino acid-mediated, salt bridges) interactions, the type of secondary structure elements (α-helices, surface loops), and others (disulphide bridges, metal binding sites)[49]. On the other hand, increase of entropy of activation ($\Delta S^{\#}$) to increase k_{cat} is not commonly reported. Entropy-driven behaviours are understood as the conformational dynamics of protein subunits as well as the complex of enzyme binding sites and its intermediate ligand in this case[51,52]. Contrary to the classical and rigid description of lock-and-key interaction between enzyme and its substrate or intermediate, polypeptide chains and their interactions are inherently flexible and undergo conformational changes as frequent as femto- and picoseconds[51,52]. One way to achieve higher disorder ($\Delta S^{\#}$) is through the displacement of water molecule(s) from the active site upon intermediate formation, which provides more freedom in protein conformation[50]. However, not much is known, and such investigations are currently experimentally challenging due to the limitations in the time-wise resolution of X-ray crystallography or NMR and typically involves large computational simulations[51–55]. Given rapid advances in the near future, the

role of increased entropy in enhanced catalytic rate may be revealed to be more common than we currently acknowledge.

In short, enhanced enzyme activity and lower enzyme stability seems to be dictated by thermodynamic law. To date, a few enzymes are known to defy the activity-stability trade-off and such enzymes seem to demonstrate a local vs global rigidity, e.g., highly flexible active sites and highly rigid protein surface[50]. In our study, increased catalytic rate was not a result of changes in amino acid sequence of a protein, but perhaps the rate-yield trade-off can be explained by the higher probability of protein conformational damage with higher conversion rate. As the conversion rate increases per enzyme, saturation level of enzymes-substrates increases, which may lead to successive reactions within a short amount of time by the same enzyme molecule. The corresponding successive and rapid changes in protein conformation to facilitate catalysis may result in enzyme decay and the observed decline in metabolite formation. To test this hypothesis that is based on enzyme decay, we adapted our non-growing cell assay (**Chapter 3**) to monitor the *in vitro* activities of beta-galactosidase[56] and aminopeptidase N[57] during long-term incubations. To modulate catalytic rate, cofactor availability and/or temperature was adjusted. However, stability of intracellular enzymes following lysis was found to be incredibly compromised and catalytic rate intervention seems to directly influence stability as well (Figure 7.4). In the case of aminopeptidase N (PepN), the rate-yield trade-off seems to be partially observed when the catalytic rate is modulated by adjustment of the reaction temperature. However, it is overall inconclusive based on the present preliminary data where the other enzyme (beta-galactosidase) or modulation (EDTA) did not support the rate-yield trade-off and dedicated experimental approaches are needed to rigorously test our hypothesis.

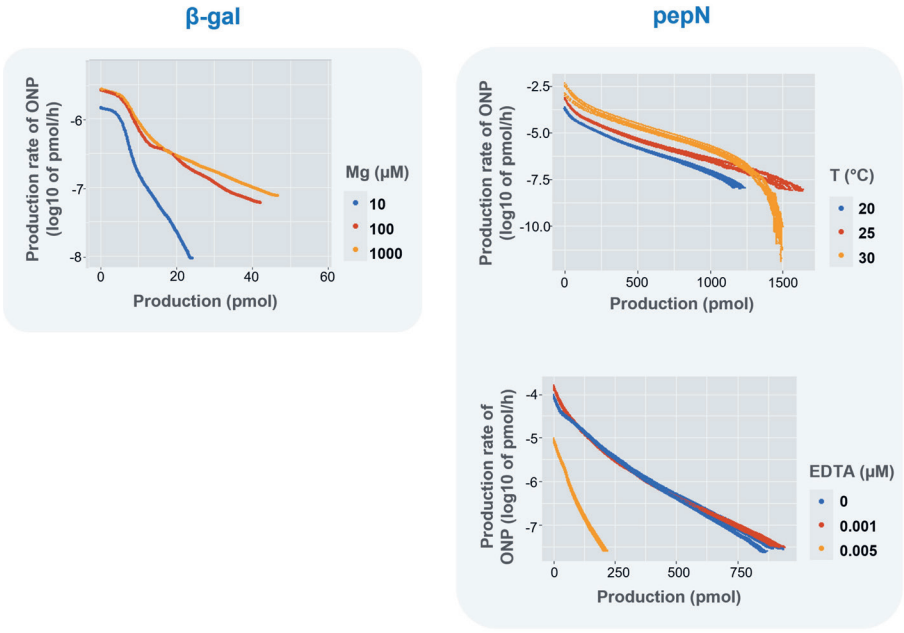

Figure 7.4 *Long term monitoring of enzyme activities (left: beta-galactosidase assay*[56] *for 72 hours, right: aminopeptidase N assay*[57] *for 162 hours) as modulated by cofactor (Mg), temperature (T), or cofactor chelator (EDTA).*

7.5 The potential application of rate-yield trade-off

Yield is not explicitly mentioned or defined in the concept of the enzyme activity and stability trade-off, but it is a crucial parameter in the work presented in this thesis (**Chapter 3-5**) and in many Biotechnological applications. Besides optimisation strategies towards the best activity/stability combination for an application, one should also consider to optimise for the rate-yield combination, to achieve a system with maximised performance. If the broader concept of the described rate-yield trade-off applies at the protein level and is generically applicable, commercial areas for applications will include various areas operating with enzymatic conversions. The most interesting target will especially be processes in which increased conversion time would be easily compensated by increased conversion yield. More specific commercial areas for applications are fermented dairy products in which acidification rate

and post-production acidification and/or flavour formation are of importance. To achieve this, several possibilities can be foreseen:

1. Increase yields of enzyme conversion by lowering the activity rate.

To lower activity rate, reduced temperature is likely to be the most convenient approach since it does not directly alter the composition of the reaction solution. In **Chapter 3-5**, the reduction of cofactor availability was used but it is likely to be either unfeasible in a complex matrix or it requires a chelating agent that may complicate downstream purification. Due to the inherent trade-off of this phenomenon, economic feasibility will depend on the cost of enzyme, processing, and product selling price, among others. The longer processing time as a result of slower conversion rate can be outweighed when using expensive enzymes for the production of high-value ingredients.

2. Faster production and improved product stability of fermented foods due to reduction in post-production activity of enzymes.

The trade-off indicates that faster fermentations will stop or slow down more rapidly. This suggests that processes with a high rate of production, produce a more stable product due to suppression of 'post-production catalysis' as a consequence of pathway decay. This could potentially be of interest for various food fermentations in which short incubation times during production are desired in combination with subsequent stagnation and stabilisation to limit changes in product characteristics. Examples could be rapid flavour formation in cheese followed by subsequent stagnation of flavour production/degradation supporting the stabilisation of the product. Another example would be the rapid acidification during the production of yoghurt, followed by acidification pathway stagnation due to its decay to prevent post-production acidification. Acceleration of the process, with intrinsically a faster stagnation of the process, may allow fast production with limited or absent post-production changes of the product, which ensures product quality, increases shelf life, as well as reduces potential food waste.

7.6 Modulations of amino-acid derived flavour formation

Next to the stability of enzymes in non-growing cells during cheese ripening, modulating the initial level of flavour-forming enzymes (**Chapter 6**) and preventing the downstream conversion of flavour compounds (**Chapter 4**) are equally important. For this reason, we investigated the formation of key-flavour compounds in cheese as a function of preculture conditions during the preparation of the starter (**Chapter 6**), but also by modifying the metal ion availability during either the preculturing phase and/or the non-growing phase (**Chapter 4**). We found that both approaches can be used to influence the amount of potent flavour compounds. A particular example of 3-methylbutanal (chocolate, nutty, fruity) formation was emphasized due to its experimental consistency that allows us to evaluate its relationship with the corresponding enzyme levels. A remaining question was how well our laboratory data can be extrapolated to industrial applications and to which extent the results hold for other lactic acid bacteria. Further discussions and other observations in milk or microcheese are elaborated in the following sections.

7.6.1 Changes in abundance of manganese and transition metals across time and environment

Transition metals are essential components of metabolism that shape the evolution of life on earth. For roughly 2.5 billion years microbes evolved many of their metabolic pathways around reactions catalysed by iron because it is the most abundant and bioavailable transition metal[58]. With the appearance of photosynthetic bacteria and the Great Oxygenation Event (GOE), iron bioavailability gradually decreased while the bioavailability of manganese, which was the second most abundant transition metal, remained relatively unchanged[58]. Diversification and incorporation of manganese into cellular metabolism prevalently occurred for approximately the next 1 billion years. As plants emerged and increased oxygen levels to its present amount, higher

copper bioavailability than manganese and iron lead to further diversification of metal cofactors[58]. Lactic acid bacteria were considered to emerge around GOE[59] with the increased metabolic prevalence of manganese. A switch to manganese as a cofactor may provide evolutionary advantages that include (1) the ability to thrive in low-iron niches, (2) prevention of iron-related DNA damage due to Fenton reactions, and (3) prevention of enzyme inactivation due to [4Fe-4S] clusters oxidation[60,61]. Accumulation of intracellular manganese ions serves as oxidative stress response in LAB[62] instead of the expression of iron-dependent stress proteins, e.g., in *E. coli*[58]. From the perspective of a cytoplasmic proteome constraint, this is arguably a more efficient strategy of oxidative stress response.

While LAB seem to prefer manganese to iron, the (fermented) dairy environments actually contain limited amount of manganese (Table 7.2), therefore LAB possess multiple systems of manganese transport[63]. The importance of maintaining proper manganese concentrations can be seen from the presence of at least 3 characterised manganese transport systems in our strain (Table 7.3). In comparison, the import of other metals is typically dependent on a single transport system. With such elaborate transport systems, one will expect this mechanism to be failproof. However, **Chapter 4** shows that non-growing cells suffer from potentially excess manganese in the range that is not normally considered toxic. Hence, to investigate non-growing LAB for cheese ripening, formulation of defined medium should ideally resemble the bioavailability and the concentration ratio of transition metals in milk and cheese environments. Up to 300-fold higher manganese concentration was found in our defined medium[64] in comparison to bovine milk[65]. This environmental difference is reflected in the expression of manganese ABC transporter (MtsAB), which is expressed in average 100-fold lower during growth in defined medium than in milk. Aside from the CorA-like magnesium and cobalt transport protein, relative protein expression levels of other metal transporters seem to be comparable between media.

Table 7.2 *Comparison of transition metal concentrations in chemically defined medium for prolonged cultivation (CDMPC[64]), bovine milk, and (semi-) hard cheese[65].*

Metal	CDMPC	Bovine milk	Cheese
Mg	200 mg/L	90-260 mg/kg	90-450 mg/kg
Ca	3 mg/L	107-133 mg/kg	730-12,000 mg/kg
Mn	4 mg/L	13-40 µg/kg	traces, lower than 1mg/kg
Fe	4 mg/L	300-700 µg/kg	1 -8 mg/kg
Co	0.3 mg/L	0.5-1.3 µg/kg	Not Available
Cu	0.3 mg/L	20-300 µg/kg	0.3-3.3 mg/kg
Zn	0.3 mg/L	740-1450 µg/kg	5 -53 mg/kg
Mo	0.3 mg/L	24-60 µg/kg	Not Available

Table 7.3 *iBAQ fraction (-log10 values) of transition metal transporters of* L. cremoris *NCDO712 in different media (**Chapter 6**). Values are average of 2 biological replicates.*

Gene ID	Protein name	CDMPC-galactose	CDMPC-glucose	Milk
mtsA llmg_1138	Mn ABC transporter substrate binding protein	5.07 ± 0.17	4.70 ± 0.05	2.79 ± 0.03
mtsB llmg_1136	Mn ABC transporter ATP binding protein	4.90 ± 0.11	5.04 ± 0.16	3.01 ± 0.01
mntA llmg_2171	Putative Mn and Fe transporters	4.62 ± 0.00	4.12 ± 0.02	4.22 ± 0.21
mntH llmg_1490	Divalent metal cation (Mn) transporter MntH	4.93 ± 0.06	4.38 ± 0.02	4.50 ± 0.16
feoA llmg_0200	Ferrous iron transport protein A	4.60 ± 0.33	4.05 ± 0.01	4.82 ± 0.01
feoB llmg_0199	Ferrous iron transport protein B	5.40 ± 0.09	5.00 ± 0.02	4.96 ± 0.08
llmg_1533	Mg and Co transport protein	3.57 ± 0.02	3.40 ± 0.01	3.92 ± 0.19
llmg_0661	CorA like Mg and Co transport protein	5.59 ± 0.40	6.22 ± 0.28	3.26 ± 0.01
copB llmg_1694	Cu-K transporting ATPase B	4.08 ± 0.04	3.90 ± 0.02	4.00 ± 0.07
copA llmg_1729	Cu/K-transporting ATPase (EC 3.6.3.4)	4.49 ± 0.07	4.31 ± 0.00	4.55 ± 0.01
zitS llmg_2400	Zn ABC transporter substrate binding protein	4.03 ± 0.02	3.97 ± 0.01	3.93 ± 0.09
zitQ llmg_2399	Zn ABC transporter ATP binding protein	4.84 ± 0.21	4.61 ± 0.02	4.57 ± 0.02

In **Chapter 4**, we investigated the effect of manganese on non-growing cells as a result of translation inhibition in defined medium. This approach provided a highly controlled and defined way to study this phenomenon. The proteome of lactococci was principally "frozen" in the state of an exponentially growing cell. In contrast, cheesemaking is a complex process where cells are

exposed to various stresses, and changes of transcriptional profiles[66] could be observed. To understand whether the addition of manganese during cheesemaking would result in behaviour consistent with observations from **Chapter 4**, we performed preliminary experiments in cheese. Figure 7.5 shows that manganese addition in cheesemaking did lead to higher accumulation of 3-methylbutanal, but the corresponding accumulation of 3-methylbutanol in the condition without manganese addition was not seen. Based on Table 7.2, metal concentrations tend to increase from milk to cheese potentially due to their interactions with casein micelles and the loss of water activity throughout cheesemaking and ripening[67,68]. To decipher this cheese observation, future experiments will need to understand whether the manganese concentration in cheese is sufficient to induce halted acidification, NADH depletion, and subsequently the lack of conversion from aldehyde to alcohol end-product, as observed earlier in defined conditions.

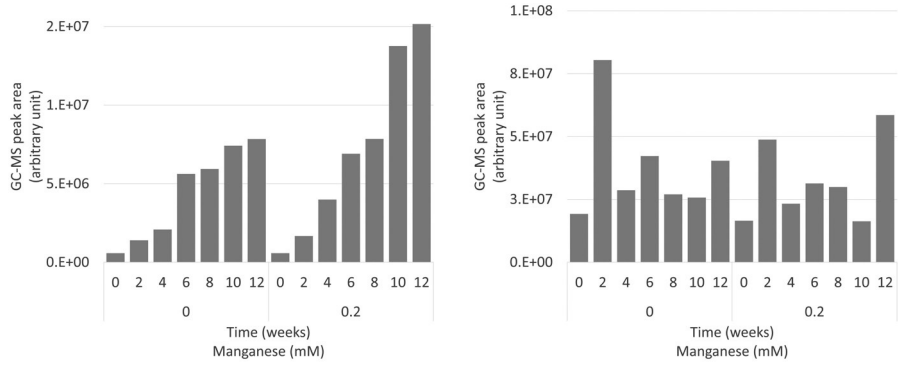

Figure 7.5 *(left) 3-methylbutanal and (right) 3-methylbutanol formation over 12 weeks of ripening with (0.2 mM) or without manganese addition in cheese.* L. cremoris *NCDO712 was precultured (100-fold dilution) in milk prior to standard microcheesemaking[67]. Manganese was added into the cheese milk at indicated concentrations. To retain Mn concentration throughout curd washing, scalding water was added with the same Mn concentration.*

7.6.2 Starter preparation and modifications of cheesemaking

Biopreservation is the original aim of cheesemaking, which is facilitated by the addition of starter culture in pasteurised milk. To modify starter preparation through growth modulation, it is important to assess the technical feasibility with regards to spoilage and altered growth rate of starter culture. In milk, post-pasteurisation contaminants typically include heat-resistant species or endospores of *Bacillus* and *Clostridium* species[69,70]. As facultative anaerobes, bacilli are more prevalent during cheesemaking. Following pasteurisation, spores of *Bacillus cereus* germinate and actively multiply within 2 hours in milk[71] and their number could increase by 100-fold within 4 hours after renneting[72]. In the final cheese, *Bacillus* may no longer be detected due to the combination of low water activity and high salt content as well as lactose depletion and high acidity caused by the activity of starter culture[72]. Nevertheless, the growth of such organism albeit transient is undesired. At around 3E+06 cells/mL, off-flavours such as bitter, putrid, stale, rancid, fruity, or yeasty were described as sensory defects[73]. At 1E+05 cells/mL, *Bacillus* can synthesize symptom-provoking amounts of cereulide toxin, which is extremely stable against heat, acid, or digestive enzymes, and, which can cause food poisoning[74,75]. To prevent these issues and reduce the risk of such spoilage microbes, rapid acidification by LAB starters is desired. Within 6 hours of inoculation in milk, LAB starters can commonly lower the pH of milk to a value between 5.2 and 5.6[67]. This period of acidification is crucial to initiate milk biopreservation. Since the reduction of growth rate is coupled to reduction of acidification rate, changes in growth rate may pose increased risk of spoilage or undesired bacteria.

In **Chapter 6**, we observed that an increase of the ribosomal fraction, due to translational subinhibition or lower temperature, led to a reduction of the growth rate as well as proteins related to flavour formation. Through the employed modulations, we demonstrated that fast growth is desired for

optimal flavour formation. However, establishing this relation for other growth modulations remains to be done. The increase of the ribosomal fraction could also be achieved through faster growth by higher nutrient quality, which may be done through the use of, e.g., glucose rather than galactose[76]. Similarly, higher ribosomal allocation at faster growth is observed in chemostat modulated through the dilution rate of the limiting nutrient[77]. Although it remains to be verified, it is likely that fast growth through this modulation will also lead to reduced flavour formation albeit via a different underlying mechanism of altered proteome allocation (translational inhibition vs. substrate limitation).

For cheese applications, cheese milk has a relatively standardised composition[67] and altering the nutrient quality of sugars or proteins in milk is practically challenging, but not impossible. An example is co-culturing of a lactose-degrading strain that lacks the ability to utilise galactose (LAC+ GAL-) with a strain that is unable to degrade lactose but is able to utilise galactose (LAC-GAL+). Growth of LAC-GAL+ strain on galactose will be slower than on glucose and will require less ribosomal allocation, which may lead to increased flavour formation. At the same time, growth of LAC+GAL- strain on glucose will allow fast acidification. This application will be similar to the use of an adjunct culture. Without fast acidifying cells, the application of slow-growing cells during cheesemaking requires ways to minimise spoilage risks. The most applicable implementation of such approach could be through higher inoculation density of starter. The most convenient method is the use of direct vat inoculation (DVI) where a highly concentrated (freeze-dried) inoculum is added together with rennet[68]. DVI application allows for more variation in growth modulations since cultivation media is less limited to milk-like media compared to bulk starter preparation. Alternatively, increased hygiene practice or the use of bio-preservative starter traits, for instance, nisin-production might be required when cells are optimised for slow growth. This provides an additional safety barrier to prevent spoilage.

The above exemplifies that growth modulations during industrial cheesemaking are rather challenging. This led to a question whether the cultivation history during starter preparation leads to a "cell memory" throughout cheesemaking and ripening. If that turns out to be true, this will be an ideal way to optimise flavour formation without implications of altered technical parameters of cheesemaking. In **Chapter 6**, cells adapted to a level of translation subinhibition were studied for flavour formation. The cells precultured in different ways were used for cheese making where complete translational blocking was present from inoculation to cheese ripening (Figure 7.6, left). As a result, the proteome present at the point of harvesting was maintained throughout the experiment. This resulted in reduced overall volatiles. To understand whether cellular memory exists, we gradually reduced the translational blockage in cheese. When erythromycin was reduced to the corresponding subinhibitory level, cells were able to grow and reach (prolonged) stationary phase in cheese. Under growing conditions, Figure 6 (middle) shows that the correlation between the overall volatiles formation and translation inhibition was still observed, but the slope seems to be less steep. This correlation remains but becomes even weaker when translation inhibition was completely removed during cheesemaking (Figure 7.6, right). Taken together, these results suggest that starter preparation may lead to altered flavour formation during cheese ripening. However, **Chapter 6** demonstrated that proteome reallocation caused by translation inhibition is much more pronounced than temperature-based proteome modulation. Considering confounding factors that were not currently measured such as maximum stationary cell numbers and viability decline rate during ripening, it remains to be seen whether other growth modulations will lead to sufficiently large proteome reallocation to elicit a lasting effect during cheese ripening.

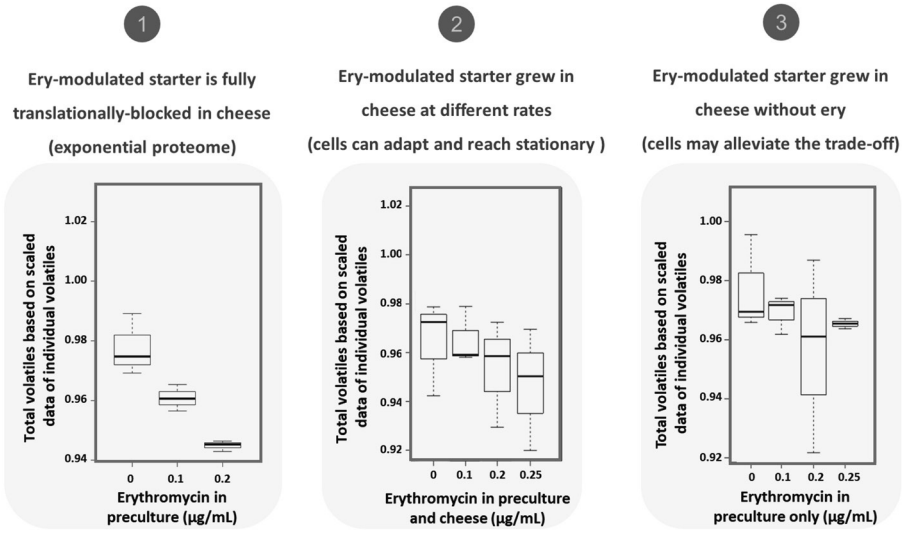

Figure 7.6 *Influence of cultivation history on overall flavour formation in cheese after 28 days of ripening. Values are average of scaled values of all detectable volatiles. All cells grew with translation subinhibition and were transferred to cheesemaking (left) with complete translation block, (middle) with the corresponding translation subinhibition, and (right) without any translation inhibition. The different erythromycin concentrations in the preculture correspond to different preculture growth rates and consequently different proteome allocations.*

7.7 Concluding remarks

This thesis reports on several studies that may bear implications for industrial applications. In the acidification of non-growing cells, we observed a trade-off between rate and yield. This is potentially relevant for the production and long-term quality of fermented dairy products. Faster production and subsequent reduction in post-production activity of enzymes leading to improved product stability is highly desired. If acidification rate can be manipulated through an approach that is regulatory compliant and technically feasible, cheese ripening and yoghurt post-acidification are examples for potential applications.

Moreover, another application is improved long-term cell viability during cell-storage through persistent ATP generation as a consequence of slower but more persistent acidification or arginine utilisation. In this case, probiotic lactic acid bacteria in liquid food products are of relevance. Additionally, any enzymatic processes where increased yields could be obtained by slowing down the conversion rate are another potential area of application. For immobilised enzymes, this may allow higher reusability and longer duration of use. For the microbial and enzymatic production of high-value ingredients, the higher yield is expected to easily overcome longer incubation cost.

We also demonstrated the relation between growth modulation and metabolic proteins relevant for flavour formation in cheese. On this topic, a potential area of application will be the preparation of starters. This understanding also allows process and production optimisation and a better decision-making for improvement in starter culture functionality. Throughout all chapters, we highlighted that lactococci are very interesting model organisms to study non-growing metabolism not only for food fermentation but also for other biotechnological applications.

References

1. Teuber, M. The genus *Lactococcus*. In *The Genera of Lactic Acid Bacteria* 173–234 (Springer, 1995).
2. Blount, Z. D. The natural history of model organisms: the unexhausted potential of *E. coli*. *Elife* **4**, e05826(2015).
3. Cooper, G. M & Hausman, R. Cells as experimental models. In *The Cell: A Molecular Approach Fourth Edition* (Sinauer Associates, 2000).
4. LeBlanc, D. J., Crow, V. L., Lee, L. N. & Garon, C. F. Influence of the lactose plasmid on the metabolism of galactose by *Streptococcus lactis*. *J. Bacteriol.* **137**, 878–884 (1979).
5. Michelsen, O., Hansen, F. G., Albrechtsen, B. & Jensen, P. R. The MG1363 and IL1403 laboratory strains of *Lactococcus lactis* and several dairy strains are diploid. *J. Bacteriol.* **192**, 1058 (2010).
6. Schwidder, M., Heinisch, L. & Schmidt, H. Genetics, toxicity, and distribution of enterohemorrhagic *Escherichia coli* hemolysin. *Toxins* **11**, 502 (2019).

7. Mirhoseini, A., Amani, J. & Nazarian, S. Review on pathogenicity mechanism of enterotoxigenic *Escherichia coli* and vaccines against it. *Microb. Pathog.* **117**, 162–169 (2018).
8. Braat, H. *et al.* A Phase I trial with transgenic bacteria expressing interleukin-10 in Crohn's disease. *Clin. Gastroenterol. Hepatol.* **4**, 754–759 (2006).
9. Wessels, S. *et al.* The lactic acid bacteria, the food chain, and their regulation. *Trends Food Sci. Technol.* **15**, 498–505 (2004).
10. Song, A. A. L., In, L. L. A., Lim, S. H. E. & Rahim, R. A. A review on *Lactococcus lactis*: from food to factory. *Microb. Cell Fact.* **16**, 1-15 (2017).
11. Wels, M., Siezen, R., Van Hijum, S., Kelly, W. J. & Bachmann, H. Comparative genome analysis of *Lactococcus lactis* indicates niche adaptation and resolves genotype/phenotype disparity. *Front. Microbiol.* **10**, 4 (2019).
12. Kazi, T. A. *et al.* Plasmid-based gene expression systems for lactic acid bacteria: a review. *Microorg.* **10**, 1132 (2022).
13. Pechenov, P. Y., Garagulya, D. A., Stanovov, D. S. & Letarov, A. V. New effective method of Lactococcus genome editing using guide RNA-directed transposition. *Int. J. Mol. Sci.* **23**, 13978 (2022).
14. Lammens, E. M., Nikel, P. I. & Lavigne, R. Exploring the synthetic biology potential of bacteriophages for engineering non-model bacteria. *Nat. Commun.* **11**, 1–14 (2020).
15. Kleerebezem, M. *et al.* Lifestyle, metabolism and environmental adaptation in *Lactococcus lactis*. *FEMS Microbiol. Rev.* **44**, 804-820 (2020).
16. Chen, Y. *et al.* Proteome constraints reveal targets for improving microbial fitness in nutrient-rich environments. *Mol. Syst. Biol.* **17**, e10093 (2021).
17. Price, C. E., Zeyniyev, A., Kuipers, O. P. & Kok, J. From meadows to milk to mucosa – adaptation of *Streptococcus* and *Lactococcus* species to their nutritional environments. *FEMS Microbiol. Rev.* **36**, 949–971 (2012).
18. Johanson, A., Goel, A., Olsson, L., Franzén, C. J. & Dudley, E. G. Respiratory physiology of *Lactococcus lactis* in chemostat cultures and its effect on cellular robustness in frozen and freeze-dried starter cultures. **86**, e02785-19 (2020).
19. Cesselin, B. *et al.* Responses of lactic acid bacteria to oxidative stress. In *Stress Responses of Lactic Acid Bacteria* 111–127 (Springer US, 2011).
20. Smit, G., Smit, B. A. & Engels, W. J. M. Flavour formation by lactic acid bacteria and biochemical flavour profiling of cheese products. *FEMS Microbiol. Rev.* **29**, 591–610 (2005).
21. Noutsopoulos, D. *et al.* Growth, *nisA* gene expression, and *in situ* activity of novel *Lactococcus lactis* subsp. *cremoris* costarter culture in commercial hard cheese production. *J. Food Prot.* **80**, 2137–2146 (2017).
22. Aleixandre-Tudó, J. L., Castelló-Cogollos, L., Aleixandre, J. L. & Aleixandre-Benavent, R. Tendencies and challenges in worldwide scientific research on probiotics. *Probiotics Antimicrob. Proteins* **12**, 785–797 (2020).
23. Li, T. T., Tian, W. L. & Gu, C. T. Elevation of *Lactococcus lactis* subsp. *cremoris* to the species level as *Lactococcus cremoris* sp. nov. and transfer of *Lactococcus lactis* subsp. *tructae* to *Lactococcus cremoris* as *Lactococcus cremoris* subsp. *tructae* comb. nov. *Int. J. Syst. Evol. Microbiol.* **71**, 004727 (2021).

24. Bachmann, H. *et al.* Availability of public goods shapes the evolution of competing metabolic strategies. *Proc. Natl. Acad. Sci. U. S. A.* **110**, 14302–14307 (2013).

25. Kim, W. S., Ren, J. & Dunn, N. W. Differentiation of *Lactococcus lactis* subspecies *lactis* and subspecies *cremoris* strains by their adaptive response to stresses. *FEMS Microbiol. Lett.* **171**, 57–65 (1999).

26. Poolman, B., Driessen, A. J. M. & Konings, W. N. Regulation of arginine-ornithine exchange and the arginine deiminase pathway in *Streptococcus lactis*. *J. Bacteriol.* **169**, 5597-5604 (1987).

27. Sun, Y., Fukamachi, T., Saito, H. & Kobayashi, H. Respiration and the F1F0-ATPase enhance survival under acidic conditions in *Escherichia coli*. *PLoS One* **7**, e52577 (2012).

28. Kuroda, A. *et al.* Role of inorganic polyphosphate in promoting ribosomal protein degradation by the Lon protease in *E. coli*. *Science.* **293**, 705–708 (2001).

29. Chowdhury, N., Kwan, B. W. & Wood, T. K. Persistence increases in the absence of the alarmone guanosine tetraphosphate by reducing cell growth. *Sci. Rep.* **6**, 1–9 (2016).

30. Kohler, C. *et al.* Proteome analyses of *Staphylococcus aureus* in growing and non-growing cells: a physiological approach. *Int. J. Med. Microbiol.* **295**, 547–565 (2005).

31. Alleron, L. *et al.* VBNC *Legionella pneumophila* cells are still able to produce virulence proteins. *Water Res.* **47**, 6606–6617 (2013).

32. Michalik, S. *et al.* Life and death of proteins: A case study of glucose-starved Staphylococcus aureus. *Mol. Cell. Proteomics* **11**, 558–570 (2012).

33. Ayrapetyan, M., Williams, T. C. & Oliver, J. D. Bridging the gap between viable but non-culturable and antibiotic persistent bacteria. *Trends Microbiol.* **23**, 7–13 (2015).

34. Frees, D., Savijoki, K., Varmanen, P. & Ingmer, H. Clp ATPases and ClpP proteolytic complexes regulate vital biological processes in low GC, Gram-positive bacteria. *Mol. Microbiol.* **63**, 1285–1295 (2007).

35. Frees, D., Gerth, U. & Ingmer, H. Clp chaperones and proteases are central in stress survival, virulence and antibiotic resistance of *Staphylococcus aureus*. *Int. J. Med. Microbiol.* **304**, 142–149 (2014).

36. Maisonneuve, E., Ezraty, B. & Dukan, S. Protein aggregates: an aging factor involved in cell death. *J. Bacteriol.* **190**, 6070–6075 (2008).

37. Hanson, A. D. *et al.* The number of catalytic cycles in an enzyme's lifetime and why it matters to metabolic engineering. *Proc. Natl. Acad. Sci.* **118**, e2023348118 (2021).

38. Gracy, R. W., Talent, J. M. & Zvaigzne, A. I. Molecular wear and tear leads to terminal marking and the unstable isoforms of aging. *J. Exp. Zool.* **282**, 18–27 (1998).

39. Markert, C. L., Scandalios, J. G., Lim, H. A. & Serov, O. L. Isozymes: organization and roles. In evolution, genetics and physiology. In *Evolution, Genetics And Physiology, Proceedings Of The Seventh International Congress On Isozymes* 1–328 (World Scientific, 1994).

40. Nugroho, A. D. W., Kleerebezem, M. & Bachmann, H. A novel method for long-term analysis of lactic acid and ammonium production in non-growing *Lactococcus lactis* reveals pre-culture and strain dependence. *Front. Bioeng. Biotechnol.* **8**, 580090 (2020).

41. Milo, R. What is the total number of protein molecules per cell volume? A call to rethink some published values. *BioEssays* **35**, 1050–1055 (2013).

42. Lahtvee, P. J., Seiman, A., Arike, L., Adamberg, K. & Vilu, R. Protein turnover forms one of the highest maintenance costs in *Lactococcus lactis*. *Microbiol. (United Kingdom)* **160**, 1501–1512 (2014).

43. Andersson, I. & Backlund, A. Structure and function of Rubisco. *Plant Physiol. Biochem.* **46**, 275–291 (2008).

44. Studer, R. A., Christin, P. A., Williams, M. A. & Orengo, C. A. Stability-activity tradeoffs constrain the adaptive evolution of RubisCO. *Proc. Natl. Acad. Sci. U. S. A.* **111**, 2223–2228 (2014).

45. Tokuriki, N., Stricher, F., Serrano, L. & Tawfik, D. S. How protein stability and new functions trade off. *PLOS Comput. Biol.* **4**, e1000002 (2008).

46. Ault, A. Enzyme catalysis and the Gibbs energy. *J. Chem. Educ.* **86**, 1069–1071 (2009).

47. Low, P. S., Bada, J. L. & Somero, G. N. Temperature adaptation of enzymes: roles of the free energy, the enthalpy, and the entropy of activation. *Proc. Natl. Acad. Sci. U. S. A.* **70**, 430–432 (1973).

48. Stearn, A. E. & Action V. L. R. Kinetics of biological reactions with special reference to enzymic processes. In *Advances in Enzymology and Related Areas of Molecular Biology* 25–74 (Interscience Publishers, 2006).

49. Siddiqui, K. S. & Cavicchioli, R. Cold-adapted enzymes. *Annu. Rev. Biochem.* **75**, 403–433 (2006).

50. Sohail Siddiqui, K. Defying the activity-stability trade-off in enzymes: taking advantage of entropy to enhance activity and thermostability. *Crit. Rev. Biotechnol.* **37**, 309-322 (2016).

51. Fragai, M., Luchinat, C., Parigi, G. & Ravera, E. Conformational freedom of metalloproteins revealed by paramagnetism-assisted NMR. *Coord. Chem. Rev.* **257**, 2652–2667 (2013).

52. Campbell, E. C. *et al.* Laboratory evolution of protein conformational dynamics. *Curr. Opin. Struct. Biol.* **50**, 49–57 (2018).

53. Åqvist, J., Kazemi, M., Isaksen, G. V. & Brandsdal, B. O. Entropy and enzyme catalysis. *Acc. Chem. Res.* **50**, 199–207 (2017).

54. Villà, J. *et al.* How important are entropic contributions to enzyme catalysis? *Proc. Natl. Acad. Sci. U. S. A.* **97**, 11899 (2000).

55. Sun, Y. & Dai, S. High-entropy materials for catalysis: a new frontier. *Sci. Adv.* **7**, eabg1600 (2021).

56. Miller, J. H. Assay of β-galactosidase. In *Experiments in Molecular Genetics.* (Cold Spring Harbor Laboratory, 1972).

57. Bachmann, H. *et al.* Regulatory phenotyping reveals important diversity within the species *Lactococcus lactis*. *Appl. Environ. Microbiol.* **75**, 5687-5694 (2009).

58. Khademian, M. & Imlay, J. A. How microbes evolved to tolerate oxygen. *Trends*

Microbiol. **29**, 428–440 (2021).

59. Champomier-Vergès, M. C., Maguin, E., Mistou, M. Y., Anglade, P. & Chich, J. F. Lactic acid bacteria and proteomics: current knowledge and perspectives. *J. Chromatogr. B* **771**, 329–342 (2002).
60. Imlay, J. A. Where in the world do bacteria experience oxidative stress? *Environ. Microbiol.* **21**, 521–530 (2019).
61. Rocha, A. G. *et al.* Life without Fe–S clusters. *Mol. Microbiol.* **99**, 821–826 (2016).
62. Archibald, F. S. & Fridovich, I. Manganese, superoxide dismutase, and oxygen tolerance in some lactic acid bacteria. *J. Bacteriol.* **146**, 928–936 (1981).
63. Siedler, S. *et al.* Competitive exclusion is a major bioprotective mechanism of lactobacilli against fungal spoilage in fermented milk products. *Appl. Environ. Microbiol.* **86**, (2020).
64. Price, C. E. *et al.* Adaption to glucose limitation is modulated by the pleotropic regulator CcpA, independent of selection pressure strength. *BMC Evol. Biol.* **19**, 15 (2019).
65. Zamberlin, Š., Antunac, N., Havranek, J. & Samaržija, D. Mineral elements in milk and dairy products. *Mljekarstvo* **62**, 111-125 (2012).
66. de Jong, A., Hansen, M. E., Kuipers, O. P., Kilstrup, M. & Kok, J. The transcriptional and gene regulatory network of *Lactococcus lactis* MG1363 during growth in milk. *PLoS One* **8**, e53085 (2013).
67. Bachmann, H., Kruijswijk, Z., Molenaar, D., Kleerebezem, M. & van Hylckama Vlieg, J. E. T. A high-throughput cheese manufacturing model for effective cheese starter culture screening. *J. Dairy Sci.* **92**, 5868–5882 (2009).
68. Bylund, G. *Dairy processing handbook*. (Tetra Pak Processing Systems, 2003).
69. Oliveira, R. B. A. *et al.* Processed cheese contamination by spore-forming bacteria: a review of sources, routes, fate during processing and control. *Trends Food Sci. Technol.* **57**, 11–19 (2016).
70. Te Giffel, M. C., Beumer, R. R., Leijendekkers, S. & Rombouts, F. M. Incidence of *Bacillus cereus* and *Bacillus subtilis* in foods in the Netherlands. *Food Microbiol.* **13**, 53–58 (1996).
71. Mikolajcik, E. M. & Koka, M. Bacilli in Milk. I. Spore Germination and Growth. *J. Dairy Sci.* **51**, 1579–1582 (1968).
72. Rukure, G. & Bester, B. H. Survival and growth of *Bacillus cereus* during Gouda cheese manufacturing. *Food Control* **12**, 31–36 (2001).
73. Meer, R. R., Baker, J., Bodyfelt, F. W. & Griffiths, M. W. Psychrotrophic *Bacillus* spp. in fluid milk products: a review. *J. Food Prot.* **54**, 969–979 (1991).
74. Dietrich, R., Jessberger, N., Ehling-Schulz, M., Märtlbauer, E. & Granum, P. E. The food poisoning toxins of *Bacillus cereus*. *Toxins* **13**, 98 (2021).
75. Tirloni, E. *et al. Bacillus cereus* in dairy products and production plants. *Foods* **11**, 2572 (2022).
76. Scott, M., Gunderson, C. W., Mateescu, E. M., Zhang, Z. & Hwa, T. Interdependence of cell growth and gene expression: origins and consequences. *Science* **330**, 1099–1102 (2010).
77. Hui, S. *et al.* Quantitative proteomic analysis reveals a simple strategy of global resource allocation in bacteria. *Mol. Syst. Biol.* **11**, 784 (2015).

Summary

Cheese and other fermented foods have been an integral part of human civilisation since ancient times. For thousands of years, fermented foods have been part of the global diet and most cultures have a long history of food fermentation. Yet, due to its complexity, much remains to be deciphered about the biology of food fermentation and its microorganism. Food fermentations often span a long period of time, and they involve diverse reactions that may occur spontaneously or facilitated by *ex vivo* enzymes or through cell metabolism. Environmental conditions can change over the course of a fermentation process, and they are often accompanied by changes in the physiological states of the microorganisms involved. Following production, fermented foods are typically subjected to storage or ripening where cells enter a non-growing but metabolically active state for an extended period (**Chapter 2**).

As we enter a world with a human population of 8 billion, ways to improve the efficiency of food manufacturing and ensure subsequent product stability become increasingly important. Extended incubation during product ripening is costly as it often relies on controlled environmental conditions. An example where product stability limits the shelf-life of a product is the post-acidification of yogurt where the increase in acidity by non-growing cells is perceived as less palatable by consumers. Understanding the metabolism of non-growing cells and how acidification rates and lactic acid yields can be modified is therefore highly relevant. Additionally, changes during storage at the distribution or consumer level are undesired and may lead to food waste. Due to current regulatory restrictions, the solution to such issues should rather be sought through modifications in culture conditions than genetic modification.

To modulate long-term metabolism, biological understanding is a prerequisite for process improvements. We developed a method resembling cheese ripening where we can monitor real-time non-growing cell activity for extended periods (**Chapter 3**). Efforts were made to follow acidification,

arginine catabolism, and branched-chain amino acid catabolism for a minimum of 1 week (**Chapter 3-5**). Non-growing cell metabolism can be steered with regards to conversion rate and/or product yield (**Chapter 3-6**). During starter preparation, strain selection (**Chapter 3**) and preculture conditions (**Chapter 3-6**) can be used to optimise desired metabolic activities. In many cases, trade-offs can be observed. The use of a slower-growing strain with higher biomass yield (**Chapter 3**) may lead to slower acidification, but the activation of arginine metabolism potentially aids in survival. In the case of acidification, the increased rate led to an increased decline in production and consequently, decreased overall lactic acid yield (**Chapter 5**). While short-term production is typically operated at the maximum rate, long-term production may benefit from operating at a suboptimal rate.

One of the demonstrated ways to modulate the acidification rate and yield was through manganese supplementation (**Chapter 4**), which we investigated in great depth. Manganese supplementation is associated with a rapid loss in culturability and NADH depletion, which allows the accumulation of key-flavour (3-methylbutanal) as a metabolic end-product by preventing further conversion to a derivative with a higher sensory threshold (3-methylbutanol). In this case, manganese omission did not lead to growth rate changes while the increase of 3-methylbutanal was observed. In contrast, growth rate reduction through translation subinhibition or reduced temperature was consistently correlated with reduced 3-methylbutanal formation (**Chapter 6**). Such reduction is not necessarily associated with the reduction of the corresponding flavour-forming enzymes. Altogether, this demonstrates that metabolite formation is influenced by many aspects of the cellular repertoire and that yield optimisation instead of growth or catalytic rate optimisation might be the preferable aim of non-growing cell metabolism and fermentation ripening. As a consequence, optimised starter culture preparation holds the potential to benefit the starter functionality in terms of flavour formation and product stability of fermented products.

Acknowledgement

The author would like to acknowledge everyone who directly and indirectly contributed to his journey to a doctoral degree, both at personal and professional levels. For inclusivity and privacy, this acknowledgment is written in haikus as a reflection tool. A haiku is an unrhymed Japanese poem, which is assembled in three parts comprising five, seven, and five syllables, respectively.

The quaint farmer's house. Late winter and silver hair. The journey started.

***Company partners**. Supplied generous funding. And prized expertise.*

***All academics**. Steering and enlightening. The promovendus.*

*To **NIZO** he went. Sometimes **WUR, TIFN, or VU. Great consortium**!*

***Colleagues** come and gone. **Friends** and **acquaintances** made. On and off the path.*

*Helpful **technicians**. Problem-solving and teaching. Fortunate, I was.*

Thousands of samples. Our daily bread and butter. To help and be helped.

Lunches in the sun. Or under the little tree. Or just the canteen.

Some strolls in the woods. Mostly, roaming through the labs. The work-life balance.

*Big pat on the back. Physically, often not. **My support system.***

*Heartfelt thanks to **you**. Rabbit, yarn, drag, ESC. You know who you are.*

***Thesis committee**. **Paranymphs** and all the rest. Cheers to the defence!*

All laughter and tears. Never to be forgotten. This upheaval ride.

Crossed! The finish line! But, finished I never be. To learn and unlearn.

Make your way to me. Challenges and obstacles. For I am ready.

About the Author

Avis Nugroho was born and raised in the metropolitan area of Surabaya, East Java, Indonesia. At a very young age, he fell in love with gardening and fermenting his harvest. One of his discoveries includes *Averrhoa bilimbi* flower wine, which fascinated him with the remarkable transformation of flavours during fermentation. At the age of 16, he enrolled for a bachelor's degree in Microbiology at Bandung Institute of Technology. The fourth year of his study was spent as a fully-funded exchange student at Tohoku University in Japan, where he experienced artisanal food and fermentation through various industrial and cultural excursions. He subsequently finished his Bachelor degree with distinction and his thesis was written on the microbial application of zero-water discharge in whiteleg shrimps cultivation. Following graduation, he eventually obtained a master scholarship and decided to concentrate on fermented food manufacture by majoring in Food Technology with specialisation of Food Biotechnology and Biorefining in Wageningen University. His team won and represented The Netherlands with a dairy substitute made of fermented soy in the European final of Ecotrophelia, which was a competition of eco-innovative product and process design. This experience combined with his Master thesis on the encapsulation of probiotic *Akkermansia muciniphila* using double W/O/W emulsion strengthened his interest on the research and development of food products and processes. With a master degree in hand, he continued to conduct his PhD study at NIZO Food Research for 4.5 years, which culminated in this thesis. His project was specialized in dairy starter culture and flavour formation by non-growing lactic acid bacteria. Afterward, for almost the next 2 years, he worked as a researcher at Vrije Universiteit Amsterdam, where he studied diverse food microorganisms for off-flavours removal in plant-based proteins. Following this education journey, he set out his industrial career and continues to enable (fermented) food innovation.

Overview of Completed Training Activities

Category A: Discipline specific activities

- Applied Biocatalysis, VLAG/RUG, Groningen, The Netherlands, 2017
- Food and biorefinery enzymology, VLAG, Wageningen, The Netherlands, 2017
- Lactic Acid Bacteria 12th conference, KNVM/FEMS, Egmond aan Zee, The Netherlands, 2017
- Nederlandse Biotechnologische 17th Conference, NBV, Wageningen, The Netherlands, 2017
- Scientific spring meeting, KNVM, Arnhem, The Netherlands, 2017
- Advanced Food Analysis, VLAG, Wageningen, The Netherlands, 2019
- New Approaches and Concepts in Microbiology, EMBL/EMBO, Heidelberg, Germany, 2019
- Big Data Analysis in The Life Science, VLAG, Wageningen, The Netherlands, 2019
- New Approaches and Concepts in Microbiology, EMBL/EMBO, Online, 2021
- Lactic Acid Bacteria 12th conference, KNVM/FEMS, Online, 2021

Category B: General courses

- Wageningen PhD symposium, WUR PhD council, Wageningen, The Netherlands, 2017
- Effective behavior in professional surroundings, WGS, Wageningen, The Netherlands, 2017
- TIFN intellectual property awareness workshop, TIFN, Wageningen, The Netherlands, 2017
- PhD week, VLAG, Baarlo, The Netherlands, 2017
- Food Friction (Technology session), Graduate School ArtEZ University of the Arts, Arnhem, The Netherlands, 2018
- Career orientation, WGS, Wageningen, The Netherlands, 2019
- Brain friendly writing and working, WGS, Wageningen, The Netherlands, 2019
- Job Coaching Workshop, IconQC, Online, 2020-2021
- Business Presentation and Communication (How to present myself and communicate in the (Dutch) Business Community), IconQC, Online, 2020-2021

Category C: Optionals

- Preparation of research proposal, HMI WUR, Wageningen, The Netherlands, 2016-2017
- Weekly group meetings, HMI WUR, Wageningen, The Netherlands, 2016-2020
- Weekly lunch meetings, NIZO, Ede, The Netherlands, 2016-2020
- Various TIFN meetings (e.g. TIFN retreats), TIFN, Wageningen, The Netherlands, 2016-2020

The studies presented in this thesis were performed within the framework of TiFN

Financial support from Wageningen University and TiFN for printing this thesis is gratefully acknowledged.

Cover design by Elma Hogeboom (GreenThesis)

The handpainted art was made with a lake pigment from annatto seeds. Annatto is a common source of food colouring that is used to enhance the perception of creaminess in dairy products, including Gouda cheese. From back to front, a trail of Lactococcal cells and various compounds related to cheesemaking and the formation of a key flavour (3-methylbutanal) are depicted. Along the trail, the color gradually becomes more saturated to represent cheese ripening.

Printed by Proefschriftmaken on FSC-certified paper